

Utah State University

DigitalCommons@USU

---

All Graduate Theses and Dissertations

Graduate Studies

---

5-2014

## Channel Adjustment and Channel-Floodplain Sediment Exchange in the Root River, Southeastern Minnesota

Michael A. Souffront Alcántara  
*Utah State University*

Follow this and additional works at: <https://digitalcommons.usu.edu/etd>



Part of the [Life Sciences Commons](#)

---

### Recommended Citation

Souffront Alcántara, Michael A., "Channel Adjustment and Channel-Floodplain Sediment Exchange in the Root River, Southeastern Minnesota" (2014). *All Graduate Theses and Dissertations*. 3334.

<https://digitalcommons.usu.edu/etd/3334>

This Thesis is brought to you for free and open access by the Graduate Studies at DigitalCommons@USU. It has been accepted for inclusion in All Graduate Theses and Dissertations by an authorized administrator of DigitalCommons@USU. For more information, please contact [digitalcommons@usu.edu](mailto:digitalcommons@usu.edu).



CHANNEL ADJUSTMENT AND CHANNEL-FLOODPLAIN SEDIMENT  
EXCHANGE IN THE ROOT RIVER, SOUTHEASTERN MINNESOTA

by

Michael A. Souffront Alcántara

A thesis submitted in partial fulfillment  
of the requirements for the degree

of

MASTER OF SCIENCE

in

Watershed Science

Approved:

---

Patrick Belmont  
Major Professor

---

R. Douglas Ramsey  
Committee Member

---

Joseph M. Wheaton  
Committee Member

---

Mark R. McLellan  
Vice President for Research and  
Dean of the School of Graduate Studies

UTAH STATE UNIVERSITY  
Logan, Utah

2014

Copyright © Michael A. Souffront Alcántara 2014

All Rights Reserved

## ABSTRACT

Channel Adjustment and Channel-Floodplain Sediment Exchange in the Root River,  
Southeastern Minnesota

by

Michael A. Souffront Alcántara, Master of Science

Utah State University, 2014

Major Professor: Dr. Patrick Belmont  
Department: Watershed Sciences

A better understanding of transport and deposition of fine sediment in alluvial rivers, including their floodplains, is essential for improved understanding of sediment budgets and prediction of river morphological changes. Previous work in the Root River indicates that channel-floodplain sediment exchange exerts strong control on the sediment flux of this system. In addition, improvements in agricultural practices and increases in high and low flows during the past five decades have led us to believe that sediment sources in the Root River may be shifting from uplands to near-channel sources. This thesis estimated the total amount of fine sediment contributed to the channel from near-channel sources due to the processes of lateral channel adjustment (channel migration and channel widening) using a quantitative approach based on the use of multiple epochs of aerial photographs (1930s-2010s), lidar data available for the entire watershed from 2008, and other GIS analysis. The results obtained in this thesis serve as another line of evidence to constrain a sediment budget for the Root River watershed and

to improve our understanding of the sediment dynamics within the watershed. In addition, we found that the Root River presents a marked division between its lateral channel adjustment trends before and after the 1970s. We also found that while increases in flows have affected lateral channel adjustment rates throughout the entire channel network, other factors like sediment supply and riparian vegetation may be playing an equally important role.

(182 pages)

## PUBLIC ABSTRACT

Channel Adjustment and Channel-Floodplain Sediment Exchange in the Root River,  
Southeastern Minnesota

by

Michael A. Souffront Alcántara, Master of Science

Utah State University, 2013

Major Professor: Dr. Patrick Belmont  
Department: Watershed Sciences

The shape and location of a river can change through time, moving large amounts of sediment in the process. This is because the land that is immediately next to the active channel of a river, known as floodplain, is considered to be part of the river system. A better understanding of how the river channel and its floodplain interact is needed to improve our ability to predict how rivers change through time. A previous study in the Root River, southeastern Minnesota, USA indicates that the relation between the channel and the floodplain in this river is very important. In addition, improvements in agriculture and changes in water flow have led us to believe that sources of sediment in the Root River may be shifting from uplands to near-channel sources (floodplain). This thesis estimated the total amount of sediment contributed to the channel from the floodplain due to lateral changes in the shape (channel widening or narrowing) and location (channel migration) of the Root River. Multiple epochs of aerial photographs together with other database and GIS (Geographic Information Systems) analyses were

used to accomplish this goal. The results of this thesis contribute to the understanding of how much sediment flows into the Root River and where it comes from. In addition, we found that the rates of channel adjustments in the Root River have changed since the 1970s. We also found that while changes in water flow are very important in the channel-floodplain relation, other factors like sediment supply and riparian vegetation may be playing an equally important role.

## ACKNOWLEDGMENTS

This thesis is the result of the work and help of many people. I want to first thank God for his many blessings and for putting such great people around me, and then all the people that in one way or another contributed to the completion of this thesis.

I am very grateful to my advisor, Patrick Belmont, for giving me the opportunity to be part of a wonderful group and for all his advice throughout this last two years. He introduced me to the field of geomorphology and without him I would literally not be here. Thanks to Justin Stout for providing the background necessary to make this project relevant. Thanks to my committee members, Joe Wheaton and Doug Ramsey, for their teachings, comments and advice throughout the entire process of developing this thesis. Thanks to Chris Garrard for her help with the python scripts developed for this thesis. I would also like to thank my lab mates for their ideas, time spent reviewing, and for their many contributions to the analyses presented here. In the same order, thanks to Toby Dogwiler and his group at Winona State University for all their help with fieldwork and with the aerial photograph analysis. Without all your help I would be far from done.

I would also like to thank Brian Bailey and Enid Kelley from the Watershed Science Department office. They would always receive me with a smile on their faces and answer my many questions regarding the watershed science program. Thanks to Shelly Ortiz Hernández and the people at the Office of International Students and Scholars for their help regarding orientation and accommodations for international students. You have being excellent hosts.

I would also like to express my appreciation to the Dominican community at Utah State University for making Logan feel more like home. Many of you have become like family. Thanks for making the stay here much more pleasurable.

Lastly, I would like to say thanks to my family for their unconditional love and for all their support. To my parents, Rafael Souffront and Tamara Alcántara, for teaching me values and for their infinite love; to my wife and to my sister, Jolyn Souffront and Yosayris Souffront, for being part of my life. You two are my motivation to become better every day, I love you.

¡Gracias a todos!

Michael Souffront

## CONTENTS

	Page
ABSTRACT.....	iii
PUBLIC ABSTRACT .....	v
ACKNOWLEDGMENTS .....	vii
LIST OF TABLES .....	xii
LIST OF FIGURES .....	xiii
 CHAPTER	
1. UNDERSTANDING NEAR-CHANNEL SEDIMENT EXCHANGE PROCESSES.....	1
1.1 Introduction.....	1
1.2 Sediment Budgets .....	2
1.3 Variables Influencing Channel Form.....	3
1.4 Channel Morphology .....	4
1.5 Channel Planform .....	6
1.5.1 Channel Migration .....	6
1.5.2 Channel Widening .....	7
1.6 Floodplain Grain Size Composition.....	9
1.7 Research Context .....	10
1.7.1 Research Questions.....	11
1.7.2 Objectives .....	11
1.8 Study Area .....	12
1.9 Methods.....	15

	x
1.9.1 Channel Migration Rate .....	17
1.9.2 Channel Width .....	18
1.9.3 Grain size distribution campaign .....	19
1.9.4 Python Scripts and Result Figures .....	19
1.10 References .....	20
2. LATERAL CHANNEL ADJUSTMENT IN THE ROOT RIVER, SOUTHEASTERN MINNESOTA .....	34
2.1 Introduction .....	34
2.2 Channel Description .....	36
2.3 Methods .....	41
2.3.1 Aerial Photograph Analysis .....	41
2.3.2 Channel Migration .....	43
2.3.3 Channel Widening/Narrowing .....	44
2.3.4 Hydrology .....	45
2.3.5 Land Cover .....	46
2.4 Error Analysis and Validation .....	47
2.5 Results and Discussions .....	54
2.5.1 Channel Migration .....	55
2.5.2 Channel Width .....	58
2.5.3 Lateral Channel Adjustment Evolution .....	61
2.6 References .....	61
3. CHANNEL-FLOODPLAIN SEDIMENT EXCHANGE IN THE ROOT RIVER, SOUTHEASTERN MINNESOTA .....	85
3.1 Introduction .....	85
3.2 Methods .....	87
3.2.1 Lidar Analysis .....	88

	xi
3.2.2 Extracting bank elevations .....	89
3.2.3 Cross Sections .....	90
3.2.4 Grain Size Distribution .....	90
3.2.5 Bulk Density .....	92
3.2.6 Sediment Mass .....	93
3.3 Error Analysis and Validation .....	94
3.4 Results and Discussions .....	96
3.4.1 Lidar Analysis .....	97
3.4.2 Grain Size Distribution and Bulk Density .....	97
3.4.3 Sediment Mass .....	99
3.5 References .....	100
4. SUMMARY AND FUTURE WORK .....	116
4.1 Summary .....	116
4.2 Future Work .....	117
4.3 References .....	118
APPENDICES .....	120

## LIST OF TABLES

Table	Page
2.1 Root River main stem planform geometry variables .....	64
2.2 Photographs analyzed .....	64
2.3 Reach vegetation coverage .....	65
2.4 Root River channel migration per reach .....	66
2.5 Tributary migration rates .....	66
2.6 Width percent change per reach.....	66
2.7 Tributary average width per reach .....	67
2.8 Highest peaks. USGS gage 05385000 near Houston.....	68
2.9 Lowest peaks. USGS gage 05385000 near Houston .....	69
3.1 Root River grain size distribution.....	102
3.2 Root River bulk density .....	103
3.3 Average sediment volume and sediment mass results per tributary .....	1034

## LIST OF FIGURES

Figure	Page
1.1 Sediment cascades transport sequence.....	25
1.2 Sediment budget Coon Creek. From Trimble, 1999.....	26
1.3 Lane’s balance. From Wilcock et al., 2009. ....	27
1.4 Threshold between meandering and braided channels .....	28
1.5 Cross section evolution of a meandering river .....	28
1.6 Root River Watershed. Counties that contain the Root River watershed .....	29
1.7 Root River watershed, channel network, lidar topography, and Driftless Area boundary.....	29
1.8 Karst map, Southeastern Minnesota. From Gao et al., 2002 .....	30
1.9 Root River decadal flow duration curves 1930s-2000s .....	30
1.10 Schematic organization of the main tasks needed to complete this project.....	31
1.11 Planform statistics toolbox.....	32
1.12 Migration rate polygons for 2000s-2010s.....	32
1.13 Polygons and centerlines for 2011 and 1947. Root River, MN.....	33
2.1 Planform geometry variables .....	69
2.2 Root River channel network and longitudinal profiles. ....	70
2.3 Reach division.....	71
2.4 Old Lake Florence, close to the city of Stewartville in the county of Olmsted, MN.....	71
2.5 Different banks characteristics from channel network .....	72
2.6 Sub-reach average width division example .....	73
2.7 Error experiment locations and Width validation sites.....	73

2.8	Average field-measured width 2013 versus average GIS-calculated width 2010	74
2.9	Cutoff between Rushford and Houston for 1990s and 2000s	74
2.10	Migration rates main stem of the Root River	75
2.11	Average migration rates per reach, main stem of the Root River	76
2.12	Average migration rates versus flow metrics	77
2.13	Migration rates for tributaries	78
2.14	Probability distributions migrations rates and different vegetation types	79
2.15	Floodplain vegetation comparison of 2010 and 1991	80
2.16	Sub-reach width plots, main stem of the Root River	81
2.17	Delta sub-reach width plots, main stem of the Root River	812
2.18	Percent width change per reach, Root River	813
3.1	Surveyed sites 2012 and sample locations 2013	105
3.2	Grain size and bulk density campaign, summer 2013	106
3.3	Equipment used in grain size and bulk density analysis	107
3.4	Control points and vegetation cover, main stem of the Root River	108
3.5	Right and left bank elevations, and Delta eta extracted from 2008 lidar	113
3.6	Bank height versus grain size metrics	114
3.7	Floodplain height distributions along the Root River	114
3.8	Fine sediment contributions due to lateral channel adjustment	115

## CHAPTER 1

### UNDERSTANDING NEAR-CHANNEL SEDIMENT EXCHANGE PROCESSES

#### **1.1 Introduction**

Developing a predictive understanding of sediment dynamics at the landscape scale has been a primary goal of geomorphology over the past half century (Hadley and Schumm, 1961; Dietrich and Dunne, 1978; Walling, 1983; Smith et al., 2011). A better understanding of transport and deposition of fine sediment in alluvial river channels and floodplains is essential for improved understanding of sediment budgets and prediction of river morphological changes (Trimble, 1999; Narinesingh et al., 1999). Sediment erosion and deposition controls the morphology of alluvial channels (Naden, 2010).

Fine sediment (grain sizes  $< 2\text{mm}$ ) is a natural component of rivers and plays an important role in the development of aquatic and riparian habitats; however, in excess amounts, it is considered a major stressor for aquatic biota and typically has negative effects on water quality and the aesthetics of the channel (Owens et al., 2005; Collins et al., 2011; Jones et al., 2011; Belmont et al., 2011). Fine sediment is responsible for the transport of many nutrients, heavy metals and other contaminants to the river channel (Walling et al., 2006; Hauer et al., 2011; Bainbridge et al., 2012). A better understanding of the mechanisms that mobilize, transport, deposit, and resuspend fine sediment is necessary to enhance our ability to predict how sediment moves through the watershed and how it affects riparian and aquatic ecosystems.

Sediment moves through the landscape in a stochastic way (Davies and Korup, 2010) and there are many pathways for sediment to move from the terrestrial environment to a channel (Figure 1.1). Prediction of fine sediment routing through a

watershed, including storage time in each stage, is complicated by multiple factors including climate, geology, and land use history. For example, sediment can be stored in floodplains for many millennia or pass through the river in short time periods (Skalak and Pizzuto, 2010). In some river systems relatively little storage occurs, while in other systems the vast majority of sediment is stored for long periods of time (Trimble, 1999; Walling and Collins, 2008). These statements highlight the need to understand how sediment moves through the river system with its respective sinks and sources instead of only focusing on downstream fluxes.

## 1.2 Sediment Budgets

Many studies have used sediment budgets to identify and quantify sediment sinks and sources (e.g., Trimble, 1999; Walling and Collins, 2008; Belmont et al., 2011). Input data to constrain a sediment budget include water and sediment gaging stations, remotely sensed data (historic and modern air photos, digital elevation models, land use and soil maps, etc.), field measurements (topographic surveys, soil dating, etc.) and other methods (e.g., geochemical fingerprinting) to understand how sediment is routed through the watershed. A simple conservation of mass equation can be used to define a sediment budget at the river reach or channel network scales, as shown in Equation 1.1.

$$I - O = \Delta S \quad (\text{Eq. 1.1})$$

where  $I$  represents sediment inputs,  $O$  represents sediment outputs, and  $\Delta S$  represents the change in sediment storage.

Accurate identification of sediment sinks and sources depends on the data available and methods used to analyze the data and account for uncertainty. Trimble (1999) presented a sediment budget for 140 years of agriculture in Coon Creek, Wisconsin, a 365 km<sup>2</sup> watershed, constrained from surveyed and monumented streams and valley cross sections. The budget, shown in Figure 1.2, was divided in three different periods (1853-1938, 1938-1975 and 1975-1993) and demonstrated that erosion was excessive in the first period, but decreased considerably in the subsequent two periods presumably due to improvements in agricultural land management. However, sediment storage within the watershed followed a similar pattern and thus, the efflux of sediment from the watershed remained relatively steady over time. This finding serves as an example of the important role that sediment storage plays within the watershed. Sediment yield measured at the mouth of a watershed cannot necessarily be an indicator of erosion within the watershed or the effectiveness of management practices (Trimble and Crosson, 2000).

### **1.3 Variables Influencing Channel Form**

Conceptually, geomorphologists consider sediment transport in terms of the relation between the amount and size of sediment being supplied to the channel relative to the slope and water discharge that make possible the movement of this sediment through the channel. A stream system that has just enough discharge and slope to transport its sediment supply is referred to as “graded”. This concept is illustrated by the Lane’s balance equation (see Figure 1.3).

$$Q_s D \sim Q S \quad (\text{Eq. 1.2})$$

where  $Q_s$  is the sediment supply,  $D$  is the sediment grain size,  $Q$  is the water discharge, and  $S$  is the channel slope.

A change in any of the factors involved in this equation could result in either aggradation or degradation of the channel (see Figure 1.2). Although this relation does not provide quantitative information about how these factors are related, it provides a useful estimate of the tendency of the channel to store or evacuate sediment (see Wilcock et al., 2009 for more detail).

#### **1.4 Channel Morphology**

Channel morphology is strongly related to the water and sediment fluxes within the channel. Montgomery and Buffington (1997) recognize three major types of channels based on bed material composition, including bedrock, colluvial and alluvial channels. Bedrock channels are usually depicted as valley-confined channels with steep slopes and a high sediment transport capacity relative to supply. Colluvial channels are generally headwater channels with sediment inputs from surrounding hillslopes and relatively shallow flows to move sediment. Alluvial channels are transport-limited channels, in that sediment supply is greater than transport capacity. Therefore, alluvial channels exhibit a large variety of morphologies depending on the different factors that control sediment dynamics (e.g., slope, discharge, sediment supply, location in the channel network, among other factors) (Hassan et al., 2005). Montgomery and Buffington (1997) also classified streams based on their reach scale longitudinal profile. They found that most common stream morphologies are cascade, step pool, plane bed, pool riffle, and dune

ripple. In planform, channels follow one of four well-defined patterns, which are meandering, braiding, straight, and anastomosing channels (Leopold and Wolman, 1957). Figure 1.4 shows the threshold at which the first three channel patterns start as a function of slope and discharge.

For the purposes of this chapter, only meandering channels are described in further detail. A meandering river is defined as a channel with a series of bends with alternate curvature. The bends in a meandering channel can move laterally or be translated downstream, reworking sediment stored in the floodplain in either process. This channel pattern coevolves as a function of associated flow and sediment fluxes (Bridge, 2003; Lauer and Parker, 2008).

Shear stress is the force exerted by the flowing water on the bed of the channel that moves bed sediment and therefore is responsible for shaping the channel (Wilcock et al., 2009). It is described by equation 1.3:

$$\tau = \rho g R S \quad (\text{Eq. 1.3.})$$

where  $\tau$  is the shear stress ( $\text{Pa} = \text{N}/\text{m}^2$ . Flow force acting per unit area of stream bed),  $\rho$  is the water density ( $\text{kg}/\text{m}^3$ ),  $R$  is the hydraulic radius (m), which is equal to channel cross-sectional area divided by wetted perimeter, and  $S$  is the bed slope. In channels where channel width is much greater than water depth,  $R$  is considered to be equal to water depth; therefore, the shear stress is sometimes referred to as the depth-slope product. This means that as depth and slope decrease, the ability of the channel to

transport sediment also decreases. Figure 1.5 illustrates how the cross section of a meandering river evolves.

## **1.5 Channel Planform**

Bank (in)stability is one of the main factors that control the mechanics of meandering rivers. A perturbation in an alluvial straight channel (e.g., deposition in one of the banks as shown in figure 1.5.b) can cause a change in the forces available to move sediment, which can subsequently make the channel meander and migrate (see Figure 1.5) (Leopold and Wolman, 1957; Lauer and Parker, 2008; Odgaard and Abad, 2008). On the other hand, laboratory flume experiments have shown that some level of bank stability is necessary to maintain a meandering pattern. Without a bank control, meandering rivers eventually develop into braided systems (Ikeda, 1989; Lewin and Brewer, 2001; Braudrick et al., 2009). Riparian vegetation provides bank strength and flow resistance, however, due to its complexity it has been difficult to establish a correlation between riparian vegetation and channel characteristics. In the last 2 decades, researchers have tried to link vegetation density and channel characteristics. For example, Gran and Paola (2001) used alfalfa sprouts to provide the bank resistance necessary to maintain a meandering river in their laboratory experiments finding that vegetation density contributed to reduced lateral channel adjustment.

### **1.5.1 Channel Migration**

Channel migration is the process in which the river moves laterally across its floodplain. This is an important mechanism in channel-floodplain formation and reworking. The mechanics of meandering channels described above cause erosion in the

outer bank of the channel and deposition in the inner bank of the channel. Therefore, the evolution of a meandering channel depends on a balance between destruction and construction of the floodplain (Wolman and Leopold, 1957; Leopold and Wolman, 1960; Wolman, 1977). This exchange of sediment between the channel and its floodplain can, but does not necessarily, result in a net contribution of sediment to the channel. The cross-sectional view in Fig. 1.5.d shows that the eroding bank is taller than the depositing bank; this is usually true for most meandering rivers (Leopold and Wolman, 1957). Lauer and Parker (2008) argued that this difference in elevation between channel banks together with extension of the outer bank and lateral migration is equal to the local, net contribution of sediment added to the channel. This can be computed using Equation 1.4:

$$E_{Local,net} = C * (H_{bf} + \Delta\eta) * \Delta S_o - C * H_{bf} * \Delta S_i \quad (Eq. 1.4)$$

where  $E_{Local, net}$  is the net volume of sediment added to the channel,  $C$  is the migration rate,  $H_{bf}$  is the bank full elevation,  $\Delta\eta$  is the difference in elevation between the outer and the inner banks,  $\Delta S_o$  is the length of the outer bank, and  $\Delta S_i$  is the length of the inner bank. For channels in equilibrium ( $\Delta s = 0$ ), this local, net contribution must be equaled by over bank deposition.

### 1.5.2 Channel Widening

Channel width is another important factor in the exchange of sediment between the channel and the floodplain. Channel width is one of the variables that control the hydraulic geometry of a river (other variables include depth, slope, sediment load, and

discharge). Alluvial channels can adjust their width by either widening or narrowing. Many studies have attempted to quantify the relationship between channel width and other hydraulic variables (e.g., Leopold and Maddock, 1953; Richards, 1976; Andrews, 1982; Parker et al., 2007). Assuming that rivers tend towards equilibrium, channel widening or narrowing will normally occur as a result of variations in any of the other factors that control hydraulic geometry.

Leopold and Maddock (1953) noted that in alluvial rivers changes in velocity, depth, and width take place as discharge increases at a particular cross section. They derived equations for these hydraulic geometry variables as a function of discharge. The resulting equation for width is expressed as:

$$W = aQ^b \qquad \text{Eq. 1.5.}$$

where  $W$  is width,  $Q$  is discharge and  $a$  and  $b$  are empirical parameters, which will vary for different rivers.

Parker et al. (2007) studied the hydraulic geometry of different sand and gravel-bed rivers around the globe and tried to develop universal relations between the factors involved in the hydraulic geometry of alluvial channels. They found clear trends of width, depth and slope in response to varying discharge over four and a half decades. However, they were only able to develop quasi-universal equations due to the effects of other factors that are difficult to account for, such as bank material properties (e.g., cohesion) or bank vegetation. Simon and Collison (2002) and Parker et al. (2011) studied the effects of bank failure and fine-grained sediment accumulation in bank toes, which

can serve as an armor for coarser non-cohesive material (gravel), reducing bank erosion rates as a result. Riparian vegetation may also constrain channel adjustment, limiting sediment transport by adding cohesion from roots and additional organic matter or increasing channel roughness (Labbe et al., 2011; Andrews, 1982). These studies highlight the importance of discharge in bank erosion, but also acknowledge the importance of other factors like bank resistance and sediment supply and the difficulty to account for such factors.

### **1.6 Floodplain Grain Size Composition**

Floodplains are recognized as important sinks for storing fine sediment in alluvial rivers (Wolman and Leopold, 1957; Howard, 1992; Howard, 1996; He and Walling, 1998; Taylor and Brewer, 2001; Knox, 2006; Lauer and Parker, 2008). The grain size composition of floodplains will vary in response to the sediment dynamics of the area (transport, deposition and remobilization) (He and Walling, 1998). Thus, an understanding of the grain size composition of floodplains is needed in order to account for the type of sediment lost from the channel during floodplain or bank deposition, as well as contributed to the channel from bank erosion. Floodplains are formed by lateral and vertical accretion (Wolman and Leopold, 1957). Point bar and overbank deposition are the mechanisms that cause lateral and vertical accretion, respectively. Point bars form typically in the inner bank of meandering rivers; in an equilibrium system, the amount of sediment eroded in the outer bank of a river cross section is roughly equal to the amount of sediment deposited in the opposite bank and floodplain (see Figure 1.5). Overbank deposition happens when flows overtop the floodplain and deposit suspended

sediment on the floodplain due to a loss of transport capacity (e.g., reduced depth, increased roughness). A general pattern of decreasing particle size as one moves away from the channel margins has been demonstrated by some studies (Pizzuto, 1987; He and Walling, 1998). However, due to the non-uniformity present in the processes of floodplain sedimentation, a detailed calculation of grain size parameters would not be out of order to understand the complexity of floodplain stratigraphy in a specific alluvial system (Taylor and Brewer, 2001).

### **1.7 Research Context**

The Root River is currently impaired for turbidity in 15 different reaches ([http://cf.pca.state.mn.us/water/watershedweb/wdip/resultsList\\_impairments.cfm?huc=07040008](http://cf.pca.state.mn.us/water/watershedweb/wdip/resultsList_impairments.cfm?huc=07040008)). Geomorphic analysis in the Root River indicates that many reaches have easily accessible near-channel sources of sediment and that channel-floodplain sediment interactions exert strong control on the flux of sediment in this river system (Stout et al., 2013). Similar to what has been observed in Coon Creek (Trimble, 1999), the primary sediment sources in the Root River appear to have shifted from upland agricultural fields to near-channel sources due to a combination of improved agricultural management practices and recent increases in high flows.

This thesis seeks to quantify the amount of sediment being added to the channel due to channel migration and widening and estimate how much of this sediment is carried by the river as wash load (sediment finer than  $67\mu\text{m}$ ). In a broad sense, this project aims to increase our understanding of near-channel sediment dynamics and document how a meandering river adjusts its planform morphology due to changes in flow and sediment

supply. In a more specific sense, this project provides constraints on the proportion of suspended sediment in the Root River that is derived from near-channel sources. This information will be used by collaborators in combination with sediment fingerprinting, sediment gaging, and other datasets to create an overall sediment budget for the Root River watershed.

In order to complete the main goal of this project, estimation of migration rates, channel widening, floodplain grain size composition and bulk density are necessary. This gives rise to the questions and specific objectives described below.

### **1.7.1 Research Questions**

1. How rapid are the migration rates in the Root River channel network? How do these rates vary spatially throughout the channel network? Have rates systematically increased or decreased in the last few decades? Does channel migration result in a net contribution of sediment to the channel?
2. Is the Root River channel systematically widening or narrowing over the past 70 years? If so, do widening/narrowing rates vary spatially throughout the channel network and what are the implications for the sediment mass balance?
3. How do grain size distributions vary spatially in the floodplains and fluvial terraces throughout the Root River watershed? What percent of the total sediment mass is transported by the river as wash load?

### **1.7.2 Objectives**

1. Measure channel migration rates and average width using multiple epochs of historical aerial photographs from 1939 to 2010.

2. Measure grain size distributions in key locations and extrapolate to entire channel-floodplain complex.
3. Compute mass of sediment exchanged between the channel and floodplain over recent decades and space scales (Root River and main tributaries).

### **1.8 Study Area**

The Root River Watershed is located in southeastern Minnesota, USA, and covers an area of ~4300 km<sup>2</sup>. Most of the watershed is within Minnesota, including the counties of Fillmore, Houston, Mower, Winona, Olmsted, and Dodge. Less than 1 % of the total area of the watershed is within Winneshiek, Iowa (see Figure 1.6). About two-thirds of the Root River drainage area is within a geologic region known as the Driftless Area, which refers to an area that was not covered by ice during the last glaciation (Hobbs, 1999) including parts of southeastern Minnesota, northwestern Iowa, southwestern Wisconsin, and northwestern Illinois. The Driftless Area is characterized by deep river valleys incised into Paleozoic bedrock, primarily composed of carbonates (Syverson and Colgan, 2004). The characteristic relief of the Driftless Area can be appreciated in Figure 1.7. River valleys in the Driftless Area were eroded as a result of incision of the Mississippi River prior to the most recent glaciation (Baker et al., 1998).

The Root River watershed is dominated by karst topography, which is characterized by underground caves, sinkholes, and springs. Karst in the Root River is mainly composed of limestone and dolostone (Witthuhn and Alexander, 1995). Underground caverns that characterize karst hydrogeology may provide paths that accelerate the flow of infiltrated water from the uplands to the channel (Ford and

Williams, 2007). Many studies mapped karst features in the study area (Witthuhn and Alexander, 1995). Gao et al. (2002) compiled existing county karst datasets in a single GIS database, which facilitates visual and statistical analysis of the data (Figure 1.8).

Changes in flow magnitude can lead to channel widening or accelerate migration rates through increased bank erosion (Leopold and Wolman, 1957; Parker et al., 2007; Leon et al., 2009). High and low flows in the main stem of the Root River have increased 60 % and 80 %, respectively since 1990 (Figure 1.9). There are different hypotheses regarding what may have caused the increase in flows in the Root River. Changes in land use, precipitation and increased flows through karst topography as explained above are plausible hypotheses (Stout et al., 2013). Average annual precipitation in the Root River watershed from 1981 to 2011 is ~863 mm; from 1990 to 2011 it ranged from 560 to 1220 mm ([http://climate.umn.edu/doc/annual\\_pre\\_maps.htm](http://climate.umn.edu/doc/annual_pre_maps.htm)). A more thorough precipitation analysis is necessary to calculate variability in annual precipitation and quantify the effects of precipitation in the hydrology of the watershed. The Root River experienced its flood of record in 2007, reaching a peak flow of 1,303 cms (46,000 cfs) ([http://nwis.waterdata.usgs.gov/usa/nwis/peak/?site\\_no=05385000](http://nwis.waterdata.usgs.gov/usa/nwis/peak/?site_no=05385000)). Based on the principle that channel width is strongly influenced by discharge, this flood was expected to have widened the channel.

The current landscape we observe in the Root River watershed is a combination of the setting and the land-use changes that have taken place in the watershed throughout its history. Prior to Euro-American settlement nearly the entire watershed was dominated by upland prairie and oak plant communities (Dogwiler, 2010). However, since early

settlement in the 1850's the land has been cleared for wheat production (Troelstrup and Perry, 1989).

The impacts of agriculture in the early 1900's are described in the first reconnaissance of the Root River by Thadeus Suber (1924). He described incision in the tributaries of the river and a recent increase in the magnitude of floods. More recently, Knox (2006) described how the development of Euro-American agriculture produced major negative impacts on runoff, soil erosion, and river morphology in the region (accelerated channel migration rates and floodplain vertical accretion).

Changes in agricultural management did not begin until the 1940's. These changes have reduced erosion from agricultural fields (Trimble, 1999; Knox, 2006). Based on this, Stout (2012) hypothesized that the Root River had been storing the eroded sediment from uplands in its floodplains and terraces and with the recent reductions of upland sediment the river may now be reworking the sediment stored in its floodplains. This is the same principle demonstrated by Trimble (1999) in Coon Creek, which is immediately across the Mississippi River from the Root River watershed.

Stout (2012) found that the Root River has a complicated erosional history with sediment sources varying throughout the watershed. Stout's main methods were the use of sediment fingerprinting to trace sediment sources in the Root River and the development of a tool to identify possible near-channel sediment sources. He found that channel-floodplain sediment exchange exerts a strong control in the sediment fluxes of the Root River. He also identified many near-channel sources of sediment that may be contributing a large amount of sediment at the present time. The sediment sources of the Root River, which are a combination of both upland and near-channel sources, could be

shifting from one source to the other (as the case of Coon Creek). Therefore, it is necessary to estimate how much sediment is being contributed to the channel from these near-channel sources as another step to prove this hypothesis.

## 1.9 Methods

Geomorphology is continually advancing with the development of new technologies. For example, the increasing availability of airborne lidar topographic data for large areas is revolutionizing the way geomorphologists address many key questions, mainly because the morphology of the Earth's surface can now be recorded at a resolution sufficient to satisfy most information demands for developing mechanistic explanations (Church, 2010). On the other hand, aerial photographs have been around for a longer time, enabling analysis of historical planform evolution of river systems (Slaymaker, 2001; Vericat et al., 2008).

In the case of the Root River, 3 m resolution lidar data is available for the entire watershed. The data were collected in November 2008 by the Minnesota Department of Natural Resources (MnDNR). The main purpose of this data was to provide high accuracy data for the National Flood Insurance Program after the 2007 floods. The data have a vertical positional accuracy of 0.287 m and a nominal point spacing of 1 m.

Complete metadata is available at:

[www.mngeo.state.mn.us/chouse/metadata/lidar\\_semn2008.html#Data\\_Quality\\_Information](http://www.mngeo.state.mn.us/chouse/metadata/lidar_semn2008.html#Data_Quality_Information).

Aerial photographs covering the study area have been collected since the late 1930's by federal (USGS, FSA), state (MnDNR, MnDOT) and private companies. The

most recent photographs (1990's-present) are natural color images with a ground sample distance of 1 m and are rectified to  $\pm 5$  m from 3.75' \* 3.75' quarter quadrangles with an over edge buffer that ranges between 50 and 300 m for all four sides. Older aerial photographs (1930's to 1970's) were georeferenced by collaborators at Winona State University. The photographs have been scanned by the MnDNR as gray-scale images at a resolution that varies from 600 to 1200 dpi and covers  $\sim 26$  km<sup>2</sup>. Most of this data is available at <http://www.mngeo.state.mn.us/chouse/airphoto/index.html>.

Stout and Belmont (2014) developed a terrace extraction tool and applied it to the Root River watershed. This tool uses a digital elevation model as its main input and extracts fluvial terrace and floodplain features based on local relief, a specific area and a distance from the channel centerline specified by the user. Stout used this tool to identify possible near-channel sources of sediment in the Root River.

Stout et al. (2013) measured the ratio of sediment smaller versus larger than 250  $\mu\text{m}$  and plotted it against terrace height and found that younger floodplains contain finer grain size distributions relative to older terrace surfaces. Further, there appears to be a fining of grain size distributions as one goes from the older terraces far from the channel to the newer floodplains closer to the channel. This provided useful insight about the fine sediment stored in the floodplains near the channel, but a more detailed grain size distribution survey is needed to determine how grain size distributions vary in order to quantify what proportion of sediment contributed to the channel is transported as wash load and therefore contributes to turbidity in the water column.

A combination of lidar and aerial photographs, together with field surveys and grain size analysis of sediment samples will be used to answer the proposed research

questions (Figure 1.10). Channel width and meander migration rates will be measured using multiple epochs of aerial photographs from 1939 to 2010, ArcMap 10 and the Channel Planform Statistics Toolbox (available online at <http://www.nced.umn.edu/content/stream-restoration-toolbox>).

For each aerial photo, both banks are manually digitized from the aerial photographs. Vegetation will be used as an indicator of bank full width to digitize the banks (Millar, 2000; Bridge, 2003). The main stem of the Root River has been divided into 10 reaches based on meander degree (big, medium and small). Tributaries reaches were divided following the same criteria.

### **1.9.1 Channel Migration Rate**

The Channel Planform Statistics Toolbox in conjunction with ArcMAP will be used to calculate channel migration and extract bank heights throughout the river network. The toolbox consists of 3 tools: the centerline interpolation tool, the migration tool, and the bank buffer tool. Figure 1.11 shows a scheme of the sequence of each tool and the inputs and outputs related to them. To begin analysis with the tool, the user must digitize channel banks, primarily based on the vegetation line on both sides of the channel. The centerline interpolation tool then creates a channel centerline from the digitized bank lines at a node spacing specified by the user (typically 25 m). The result is a new polyline that defines the center of the channel. The migration tool yields migration rates from centerlines from two different years by calculating the average normal distance between the nodes of the two centerlines. Migration rate results are stored in polygon shapefiles created by the tool (see Figure 1.12). The bank buffer tool creates polygons of

user-specified width along the outside of each digitized bank line. The difference in opposing bank elevations ( $\Delta\eta$  in Equation 1.4) is then extracted from the 2008 lidar using these polygons. Once these values are obtained (length, migration rate and bank height), the net sediment contribution can be computed using Equation 1.4.

### 1.9.2 Channel Width

The method used to determine average channel width for each photograph consisted of three main steps described as:

1. Conversion of previously hand digitized bank lines to polygons. This was done using the trace tool of the editor toolbox in ArcMap10. The area of the channel polygon was then calculated using the geometry calculator of ArcMAP 10.
2. Reach average channel width was calculated as:

$$w_{\text{mean}} = \text{Polygon Area/Polygon Length}$$

3. Percent change within a specific period of time was then calculated from the results of each photograph analysis as:

$$\% \text{ Change} = ((w_2/w_1) - 1) \times 100$$

where  $w_2$  is closer to present time than  $w_1$ .

### **1.9.3 Grain size distribution campaign**

Sediment grain size distributions for the selected floodplains were measured from samples to be collected in summer 2013. Selection of sample locations will be based on floodplain characteristics, including height above the channel, migration rate of the channel, vegetation cover, and accessibility. The samples will be weighted and analyzed for grain size using a Sequoia Scientific LISST-Portable particle size analyzer, which measures the grain size distribution and volume concentration of a sample suspended in a liquid (deionized water) using a laser diffraction method (Sequoia, 2011).

The total sediment mass contributed to the channel from the floodplain due to lateral adjustment was computed from the volumes obtained from channel migration and widening and the sediment bulk density obtained from field samples ( $\text{Mass} = \text{Density} * \text{volume}$ ). The percent of this mass composed by fine sediment will be estimated from the grain size distributions by multiplying the volumes by the percent of sediment finer than 67  $\mu\text{m}$ .

### **1.9.4 Python Scripts and Result Figures**

Python code was developed to create plots of migration rates, width, and delta eta values versus downstream distance and to facilitate analysis in general. The scripts, attached in the appendix section, use many different modules. ArcMAP10 tools were used through the Arcpy module. The main Arcpy functions used include the use of cursors in order to access vector data tables and ArcMAP tools in order to create new vector and raster data. The os (operating system) and numpy modules of python were used to organize and perform mathematical calculations with the data. Finally, the pyplot

and pylab modules of the Matplotlib library, a python 2D plotting library which produces publication quality figures, were used to generate the figures presented in the results sections (The matplotlib library is available for free at <http://matplotlib.org/>).

## 1.10 References

- Andrews, E.D., 1982. Bank stability and channel width adjustment, East Fork River, Wyoming, *Water Resour. Res.* 18 (4): 1184-1192.
- Bainbridge, Z.T., Wolanski, E., Álvarez-Romero, J.G., Lewis, S.E., Brodie, J.E., 2012. Fine sediment and nutrient dynamics related to particle size and floc formation in a Burdekin River flood plume, Australia. *Marine Pollution Bull.* 65(4-9): 236-248.
- Baker, R.W., Knox, J.C., Lively, R.S., Olsen, B.M., 1998. Evidence for early entrenchment of the upper Mississippi River valley. Patterson, C.J. & Wright, H.E., Jr. (Eds.) *Contributions to Quaternary studies in Minnesota. Minnesota Geol. Survey Report of Investigations.* 49: 113-120.
- Belmont, P., Gran, K.B., Schottler, S.P., Wilcock, P.R., Day, S.S., Jennings, C., Lauer, J.W., Viparelli, E., Willenbring, J.K., Engstrom, D.R., Parker, G., 2011. Large Shift in Source of Fine Sediment in the Upper Mississippi River. *Environ. Sci. & Technol.* 45 (20): 8804-8810.
- Braudrick, C.A., Dietrich, W.T., Leverich, G.T., Sklarb, L.S., 2009. Experimental evidence for the conditions necessary to sustain meandering in coarse-bedded rivers. *Proceedings of the National Academy of Sciences USA.* 106 (40): 16936-16941.
- Bridge, J.S., 2003. *Rivers and Floodplains: Forms, Processes, and Sedimentary Record.* Blackwell Sci. Ltd., Oxford.
- Church, M., 2010. The trajectory of geomorphology. *Progress in Physical Geography.* 34(3): 265-286.
- Collins, A.L., Naden, P.S., Sear, D.A., Jones, J.I., Foster, I.D.L., Morrow, K., 2011. Sediment targets for informing river catchment management: international experience and prospects. *Hydrol Processes.* 25: 2112-2129.
- Davies, T.R.H., Korup, O., 2010. *Sediment Cascades in Active Landscapes, Sediment Cascades.* John Wiley & Sons, Ltd. Chichester, UK.
- Dietrich, W.E., Dunne, T., 1978. Sediment budget for a small catchment in mountainous terrain. *Zeitschrift für Geomorphologie.* 29: 191-206.

- Dogwiler, T., Wicks, C.M., 2004. Sediment entrainment and transport in fluvio karst systems. *J. of Hydrol.* 295 (1-4): 163-172.
- Dogwiler, T., 2010. Rush-Pine Creek Watershed Preliminary Assessment and Scoping Plan, Southeastern Minnesota Water Resour. Center, Winona State University, Winona, MN.
- Ford D.C and Williams P.W., 2007. Karst hydrogeology and geomorphology. Wiley, Chichester. pp. 562.
- Gao, Y., Alexander, E.C. Jr., Tipping, R.G., 2002. The development of a karst feature database for southeastern Minnesota. *J. of Cave and Karst Studies* 64 (1): 51-57.
- Gran, K., Paola, C., 2001. Riparian vegetation controls on braided stream dynamics. *Water Resour. Res.* 37(12): 3275-3283.
- Hadley, R.F. and Schumm, S.A., 1961. Sediment sources and drainage-basin characteristics in upper Cheyenne River basin. USGS Water Supply Paper: 1531-B.
- Hassan, M.A., Church, M., Lisle, T.E., Brardinoni, F., Benda, L., and Grant, G. E., 2005. Sediment transport and channel morphology of small, forested streams. *Jawra J. of the American Water Resour. Association.* 41: 85-876.
- Hauer, C., Unfer, G., Tritthart, M. and Habersack, H., 2011. Effects of stream channel morphology, transport processes and effective discharge on salmonid spawning habitats. *Earth Surface Processes.* 36: 672-685.
- He, Q. and Walling, D.E., 1998. An investigation of the spatial variability of the grain size composition of floodplain sediments. *Hydrol Processes.* 12: 1079-1094.
- Hobbs, H., 1999. Origin of the Driftless Area by subglacial drainage - a new hypothesis. In: Mickelson, D.M., Attig, J.W. *Glacial Processes Past and Present.* Geol. Soc. Am. 337: 93-102.
- Howard, A. D., 1992. Modelling channel migration and floodplain sedimentation in meandering streams. *Lowland Floodplain Rivers: Geomorphological Perspectives.* P. Carling and G. Petts. Chichester. John Wiley and Sons. pp. 1-41.
- Howard, A. D., 1996. Modelling channel evolution and floodplain morphology. M. A. Anderson, D. E. Walling, and P. D. Bates. *Floodplain Processes.* Chichester. John Wiley & Sons. pp. 15-62.
- Ikeda, H., 1989. Sedimentary controls on channel migration and origin of point bars in sand-bedded meandering rivers. Ikeda, S., Parker, G. Ž. *River Meandering.* American Geophys. Union, Water Research Monograph. 12: 51-68.
- Knox, J.C., 2006. Floodplain sedimentation in the Upper Mississippi Valley: Natural versus human accelerated. *Geomorphology,* 79 (3-4): 286-310.

- Labbe J.M., Hadley, K.S., Schipper, A.M., Leuven, R.S., Gardiner, C.P., 2011. Influence of bank materials, bed sediment, and riparian vegetation on channel form along a gravel-to-sand transition reach of the Upper Tualatin River, Oregon, USA. *Geomorphology*. 125 (3): 374-382.
- Lauer, J.W., Parker, G., 2008. Net local removal of floodplain sediment by river meander migration. *Geomorphology*, 96 (1-2): 123-149.
- Leon, C., Julien, P.Y., Baird D.C., 2009. Case Study: Equivalent Widths of the Middle Rio Grande, New Mexico. *J. of Hydraulic Engineering*. 135 (4): 306-315.
- Leopold, L.B., Maddock, T.J., 1953. The hydraulic geometry of stream channels and some physiographic implications. USGS Professional Paper, 252, 57 pp.
- Leopold, L.B., Wolman, M.G., 1957. River Channel Patterns: Braided, Meandering and Straight. USGS Professional Paper 282-B: 39-103.
- Leopold, L.B., and Wolman, M.G., 1960. River meanders: *Geol. Soc. Am.* 71: 769-794.
- Lewin, J., Brewer, P.A., 2001. Predicting channel patterns. *Geomorphology*. 40 (3-4): 329-339.
- Millar, R.G., 2000. Influence of bank vegetation on alluvial channel patterns. *Water Resour. Res.* 36 (4): 1109-1118.
- Montgomery, D.R. and Buffington J.M., 1997. Channel-reach morphology in mountain drainage basins. *Geol. Soc. Am.* 109 (5): 596-611.
- Naden, P.S., 2010. The Fine-Sediment Cascade, Sediment Cascades. In: Burt, T., Allison, R. (Eds.), *Sediment Cascades: An Integrated Approach*. John Wiley & Sons, Ltd. Centre for Ecology and Hydrology, UK, pp. 271-305.
- Narinesingh, P., Klaassen, G.J., and Ludikhuizen, D., 1999. Floodplain sedimentation along extended river reaches. *J. of Hydraulic Research*, 37 (6): 827-845.
- Odgaard, A.J., Abad, J.D., 2008. River meandering and channel stability. *ASCE Manual of Practice 110: Sedimentation Engineering*, M.H. Garcia. Reston, VA, pp. 439-459.
- Owens, P.N., Batalla, r. j., Collins, A.J., a. j., Gomez, B., Hicks, D.M., Horowitz, A.J., Kondolf, G.M., Marden, M., Page, M.J., Peacock, D.H., Petticrew, E.L., Salomonsk, W., and Trustruml, N.A., 2005. Fine-grained sediment in river systems: environmental significance and management issues. *River Research and Applications*. 21: 693-717.
- Parker, G., Wilcock, P.R., Paola, C., Dietrich, W.E., and Pitlick, J. 2007. Physical basis for quasi-universal relations describing bankfull hydraulic geometry of single-thread gravel bed rivers. *J. of Geophys. res.* 112, F04005.

- Parker, G., Shimizu, Y., Wilkerson, G.V., Eke, E.C., Abad, J.D., Lauer, J.W., Paola, C., Dietrich, W.E. and Voller, V.R., 2011. A new framework for modeling the migration of meandering rivers. *Earth Surface Processes and Landforms*. 36: 70-86.
- Pizzuto, J.E., 1987. Sediment diffusion during overbank flows. *Sedimentology*. 34: 301-317.
- Richards, K.S., 1976. Channel width and the riffle-pool sequence. *Geol. Soc. Am. Bull.* 87 (6): 883-890.
- Sequoia, 2011. LISST-Portable User's Guide Version 3.11. S.S. Inc.
- Simon, A. and Collison, A.J.C., 2002. Quantifying the mechanical and hydrologic effects of riparian vegetation on streambank stability. *Earth surface processes and Landforms*. 27: 527-546.
- Skalak, K. and Pizzuto, J., 2010. The distribution and residence time of suspended sediment stored within the channel margins of a gravel-bed bedrock river. *Earth Surface Processes and Landforms*, 35: 435-446.
- Slymaker, O., 2001. The role of remote sensing in geomorphology and terrain analysis in the Canadian Cordillera. *International J. of Applied Earth Observation and Geoinformation*. 3 (1): 11-17.
- Smith, S.M.C., Belmont, P., Wilcock, P.R., 2011. Closing the gap between watershed modeling, sediment budgeting, and stream restoration. *Stream restoration in dynamic fluvial systems: scientific approaches, analyses, and tools*. AGU, washington, dc. 194: 293-317.
- Stout, J.C., 2012. Identifying and quantifying sediment sources and sinks in the Root River, Southeastern Minnesota. All Graduate Theses and Dissertations. Paper 1304.
- Stout, J.C., Belmont, P., Schottler, S.P., Willenbring, J.K., 2013. Identifying Sediment Sources and Sinks in the Root River, Southeastern Minnesota. *Annals of the assoc. Am. Geographers*. 104(1): 20-39
- Stout, J.C., Belmont, P., 2014. TerEx Toolbox for semi-automated selection of fluvial terrace and floodplain features from lidar. *Earth Surf. Process. Landforms*. 39: 569-580.
- Surber, T., 1924. A biological reconnaissance of the Root River drainage basin southeastern Minnesota: Minnesota State Game and Fish Department.
- Syverson, K.M., Colgan, P.M., 2004. The Quaternary of Wisconsin: A review of stratigraphy and glaciation history. J. Ehlers, P.L. Gibbard. *Developments in Quaternary Sciences*. Elsevier, pp. 295-311.

- Taylor, M.P. and Brewer, P.A., 2001. A study of Holocene floodplain particle size characteristics with special reference to palaeochannel infills from the upper Severn basin, Wales, UK. *Geol. J.* 36: 143-157.
- Trimble, S.W., 1999. Decreased Rates of Alluvial Sediment Storage in the Coon Creek Basin, Wisconsin, 1975-93. *Sci.* 285 (5431): 1244-1246.
- Trimble, S.W., Crosson, P., 2000. U.S. Soil Erosion Rates: Myth and Reality. *Sci.* 289(No. 5477), 248-250.
- Troelstrup Jr., N.H. and Perry, J.A., 1989. Water quality in southeastern Minnesota streams: Observations along a gradient of land-use and geology. *J. of the Minnesota Academy of Sci.* 55: 6-13.
- Vericat, D., Brasington, J., Wheaton, J.M. and Cowie, M., 2008. Accuracy Assessment of Aerial Photographs Acquired using Lighter-Than-Air Blimps: Low-Cost Tools for Monitoring Fluvial Systems. *River Research and Applications*.
- Walling, D.E. 1983. The sediment delivery problem. *J. of Hydrol.* 65:209-237.
- Walling, D.E., Collins, A.L., 2008. The catchment sediment budget as a management tool. *Environ. Sci. & Policy.* 11 (2): 136-143.
- Walling, D.E., Collins, A.L., Jones, P.A., Leeks, G.J.L., Old, G., 2006. Establishing fine-grained sediment budgets for the Pang and Lambourn LOCAR catchments, UK. *J. of Hydrol.* 330: 126-141.
- Wilcock, P., Pitlick, J., Cui, Y., 2009. Sediment transport primer: Estimating bed-material transport in gravel-bed rivers. General Technical Report. RMRS-GTR-226. Fort Collins, CO: U.S. Department of Agriculture, Forest Service, Rocky Mountain Research Station. pp. 78.
- Witthuhn, K., and Alexander, E. Jr., 1995. Sinkholes and Sinkhole Probability. County Atlas Series Atlas C-8, Part B. Minnesota Department of Natural Resour.
- Wolman, M.G. and Leopold, L.B., 1957. River flood plains: some observations on their formation. Washington, DC: USDA Geol. Survey. 282-C: 86-109.
- Wolman, M.G., 1977. Changing needs and opportunities in the sediment field. *Water Resour. Res.* 13 (1): 50-54.

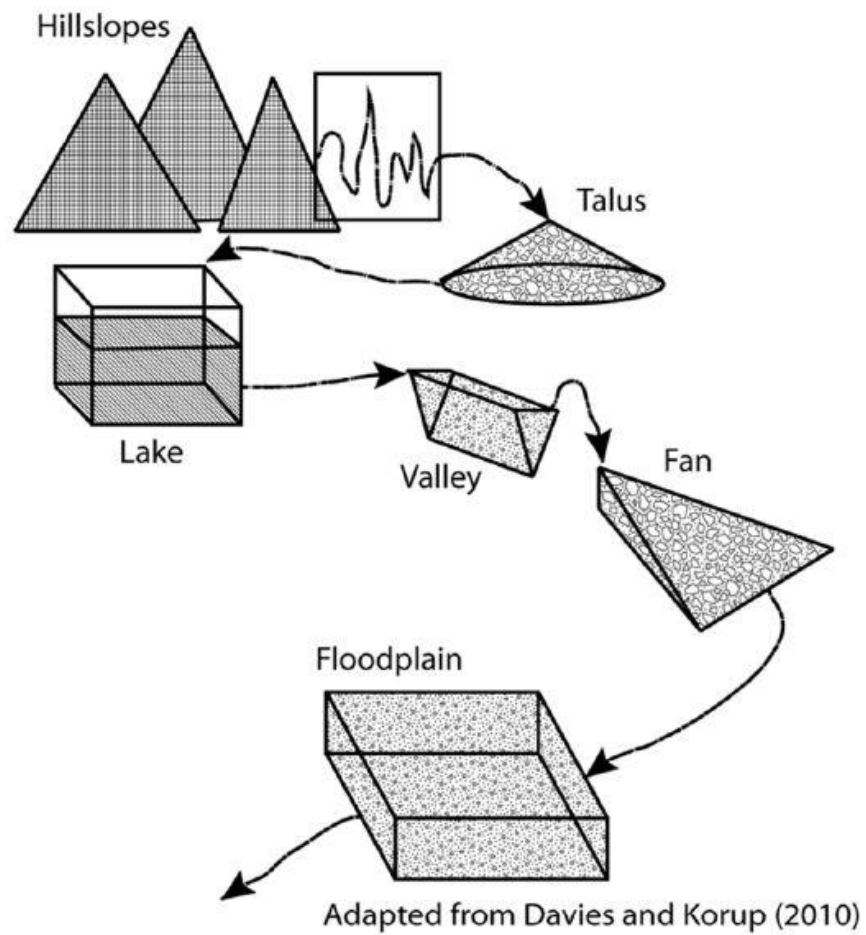


Figure 1.1. Sediment cascades transport sequence. A generic depiction of a sediment cascades, involving multiple landforms where sediment is temporarily stored. Original from Davies and Korup, 2010.

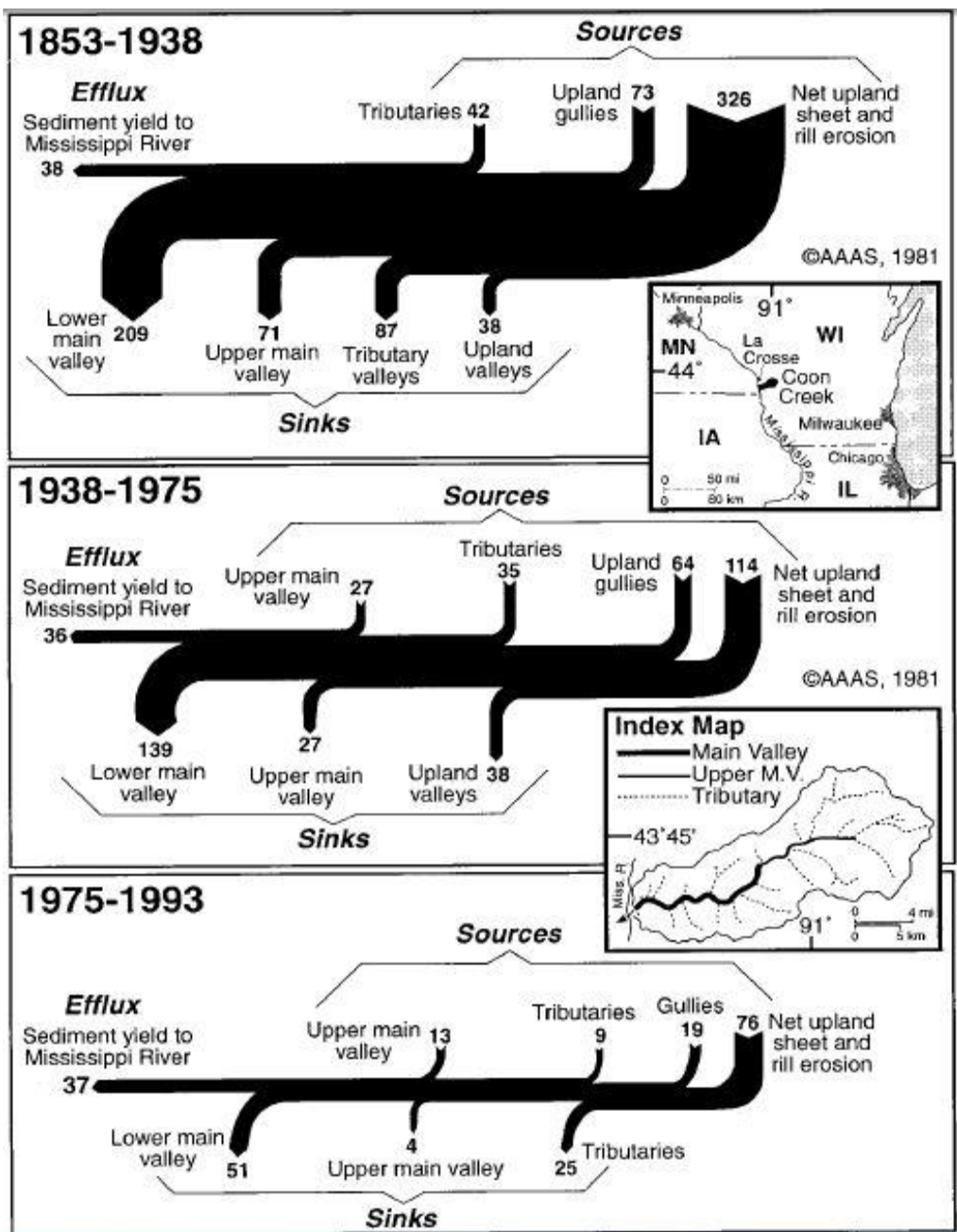


Figure 1.2. Sediment budget, Coon Creek. From Trimble, 1999.

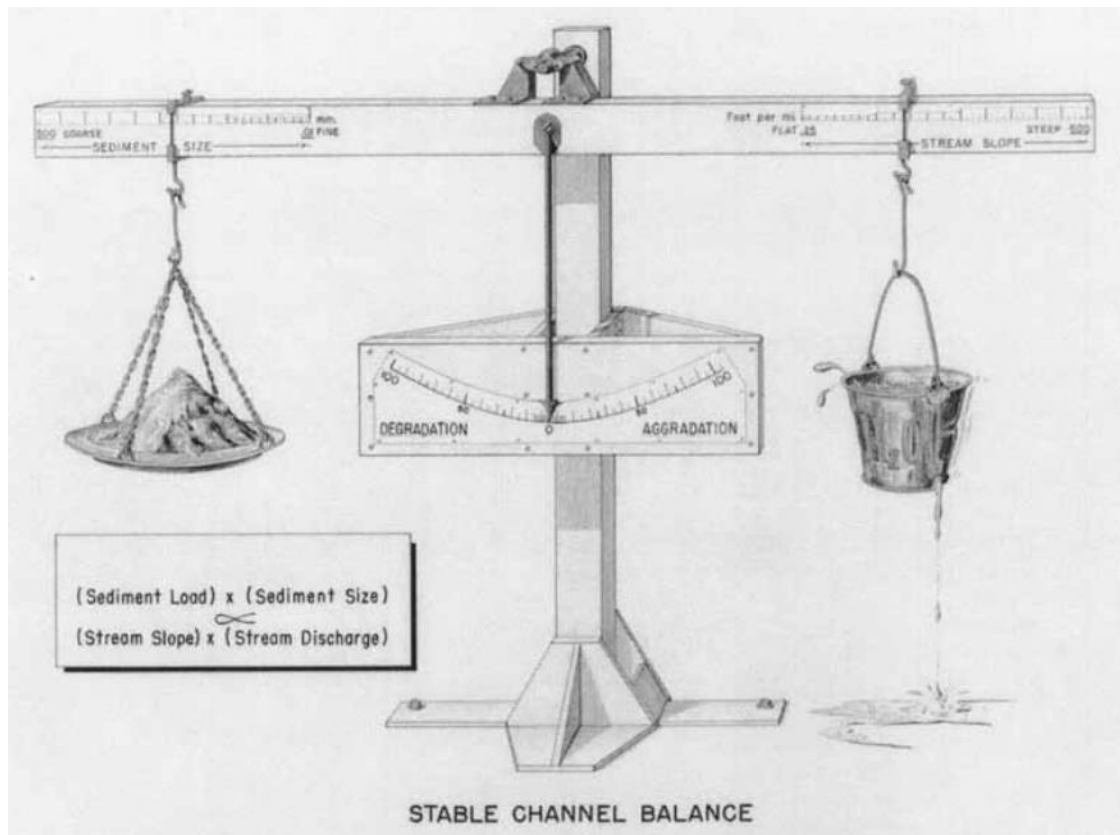


Figure 1.3. Lane's balance showing channel stability, presented first in Borland, 1960 (cited in Wilcock et al., 2009).

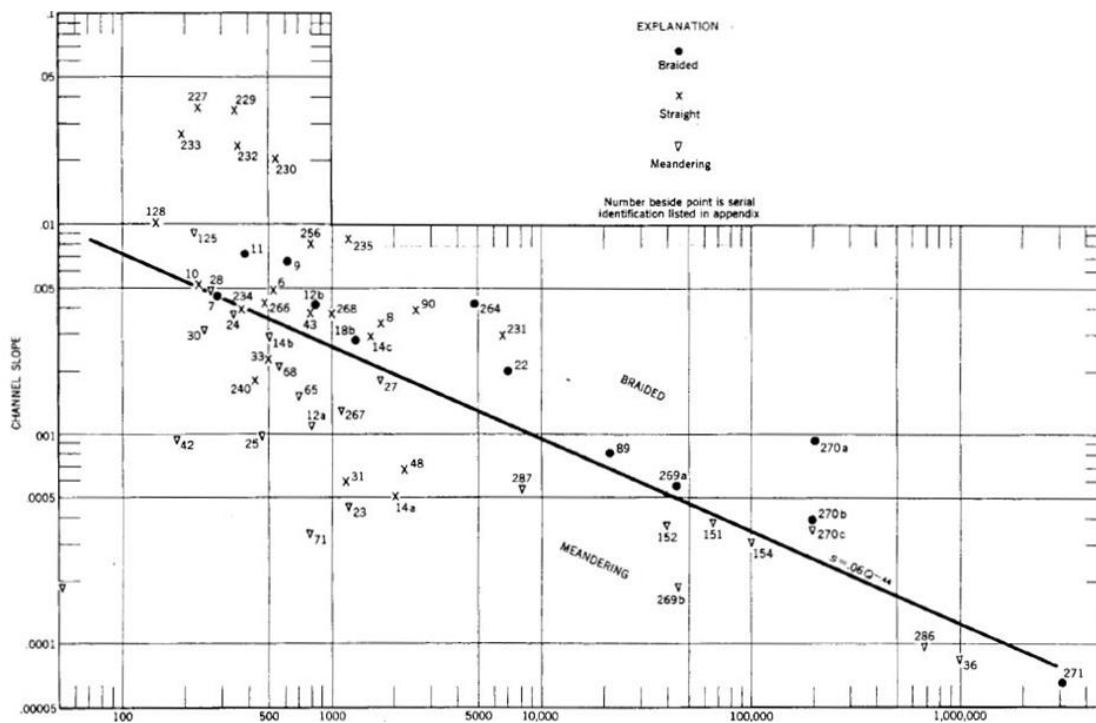


Figure 1.4. Threshold between meandering and braided channels. From Leopold and Wolman , 1957.

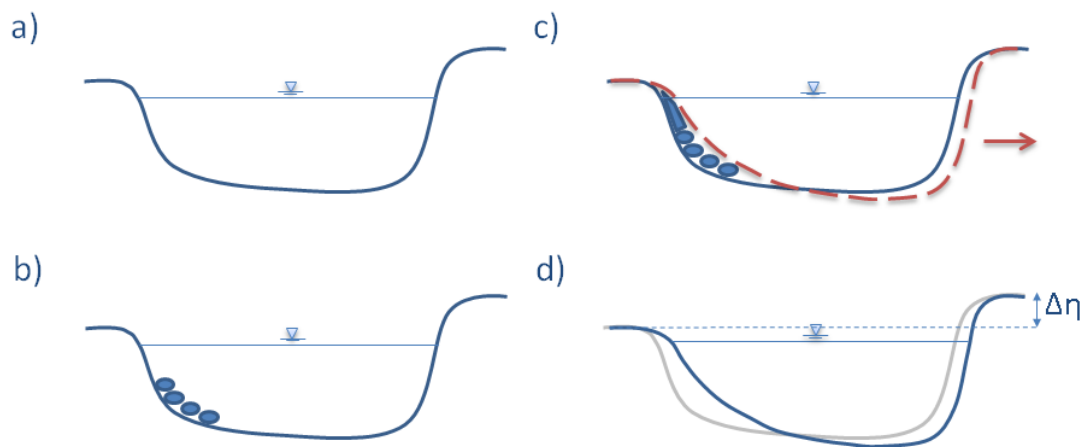


Figure 1.5. Cross section evolution of a meandering river. a) Initial condition, b) deposition of sediment in one of the bank sides, c) erosion response to deposition in opposing bank, d) new cross section. The red arrow in (c) shows the direction in which the channel migrates; red dashed line represents the new cross section.  $\Delta\eta$  in (d) is the difference in bank height; the gray line represents the old cross section.

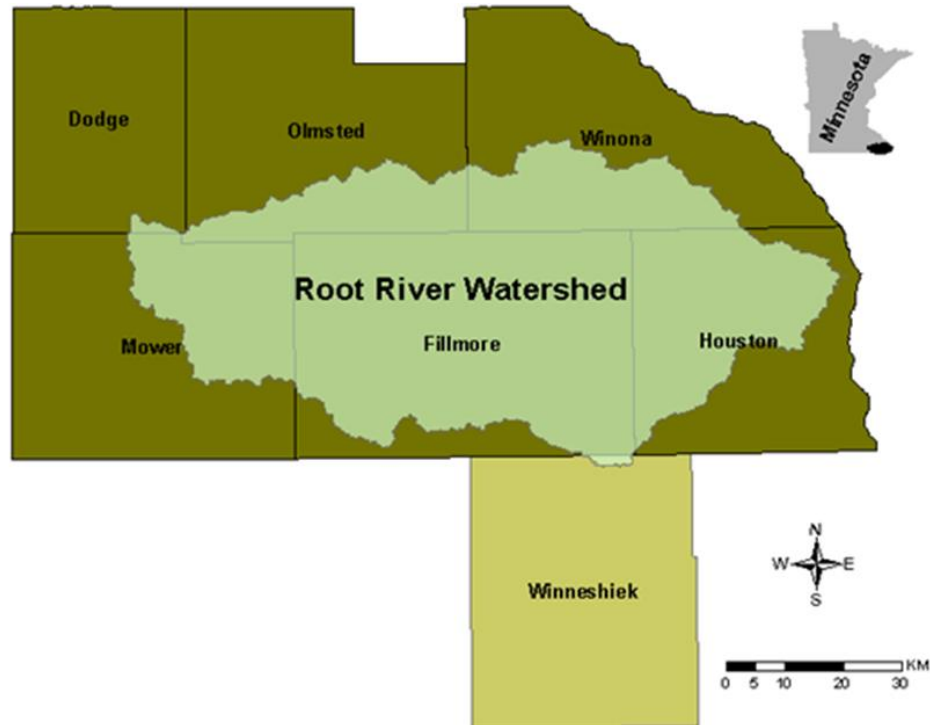


Figure 1.6. Root River Watershed location within Minnesota. Counties that contain the Root River watershed.

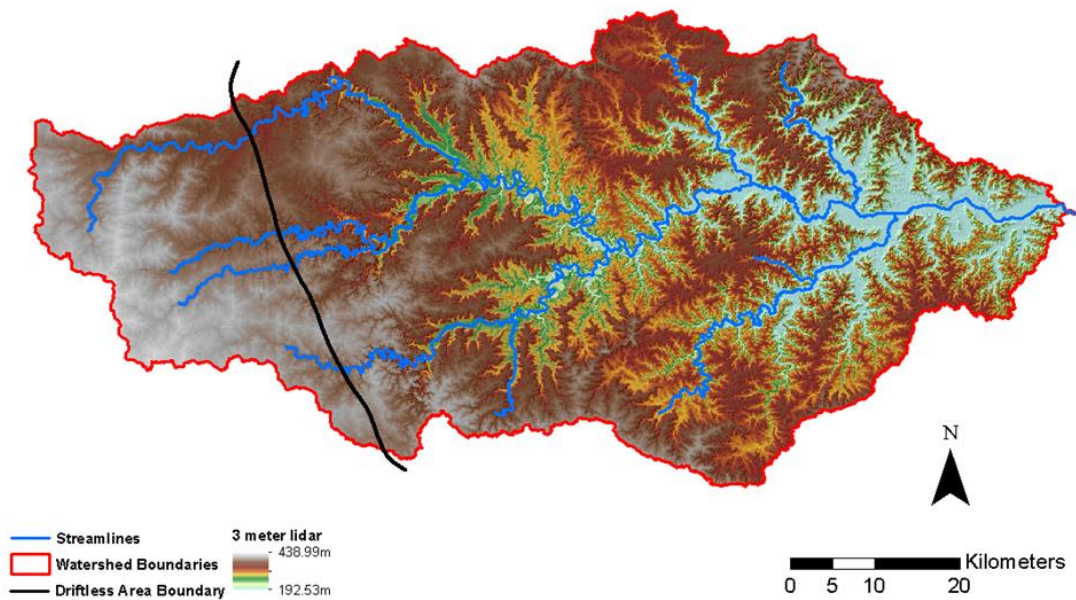


Figure 1.7. Root River watershed showing channel network, lidar topography and boundary between glaciated terrain and the Driftless Area (to the left and right of black line, respectively).

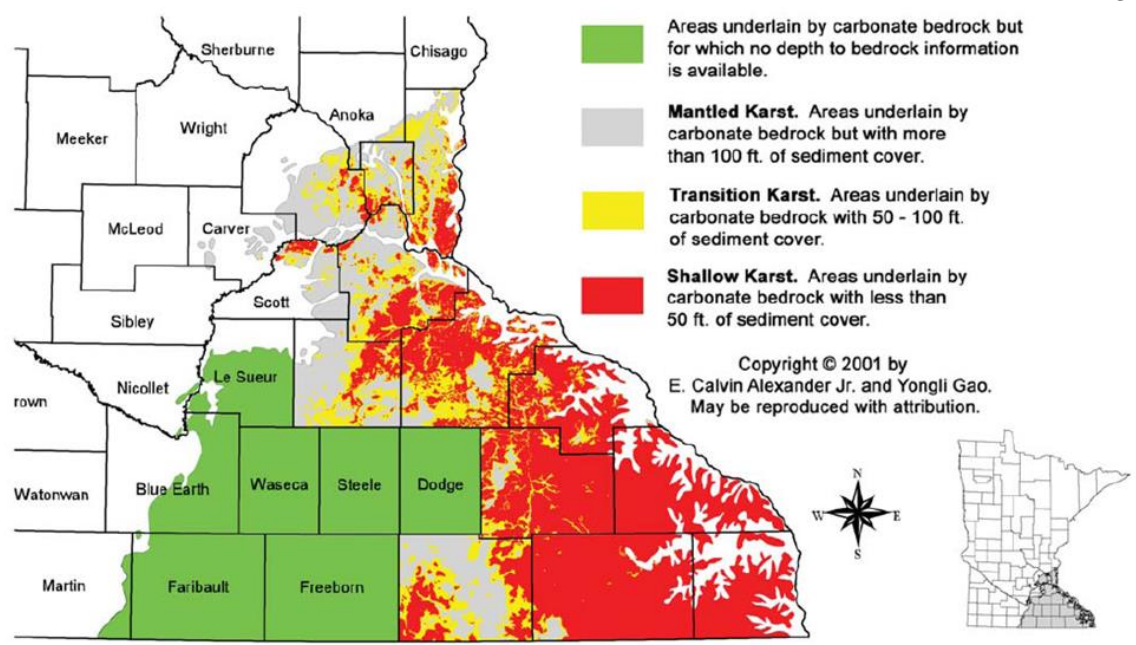


Figure 1.8. Karst map, Southeastern Minnesota. From Gao et al., 2002.

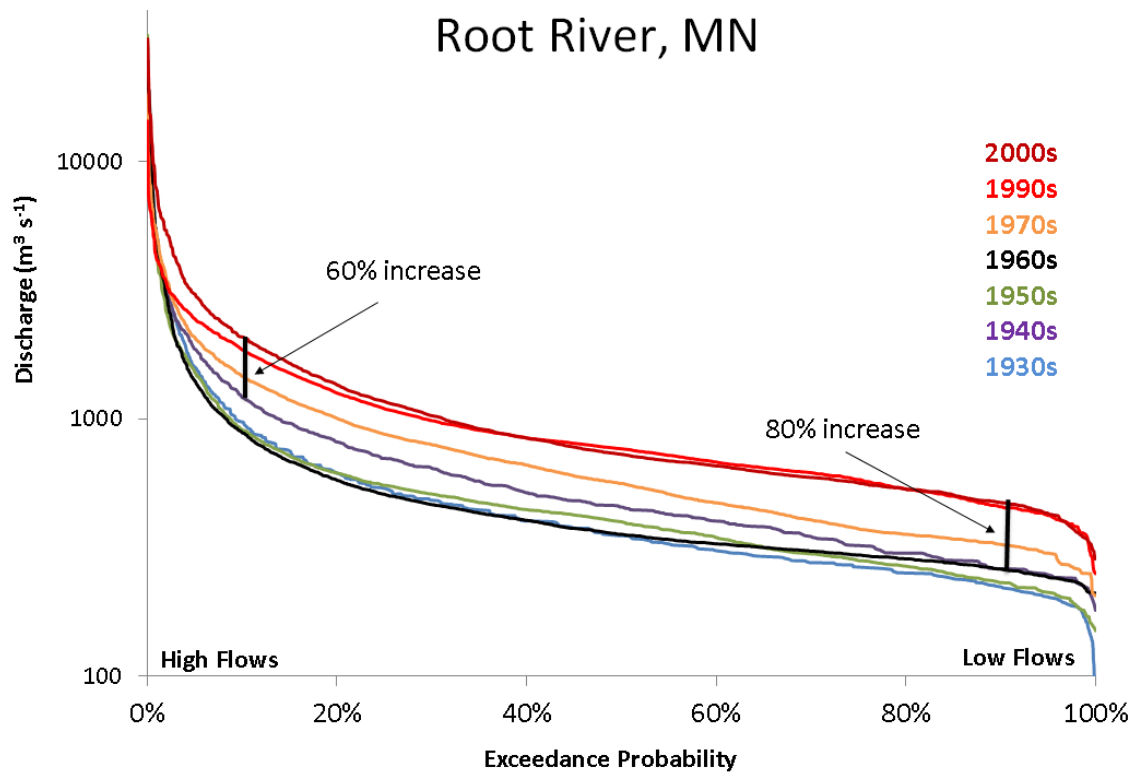


Figure 1.9. Root River decadal flow duration curves 1930s-2000s. Modified from Stout et al., 2013.

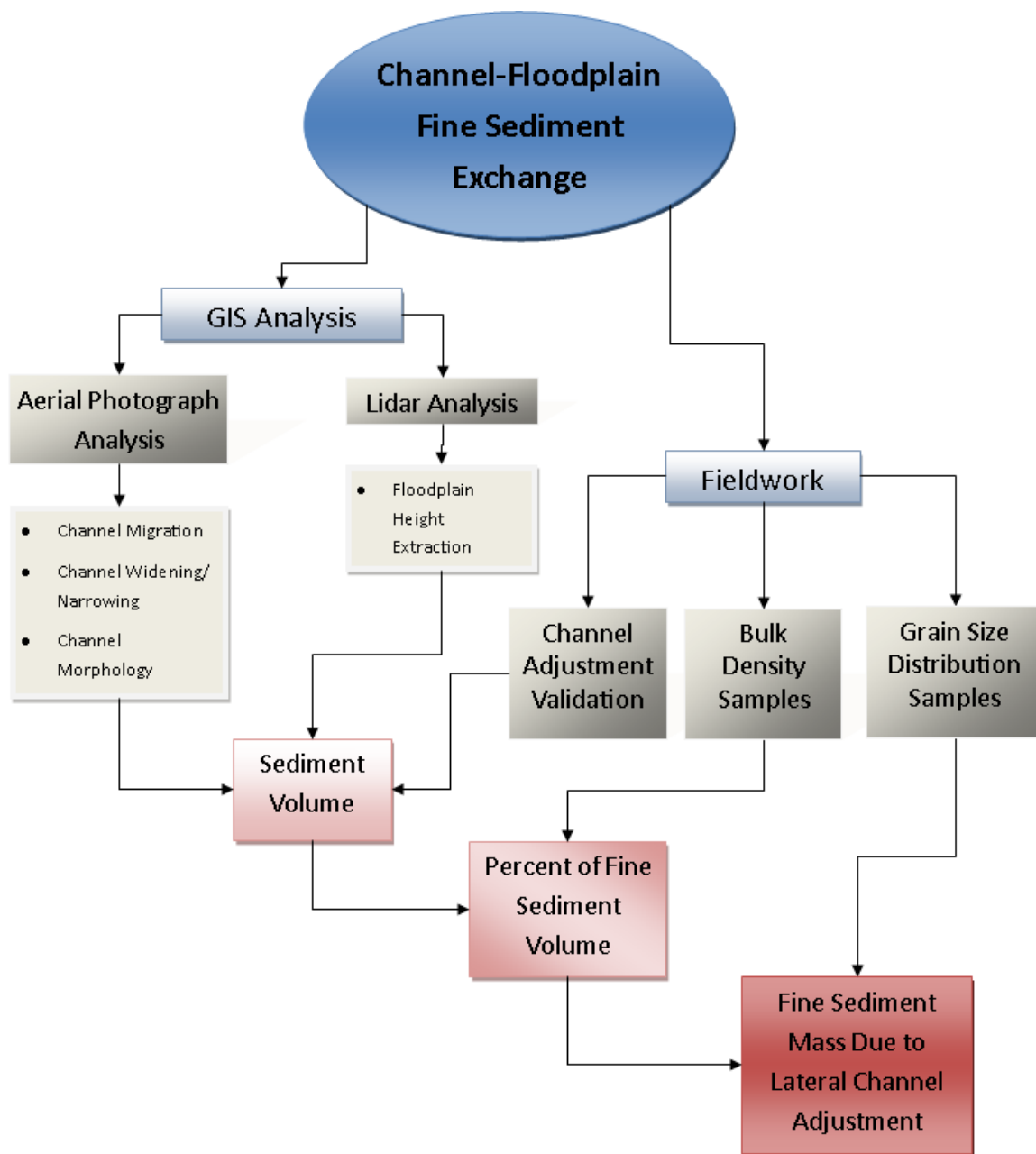


Figure 1.10. Schematic organization of the main tasks needed to complete this project.

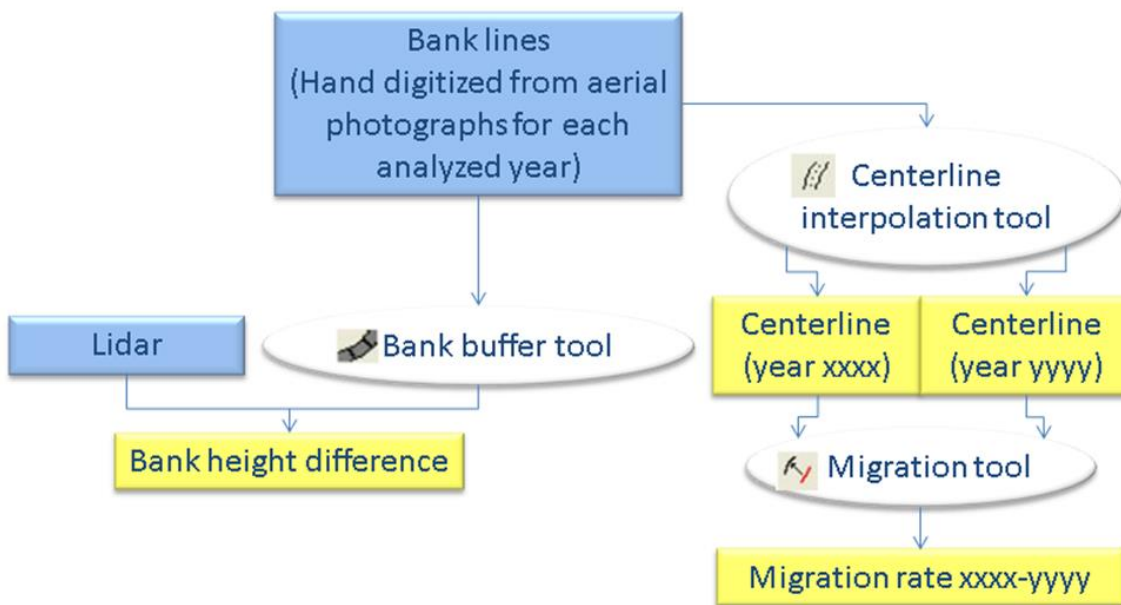


Figure 1.11. Planform Statistics Toolbox tool sequence to obtain bank height difference and migration rate. Blue boxes represent inputs, white circles represent the tools and yellow boxes represent the tool outputs.

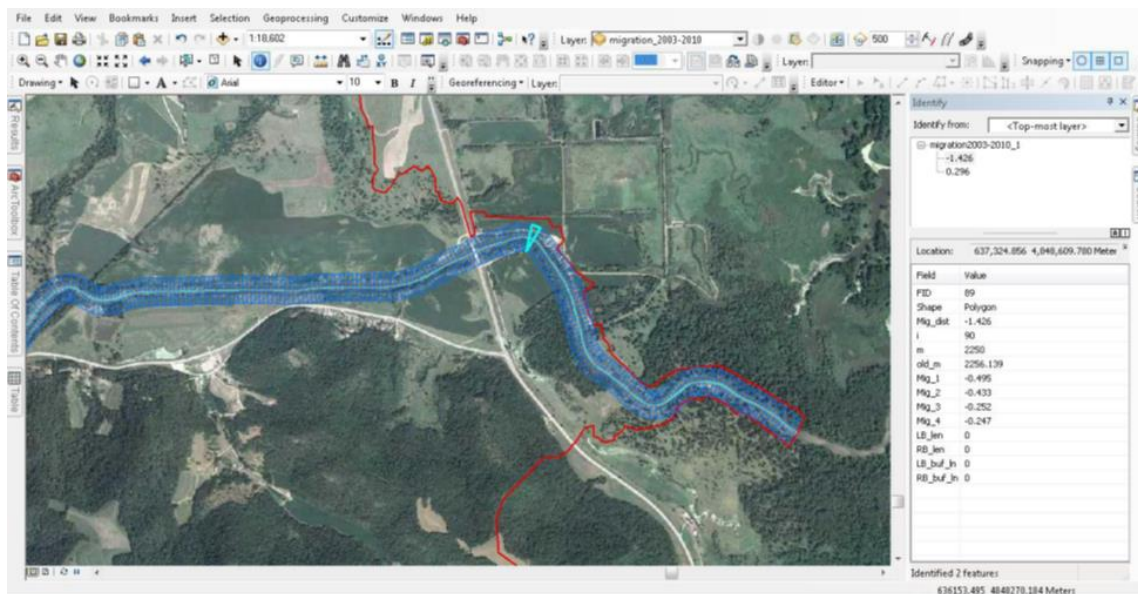


Figure 1.12. Migration rate polygons for 2000s-2010s aerial photograph at the mouth of the Root River.

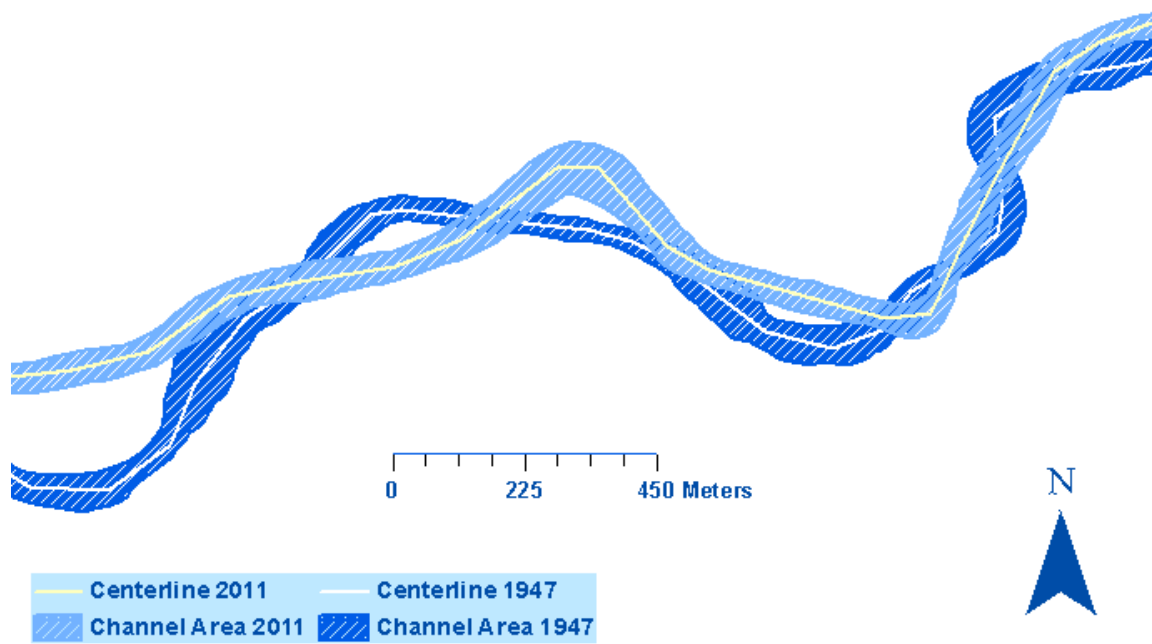


Figure 1.13. Polygons and centerlines for 2011 and 1947. Root River, MN.

## CHAPTER 2

LATERAL CHANNEL ADJUSTMENT IN THE ROOT RIVER, SOUTHEASTERN  
MINNESOTA**2.1 Introduction**

Alluvial rivers are dynamic systems. As channel morphology evolves through time, sediment is being reworked from the floodplain to the channel and vice versa with some frequency. Understanding river behavior and how channel adjustment results in sediment erosion and deposition have remained among the most important topics in fluvial geomorphology (Leopold and Wolman, 1957; Andrews, 1982; Montgomery and Buffington, 1997; Lauer and Parker, 2008; Belmont, 2011).

For the purpose of this thesis, I use the term ‘lateral channel adjustment’ to refer to two important processes that exchange sediment between the channel and floodplain, channel migration and channel widening/narrowing. Channel migration is the process by which the channel moves laterally across its floodplain and channel widening/narrowing is the process by which the channel either increases or decreases its width. Lateral channel adjustment is affected by many different factors (e.g., water discharge, sediment supply, riparian vegetation), as discussed in chapter one. Changes in any of the variables involved in the hydraulic geometry of a river system can result in the alteration of any of the other variables (see variables influencing channel form, chapter 1). The Root River has experienced changes in several of these variables over the past few decades, as explained below.

The Root River has experienced an increase in both its high and low flows since the 1990s (Stout et al., 2013) (see Figure 1.9). A discharge analysis comparing different flow metrics to lateral channel adjustment rates was included in this chapter to better understand the hydrology of the Root River and the relation between channel adjustment and the increased flows.

Lateral channel adjustment is also strongly influenced by the resistance to erosion caused by channel banks. Vegetation can exert a significant influence on channel morphology (see channel planform section, chapter 1). For this reason, an analysis comparing migration rates relative to local vegetation types along the channel (forested, low vegetation, and cultivated) was conducted in order to better understand the relation between channel migration and riparian vegetation.

Channel migration and channel widening can both result in contributions of sediment to the channel. Reduced sediment coming from agricultural fields and easily accessible near-channel sediment sources were strong reasons to believe that sediment sources in the Root River were shifting from upland sources to near-channel sources (Trimble, 1999; Stout et al., 2013). With less sediment coming from uplands, the river could now be mobilizing the sediment that it had been storing in its floodplains just as the Coon Creek case (see sediment budget, chapter 1). The fact that there is material that could easily be eroded and that flows have been increasing since the 1960s would help explain this shift.

In this chapter, recent and historical lateral channel adjustment rates were estimated to answer a few key basic and applied questions. From a basic science perspective, I sought to measure the spatial and temporal variability of lateral channel

adjustment to better understand how single-threaded meandering rivers change and create the complex patterns that can be observed in aerial photos and lidar data. From an applied perspective, I sought to determine if trends have changed during the past decades and (in chapter 3) use the lateral adjustment rates to estimate how much sediment is being contributed to the channel from these near-channel sources, thereby contributing to the broader goal of closing a sediment budget for the Root River.

## **2.2 Channel Description**

Streams can be classified by various methods depending on the questions and characteristics of interest. One simple example of a stream classification method is the Strahler stream order method, which loosely classifies streams according to size, assigning an order number to streams (i.e., headwaters are first order) and increasing the number each time two tributaries of the same order meet (Strahler, 1957). Physical characteristics like planform, slope or morphology in general are not considered in the Strahler method. In order to perform a lateral channel adjustment analysis, it is useful to divide the stream into representative reaches and classify the reaches using a system that accounts for these variables. The goal of a reach delineation exercise is to provide insight into the response of a river system, such as identifying unstable reaches, reaches prone to channel migration or sensitive areas (Kondolf et al., 2005). The specific goal of the reach delineation used here was to facilitate analysis by separating areas with different characteristics (i.e., width, meandering pattern, bank heights, valley confinement, etc.) and to determine which reaches are more prone to lateral channel adjustment. This

division also helped identify some of the characteristics that these active reaches have in common.

The characteristics used to divide the Root River channel network into meaningful reaches for analysis were planform geometry, valley confinement and channel morphology features. Planform geometry variables included meander amplitude, wavelength, sinuosity, and bankfull width (figure 2.1). Table 2.1 shows the planform geometry values measured for the ten distinct reaches delineated for the main stem Root River. The presence of point bars and other depositional features was also considered in the reach delineation. The reaches designated within each stream are about 8 to 17 km long.

The Root River watershed has a channel network of about 630 km including its major tributaries. The streams analyzed within the Root River watershed, from shorter to longer, are Bridge Creek (10.6 km), Crystal Creek (20.1 km), Rushford Creek (34.3 km), Money Creek (41.9 km), the Middle Branches (51.5 km and 74.9 km respectively), South Fork (76.5 km), the main stem of the river (83.7 km), South Branch (84.5 km) and North Branch (152.9 km). The slope of a river, which normally decreases in the downstream direction, is another important factor to consider in the description of a channel. Channel slope contributes to stream power (see channel morphology chapter 1). Stout (2012) created longitudinal profiles for the Root River and its mayor tributaries. Figure 2.2 shows the Root River channel network and the longitudinal profiles for these streams.

The main steam of the Root River was separated into 3 sections with 10 different reaches (figure 2.3). The third section, comprising reaches 7 to 10, includes part of the North Branch and the main stem of the Root River. Part of the North Branch was

included due to the transitional character of the channel in this area and because it is within the Driftless Area. The reaches of this section start at the confluence with the Middle Branch and end after the confluence with the South Branch. The third section is part of a transitional zone between the glaciated area, a relatively flat area covered by glacial till; and the Driftless Area, an incised area dominated by karst topography that has not been glaciated in the past half million years (see figure 1.7). The alluvial channel in this area is surrounded mostly by sandy soils. Just as the rest of the watershed, the vegetation cover here is a combination of cultivated land, low vegetation and large patches of forested land. Forested land dominates the area immediately adjacent to the channel. The reaches in this section are 3<sup>rd</sup> order streams with an average width of about 44 m and long bends of more than 600 m. These bends have not been very active laterally throughout the interval of aerial photographs analyzed most likely due to the semi-confined character of the channel in this area, the grown vegetation, and the tall terraces that range between 2 and 8 m along the channel. The slope in these reaches ranges between 0.00071 and 0.00117 m/m. Reach 7 serves as transition from a semi-confined to an unconfined channel with floodplains dominated by cultivated land.

The second section of the main stem of the Root River, comprising reaches 4, 5, and 6, is currently the most active area of the entire watershed regarding lateral channel adjustment. The photograph analysis shows that the meanders in this area evolve relatively fast. Many avulsions were identified in these reaches, throughout all the photographs analyzed a total of 12 cutoffs were identified. After the confluence with South Branch, the main stem of the Root River is a 4<sup>th</sup> order stream. Sediment contributions from the third section upstream and from Rushford Creek have a visible

influence on how the channel looks in this section. Point bars and mid-channel bars are abundant. The average width in this section is about 55 m and the meanders are smaller in amplitude and more numerous compared to the third section. Terrace height decreases significantly in the proximity of the city of Rushford, ranging 2 to 4 m. In the same stretch, channel slope ranges between 0.0006 and 0.0007 m/m.

The first section of the main stem comprises reaches 1, 2 and 3. These three reaches are fairly straight with a maximum sinuosity of 1.2 and have an average width of about 62 m. Channel slope and terrace height range from 0.00055 to 0.00042 m/m and 1 to 4 m, respectively. Floodplains in this section are also dominated by cultivated land. Bed load sheets of sand could be seen in multiple locations throughout this section in the aerial photographs, which suggests high loading and transport of sand through these reaches. Relatedly, the channel does not present any major point bars or mid-channel bars in this section. As expected, the channel generally gets wider and channel slope drops in order to adjust to the increased discharge coming from all the tributaries and the main stem and to the Mississippi level as the latter aggraded after the introduction of euro-american agriculture to the area (Knox, 2006). Preliminary assessment of aerial photographs indicated that this section has remained stable during the past few decades.

Tributaries of the Root River were divided into reaches following the similar criteria as the main stem. Figure 2.2.b shows longitudinal profiles for the major tributaries of the Root River. All the tributaries follow a meandering pattern with the exception of areas where the channel has been straightened. Forested land is dominant along the tributaries. The headwaters of the North, Middle and South branches of the Root River are upstream of the Driftless Area. This glaciated area is characterized by a

more homogeneous terrain and lower relief compared to the incised valleys of the Driftless Area. Generally, this area is characterized by short banks and channels narrower than 20 m. Many of these channels are used as agricultural ditches. The South Branch contains a hydro-electric power dam originally built in 1868. The dam is classified as a run-of-river dam and is about 60 m wide and 6.5 m tall (Gulliver et al., 1982). The North Branch also had a dam located in the County of Olmsted that was removed in the early 1990s (Figure 2.4). The rest of the tributaries are completely within the Driftless Area.

Rushford Creek is one of the most active tributaries. It drains a watershed characterized by sandy soils. The channel is characterized as having rapidly eroding banks that vary from 1 to 4 m tall (Figure 2.5.d). Upstream, the near-channel area is heavily forested. Near the confluence with the main stem of the Root River the channel has been straightened to prevent lateral movement as it passes through the city of Rushford.

Money Creek is less active than Rushford Creek, with tall terraces that exceed 6 m. Even though not very active under normal circumstances, Money Creek was very affected by the floods of 2007, which caused the collapse of a bridge on highway 76 and caused major road damages. The headwaters of Money creek are densely vegetated to the point of covering the stream channel. The last kilometer of Money Creek before its confluence with the Root River has also been channelized.

Stout et al. (2013) estimated that most of the suspended sediment added to the main stem from South Fork comes from near-channel sources based on data available from the monitoring sites and a fingerprinting analysis. The Minnesota Department of

Agriculture has a monitoring site in the headwaters of the South Fork, which monitors the quality and quantity of sediment and water coming from agricultural fields. Most of the banks of South Fork are higher than 4 m. The channel near the confluence of South Fork and the Root River presents a meandering pattern, but has been reinforced to prevent channel migration.

## **2.3 Methods**

Our analysis of channel lateral adjustment included quantification of two related processes, channel migration and channel widening/narrowing. An aerial photograph analysis was used to estimate lateral channel adjustment. Hydrology and land cover analyses together with an assessment of planform variables were also conducted to determine their relation with lateral channel adjustment. The following paragraphs describe the methods used to estimate channel adjustment as well as the different supplemental analyses conducted to answer the research questions posed in this work.

### **2.3.1 Aerial Photograph Analysis**

Aerial photographs from 1930s, 1950s, 1970s, 1990s, 2000s, and 2010s were analyzed. For more detail about the photographs see methods, chapter 1. The most recent photographs (1990s-2010s) are national agricultural Imagery Program (NAIP) photos for the years of 1991, 2003 and 2010. For the older photographs (1930s-1970s), a composite of photos from different years was used because photographs from one year did not cover the watershed in its entirety. A peak flow analysis was conducted to make sure that events that could significantly affect the shape of the channel did not happen in between years of the photographs that were combined to represent a given decade (see

hydrology section). Table 2.2 shows the years that were combined for each decade.

Older photographs were collected from different sources like the Minnesota department of Natural Resources (MnDNR), county agencies and university libraries. These older photographs had to be georeferenced.

Older photographs were georeferenced using the georeferencing toolbar of ArcMap. Hard points were used in the photographs, with road intersections being the most commonly used points. From Hughes et al. (2006), hard points were considered to be any feature with sharp edges or corners, usually road intersections or buildings. Generally 6 to 12 points were selected for each photo. First and second order transformations were used. According to Hughes et al. (2006), a first order transformation would work well when most of the points are in the floodplain; however, when the points selected extend out of the floodplain the number of outliers increased due to poor transformation in areas of higher elevation. Therefore, a second order transformation is needed in these areas. The latter, was the case for many of the older photographs as the hard points within the floodplain that remained in the most recent base layer photograph decreased.

Banklines for the channel adjustment analysis were extracted from aerial photographs for the decades of 1930, 1950, 1970, 1990, 2000, and 2010. Banklines were manually digitized following the bankfull width of the channel. Bankfull width is defined by the edge of the banks when they are filled with water to the top of the banks. Indicators of bankfull width were selected to digitize the banklines so that the same criterion was used for all parts of the Root River channel network. Vegetation line along the edge of depositional features were the main indicators used, followed by visual

assessment of previous and subsequent aerial photographs to better understand if and how the channel was evolving, and the use of the 2008 lidar. In forested areas, riparian vegetation obscured the banks. In such cases, interpolation between visible points of the bank was used in cases where trees were obscuring the banks.

Current planform geometry characteristics were estimated from the 2010 photographs. Planform metrics were calculated to determine the average values shown in table 2.1. Valley width and length, and meander wavelength and amplitude were measured at 10 locations distributed along each reach and then averaged to represent the entire reach. Valley confinement was calculated by dividing valley width and average channel width (see Channel Widening/Narrowing section below). Sinuosity was calculated for each reach by dividing reach length and valley length, the latter being the straight distance between the starting and ending points of each reach.

### **2.3.2 Channel Migration**

Channel migration was calculated from the banklines using the Planform Statistics Toolbox developed by J. Wesley Lauer (<http://www.nced.umn.edu/content/stream-restoration-toolbox>). This tool, described in the methods section (chapter 1), interpolates a channel centerline from digitized banklines and calculates the average normal distance between centerlines from different years (see methods, chapter 1). For this analysis the centerlines created were set to have 25 m node spacing, thus channel migration was calculated from these centerlines each 25 m increment of the channel. Results were stored in polygons of 25 m long and 80 m wide along the channel, which were generated by the Planform Statistics Toolbox. The 80 m

width of the polygon boxes is simply to secure that the entire channel is covered.

However, there are no repercussions in places where the channel is not fully covered since the polygons' only purpose was to store values in their attribute tables. Migration distances were then divided by the number of years between the photographs of analysis to obtain an average migration rate (m/yr). Migration results were calculated for the periods of 1930-1950, 1950-1970, 1970-1990, 1990-2000, and 2000-2010. Older rates were used to study the evolution of the channel and the channel migration history, while the most recent decades (1990-2000 and 2000-2010) were used to estimate the net contribution of sediment delivered to the channel as a result of channel migration (see chapter 3).

### **2.3.3 Channel Widening/Narrowing**

Channel widening/narrowing was calculated from the same banklines used for migration analysis. The editor toolbox of ArcMap together with other ArcMap tools were used to convert the banklines to polygons and to divide these into smaller polygons from which the average width was calculated as detailed in the methods section (chapter 1). Polygons created from the banklines were divided into sub-polygons of 10 times the average width of the bankline polygons, which varied from about 30 to 80 m. Average width was then calculated for these sub-polygons using a Python script. This script also produced box plot figures of the width distributions within a reach for each decade analyzed. A second script was used to compute average sub-reach width for each reach from upstream to downstream, providing more detail about the variability within each reach that the box plots do not reflect. Automating the calculation of channel width

allowed us to use smaller polygons, thus obtaining a better representation of the reaches, that is, averages widths each 10 times the average width of the reach as opposed to one average width for the whole reach (Figure 2.6). The figures provided useful statistic metrics and aided in the visual assessment of the variability and the overall distribution of the channel widths throughout the whole Root River watershed.

### 2.3.4 Hydrology

The hydrology of the Root River Watershed was analyzed using data from USGS gage 05385000 near Houston, Minnesota. Flow duration curves were calculated for multiple time intervals that match the time periods for which lateral channel adjustment was measured spanning a total time from 1930 to 2008. Daily flow data was used to produce the flow duration curves.

The change in the 1, 5 and 10 % exceedance probability from one decade to another was calculated to study their influence in channel adjustment. The difference between the 1, 5, and 10 % exceedance flows was calculated as:

$$\Delta Q_{n\%EP} = \frac{Q_{n\%EP Dec_{Recent}}}{Q_{n\%EP Dec_{Older}}} \quad (Eq. 2.1)$$

where  $\Delta Q_{n\%EP}$  is the difference between the n exceedance provability of two different decades.  $Q_{n\%EP Dec_{Recent}}$  is the flow exceeded for the more recent decade and  $Q_{n\%EP Dec_{Older}}$  is the flow exceeded for the older decade.

Peak flow data from 1910 to 2011 was used to calculate the magnitude of flows with respect to each other and to calculate the 5-, 10-, and 25-year return interval floods

of the watershed. Peak flow data was organized and ranked in order to associate lateral channel adjustment rates to specific floods that happened within a period of time. This data helped in understanding how the timing of these floods affected lateral channel adjustment. A Log Pearson Type III method was used to calculate the return intervals. The 10-year return interval was used as the maximum flood allowed in between aerial photographs to make sure that events that could significantly affect the shape of the channel did not happen in between years of photographs that were combined to represent a decade. The highest peak for the years used to represent a decade was not to exceed the 10-year return interval. In this way, we reduced the probability that major channel adjustment changes happening in between the years combined in a decade.

### **2.3.5 Land Cover**

A land cover analysis was conducted to determine the effect of vegetation on channel migration. The land cover analysis consisted of a supervised classification of a 30 m resolution 2011 multi-band Landsat image using Erdas Imagine 2011. The satellite image was downloaded from EarthExplorer (<http://earthexplorer.usgs.gov/>). The image was cropped to the area of interest, which was the floodplain area of the main stem of the Root River. The classes used for analysis were forested, cultivated, low vegetation (including hay, pasture, grassland and other low vegetated areas), water and urban. Four training areas were averaged to get each class in the classification. The resulting raster was converted to a polygon using ArcMap and then a spatial join was used to link migration rates from 2000-2010 and land cover per reach side (left and right). Probability distributions were calculated for the migration rates of each one of the three

vegetation types used in the analysis. Percent coverage was calculated for both sides of each of the 10 main stem reaches (table 2.3) using a python script to determine the vegetation type for each side. The script grouped together and estimated the total areas of land cover polygons that touched the banklines of each reach and then calculated the dominant land cover for each bank side by dividing the three land cover areas by the total land cover area.

## **2.4 Error Analysis and Validation**

There are multiple sources of error involved in estimating channel lateral adjustment from aerial photographs. Even though there is not a standard protocol to deal with all possible sources of error for this type of analysis on aerial photographs, the most common sources of error have been studied individually by many different authors (Hughes et al., 2006; Day, 2012). Estimating lateral channel adjustment from aerial photographs consists, for the most part, of comparing photographs of the same areas taken at different times to estimate how the river channel has changed. The distance that the channel migrated or widened from one photograph to another divided by the time interval between the photographs analyzed is the adjustment rate of the channel. Therefore, the sources of error in this type of analysis are related to the accuracy of the photographs with respect to each other and our ability to estimate distances between points within the photographs. The main sources of error analyzed here include georeferencing error, error due to the resolution and overall quality of the photographs, and digitizing error.

Error due to georeferencing aerial photographs is one of the most common errors considered in analyzing lateral channel adjustment. Improper georeferencing of photographs results in distances that depart from their real value due to the points measured being in an incorrect location in the first place. Hughes et al. (2006) provides excellent guidelines on how to increase the accuracy of the photographs. In his study, he demonstrated that the georectification accuracy of aerial photographs could be increased by using more than 8 ground control points, increasing the spatial density of the ground control points near the area of interest and avoiding the use of third order transformations. These suggestions were followed for our analysis.

The set of aerial photographs analyzed were acquired from two sources. The most recent photographs (1990s, 2000s, and 2010s) were collected by the Farm Service Agency (FSA) through their National Agriculture Imagery Program (NAIP) for the whole state of Minnesota using a ground sample distance of 1 m and were georeferenced to a horizontal accuracy of  $\pm 5$  m from 3.75' \* 3.75' quarter quadrangles using a Root Mean Squared Error (RMSE) to report their error. Older photographs (1930s to 1970s) were georeferenced in collaboration with colleagues from Winona State University using the georeferencing toolbar of ArcMap (see aerial photograph analysis. methods, chapter 2). A methodology similar to the one used with the more recent photographs was used to ensure consistency.

$$RMSE = \sqrt{\frac{e_x^2 + e_y^2}{2}} \quad (Eq. 2.2)$$

where  $e_x$  is the error in the x-axis and  $e_y$  is the error in the y-axis.

RMSEs were calculated from the reference points in each photograph, chosen following the criteria from Hughes et al. (2006). An average RMSE was estimated from these values. The horizontal accuracy for the older photographs was estimated to be  $\pm 15$  m. Error estimates obtained from the georeferencing tool of ArcMap accounted for the error for the entire area of the photographs. However, when possible, photographs were georeferenced using control points close to the channel to increase their accuracy near the area of interest. Most of the time, the channel-floodplain area in the photographs covered about a quarter of the entire photograph. Therefore, the error due to georeferencing in the 1930s-1970s photographs is likely smaller than the RMSE that was estimated for the analysis.

RMSEs were calculated using the 2010 NAIP photo as a base. To ensure that the error calculated was relevant for the lateral channel adjustment, RMSE was calculated from control points in photographs that were georeferenced one to another in decadal sequences (e.g. 1970s georeferenced to 1990s, 1950s to 1970s and so on). Control points varied from 15 to 30 along the main stem of the Root River. This check was done in this way because lateral channel adjustment was calculated in two decade periods using the exact same intervals (1930s-1950s, 1950s-1970s, and 1970s-1990s), therefore, the error in between this two decade periods would more likely represent the actual error.

A source of error that is not inherent in the photographs is the error due to the digitizer's judgment when creating the banklines. Delineation of channel banks is a somewhat subjective process that can vary depending on the interpretation of the analysis. To minimize the error due to this subjectivity, a set of guidelines were

established, as described in the methods section. Day (2012) estimated the error due to tracing bluffs in the Le Sueur River, southern Minnesota by having a single user digitize the same bluff ten times with several hours or days between each of the traces. She quantified the differences between traces for ten bluffs in her study watershed as an estimate of error from digitizing. Day (2012) estimated that the combined error in the total volume of sediment calculated from aerial photographs was 11 to 20 %. A similar method for the error due to digitizing was used in this error analysis, except that multiple users digitized the same portion of the river.

Two experiments were conducted to determine how the estimation of channel adjustment was affected depending on the judgment of the digitizer (Figure 2.7.a). The first experiment consisted of having four people digitize banklines for the same reach of the river using the same photographs. The digitizers chosen for the experiment had all a graduate level training in geomorphology, including the author. Experimental digitizers were given the same instructions and the same starting and ending points. The reach digitized for the experiment was located in one of the most active areas of the river where judgment would likely be a significant factor. This area is located in the main stem of the river between Rushford and Houston ( $91^{\circ}40'32''$  W  $43^{\circ}46'16''$  N to  $91^{\circ}38'12''$  W  $43^{\circ}46'30''$  N). The total length of the reach was  $\sim 5.4$  km. Centerlines were created from each set of digitized banklines and the average distance between the interpolated centerlines was calculated. Since the centerlines were generated by each digitizer from the same photo, the average distance between each centerline was considered to be the error due to the digitizer's judgment.

The second experiment consisted of calculating the change in channel width at 12 random points along ~40 km of channel in the main stem of the river using banklines digitized by two different digitizers. The digitizers for this second experiment were collaborators from Winona State University with undergraduate training in GIS and geomorphology. Channel width was measured manually for two sets of banklines at each random point. The difference in width at each random point was considered to be the error due to the digitizer's judgment in this process.

The errors due to georeferencing, quality of the aerial photographs, and to digitizing of the banklines were aggregated into a common RMSE.

$$RMSE = \sqrt{\frac{e_1^2 + e_2^2 \dots + e_n^2}{n}} \quad (Eq. 2.3)$$

where  $e_n$  represents the different sources of error taken into consideration for this error analysis.

A field-based channel width validation was conducted in the Root River by collaborators from Winona State University. Validation sites were selected upstream and downstream the confluences of the main stem of the Root River with its major tributaries as well as further upstream in several of the tributaries. The method consisted of locating the validation sites (Figure 2.7.b) and determining the average width of the channel for each site using a laser range finder (Nikon Laser Forestry 550) to define a reach 10 times that width. Channel width was measured at 10 to 12 locations along the delineated reach using the laser range finder. GPS coordinate points were taken at the upstream and

downstream ends of the reach. For the comparison analysis, the average width of the 10 to 12 locations was calculated for each site and compared to the average width obtained from the aerial photograph-based analysis of the 2010 channel corresponding to the same locations.

Finally, the largest channel adjustment values (migration rates, widening rates) were spot-checked for accuracy. The Planform Statistics Toolbox (see methods, chapter 1) considers the average distance between two centerlines from different years to be the channel migration for the interval of time between the photographs used. Therefore, other channel processes like cutoffs and development of mid-channel bars are erroneously considered to be channel migration by the toolbox. Channel cutoffs were observed to occur every 1 to 2 decades, primarily within the relatively short reach, between the cities of Rushford and Houston. The cutoff process abruptly changes the path of the channel, leaving an oxbow lake in the floodplain that is eventually filled with sediment. Channel migration results were also erroneous when mid-channel bar development resulted in attachment of the middle bar to one of the bank sides or where the channel widened or narrowed greatly due to any process changing only one of the banks. Both of these processes are important for this analysis because they reshape the channel in a way similar to channel migration and are indistinguishable in the results from the Planform Statistics Toolbox. In all observed cases, migration rates associated with channel cutoffs and development of mid-channel bars were extremely high (between 25 to 50 m/yr). Therefore, a manual check of the largest values obtained from the channel migration analysis was conducted to exclude erroneous values. Aerial photographs and banklines from the interval period were used to do the check. High

values in areas found to be associated with channel avulsions or processes other than channel migration were deleted.

#### **2.4.1 Error Analysis Results**

Errors due to georeferencing, quality of the photographs and the digitizer's judgment were combined in a root mean square error (RMSE). This method was chosen because all these errors ultimately influence the position of the banklines. The RMSE was calculated separately for the more recent and for the older photographs because of the different values associated to each source of error for both groups. Error due to georeferencing for the more recent and the older photographs were estimated to be 5 and 15 m, respectively. The error due to digitizing was estimated to be 7 m for both sets of photographs.

The check conducted with the control points estimated that the error due to the georeferencing of the photographs was an average 13 m. The RMSE assumed for the older photographs using the 2010 NAIP photo as the base was 15 m. The latter was used in the combined RMSE due to the closeness to the error in between decades and the consistency inherent in the use of the same base photograph to georeference the older photographs.

The combined RMSE was estimated to be 6 and 12 m for the more recent and the older decades, respectively. Lateral channel adjustment was estimated in m per year (m/yr). Therefore, to determine which rates are above the level of error we divided the combined RMSE by the number of years between aerial photographs to obtain error in units of m/yr. Yet it is important to recognize that the error itself is a function of the

distance, so even very low rates (below the reported error rate) could be measured if the time frame is sufficiently long.

Width validation results showed that field-measured widths tended to be wider than the GIS-calculated widths. The field-measured values were, on average, 13 % wider than the GIS-calculated values; this means that on average the field-measured values were 5 m wider than the GIS-calculated values (Figure 2.8). Some fraction of this systematic offset may be accounted for by widening that has occurred between 2010 (last year of air photos analyzed) and 2013 (when field measurements were conducted). If the Root River had widened during this time at a rate consistent with the average widening rate computed for the time period 2000s-2010s we predict that it would have widened 4 m on average. However, 2010 (13900 cfs) and 2011 (12000 cfs) were high flow years, and thus we expect that the channel widening rate may have been substantially higher than the 2000s-2010s average.

Spot-checking was conducted for all of the migration rates calculated. Over 2 km of channel from the period of 1990s-2000s and 5 km for most of the older photographs were extracted from the analysis due to avulsions and mid-channel bar development (Figure 2.9).

## **2.5 Results and Discussions**

This analysis of lateral channel adjustment was necessary in order to estimate the amount of sediment contributed to the channel due to the processes of channel migration and channel widening as well as to better understand the planform evolution of the Root River and how it relates to factors like discharge and vegetation cover. Based on the

observed increases in flows (see Figure 1.9), we expected to see gradual increases in channel migration and channel widening. What we found was that while channel adjustment results follow these trends, there were specific areas where channel migration was more active than others and higher flows are not necessarily the main factor influencing channel adjustment rates.

### **2.5.1 Channel Migration**

Channel migration analysis shows that migration rates were more evenly distributed along the channel network in the past. Even though the high and low flows have increased, most of the channel migration for the last two decades (1990s-2000s and 2000s-2010s) is now concentrated in specific, active areas of the channel network. As a result, average migration rates in the river have decreased (table 2.4). The most active reaches were located half way downstream of the main stem of the Root River (reaches 4 and 5). Besides being located after the confluences of four of the major tributaries of the Root River (The North, South and Middle branches and Rushford Creek), this area coincided with a decrease in bank height and the widening of the valley, which allowed the channel to migrate more freely. This is consistent with our hypothesis that the most active areas would have relatively low floodplains due to the fact that the floodplains would be constantly reworked through the processes of lateral channel adjustment.

High channel migration rates in these active reaches resulted in frequent avulsions. When the meander loops become too big, channel cutoffs reset the channel to a straight shape leaving an oxbow to be filled in the floodplain. This process happens every 1 to 2 decades in this section. The number of avulsions in reaches with high

migration rates has decreased for the last two decades. The number has decreased from having at least two cutoffs happen in the Root River to no cutoffs in the 2000s-2010s decade. The highest number of avulsions occurred in the main stem of the Root River during the period between 1950s-1970s with a total of seven avulsions occurring in this period (see Figure 2.10).

Figure 2.10 shows migration rates for the main stem of the Root River for all the epochs of photographs analyzed. Reaches 4 and 5 have remained the most active throughout the years analyzed. These reaches, between the cities of Rushford and Houston and described in the Channel Description section (section 2), present a combination of factors that encourage channel migration. South Branch and Rushford Creek tributaries upstream from these reaches add considerable amounts of water and sediment to the system. Evidence of this is the marked change in the morphology of the channel, which presents many point bars and transitory depositional features. The valley also widens, allowing the channel to meander more freely than in reaches upstream. The uncertainty associated with these rates was 0.55 m/yr. Channel migration rates below this value cannot be validated as real values.

Average migration rates for the Root River for epoch analyzed are shown in Figure 2.11. Oldest decades (1930s-1950s) had higher average migration rates in all cases. This decrease in migration rates comes in contrast to what might be expected, given the observed increases in high flows over the past few decades. Channel migration has been reduced in both magnitude and variability. Thus, flow metrics do not seem to be strongly related to channel migration in the Root River. However, several other variables have changed and the observed decrease in migration rates could be, at least in

part, due to factors such as a decline in sediment supply and changes in riparian vegetation, which adds resistance to the banks. Sediment supply has very likely been reduced due to the use of best management practices in agriculture. Riparian vegetation has visibly increased in more recent aerial photographs as well. In addition, according to our analysis of flood events within each decade the early 1930s were an exceptionally dry decade. Therefore, the channel may also have adjusted rapidly after this extreme drought period.

Even though high flows alone do not appear to be a dominant control for channel migration in the Root River, a comparison between migration rates and different flow metrics was done in order to determine if there was a relation. Figure 2.12 shows average migration rates versus different flow metrics. The 1 % exceedance probability is the only flow metric that seems to have a directly proportional relation with average migration rates with an  $R^2$  of 0.34. The fact that negative relations are observed between migration rate and peak flow as well as the 5 and 10 % exceedance flows is surprising and may cast some doubt on whether or not the positive correlation observed between migration rate and the 1 % exceedance flow is truly causative or spurious.

Migration rates followed a similar pattern in the tributaries. Figure 2.13 shows a comparison between the migration rates for the decades of 1990s-2000s and 2000s-2010s at South Fork and Rushford Creek. Table 2.5 shows the average migration rates for the tributaries of the Root River.

A land coverage analysis was conducted in order to determine the effect of riparian vegetation on channel migration. Figure 2.14 shows probability distributions for the migration rates of forested, low vegetation (hay, pasture, grassland, and other low

vegetated areas), and cultivated areas. Results show that while low migration rates (0 to 1.5 m/yr) occur similarly through the three vegetation types, there is a higher occurrence of high and extremely high migration rates ( $> 1.5$ ,  $>3$  m/yr) in cultivated areas. This higher occurrence can be seen in the heavy tail of the distribution associated with cultivated land, as compared to the other two distributions. This plot highlights the importance of riparian vegetation and how it helps increase bank resistance preventing lateral adjustment as a result. According to these results, we hypothesize that an increase in riparian vegetation has been one of the factors contributing to reduced migration rates in the past two decades by increasing bank stability and therefore contrasting the increase in flows. This would help explain why migration rates have decreased in spite of the increase in water discharge. Figure 2.15 offers a visual comparison of the land coverage between the 1991 and 2010 aerial photographs. A more detailed study of land use change would be necessary in order to quantify if and how riparian management has affected channel migration rates over the past several decades.

### **2.5.2 Channel Width**

Channel widening results in the Root River offer evidence that channel widening or narrowing is the result of a combination of processes that are interrelated. Water discharge is usually considered to be one of the main drivers of channel widening; however, other factors like sediment supply or bank resistance may also play significant roles.

We found that the Root River has generally been widening since the 1930s with a few exceptions following large events (table 2.6). Figure 2.16 shows the overall

distribution of widths along the Root River. Channel narrowing was observed after decades of extreme channel widening in the period between the 1930s and the 1970s. From the 1930s to the 1950s, the channel widened 18 % on average (Figure 2.18). This is consistent with the fact that the Root River experienced its second and fifth largest peak flows during this period (table 2.8). However, the channel narrowed 14 % from the 1950s to the 1970s. This period had the fourth, fifth and seventh largest peaks; however, it also included 5 of the 8 lowest peak flows from 100 years of record. This highlights the importance of the timing and sequence of floods in how channel adjustment is affected.

In order to further study channel width changes between decades, we created plots indicating the change in width between the time periods of interest (Figure 2.17). These plots show average channel width change in the main stem of the Root River every 10 times the average width of the channel (represented by each blue dot) for a total distance of ~127 km. This high level of detail along the entire main stem of the Root River allowed us to more easily identify widening and narrowing trends in a very fine scale. Besides this, the overall widening/narrowing trends discussed above and visible in Figure 2.16 are more easily identified in this plot.

The rate at which the channel widens has decreased since the 1950s, but the general trend has continued to be in the direction of widening. Notwithstanding the fact that both high and low flows have increased by 60 and 80 %, respectively, the rate at which the channel increases its width has decreased from 18 % (1930s-1950s) to an average 5.3 % after the 1970s. This reduction in the rates may be related to a reduction in sediment supply as a consequence of conservation and improved agricultural practices

and/or changes in riparian vegetation. If this is true, prior to the 1970s the river had more sediment coming from uplands and at the same time offered less resistance to bank erosion. Therefore the river was more active adjusting its shape (widening and narrowing) depending on water supply. As sediment coming from uplands decreased and channel banks became more stable due to vegetation feedbacks, the channel has been losing that interplay of widening and narrowing resulting in a slower but constant widening for the past four decades. Narrowing still takes place, as evidenced in reaches 10, 9, and 8 of the main stem of the Root River during the 1990s-2000s decade, but the overall tendency is to widen.

A simple regression analysis between width percent change and various flow metrics revealed channel widening to be most closely related to the flows that were exceeded on 1 % of the time. Figure 2.19 shows width percent change versus the percent difference between the 1 %, 5 %, and 10 % flows for each of the time periods measured. Evaluating width change against the difference between different flow metrics allowed us to determine how the channel adjusted depending not on the amount of a specific flow, but on the percent increase or decrease of a specific percent exceedance flow with respect to the same exceedance flow for a prior period of time.

Channel widening results for the tributaries of the Root River for the last two decades still follow the widening-narrowing pattern. Table 2.7 shows the average widths for the tributaries of the Root River for the last two decades. This analysis shows that tributaries stored sediment in their floodplain by narrowing during the decade of 1990s-2000s and that they have since been eroding this sediment as part of the widening - narrowing adjustment pattern.

### **2.5.3 Lateral Channel Adjustment Evolution**

Lateral channel adjustment patterns in the Root River have changed since the 1970s. Channel migration and channel widening results show that prior to the 1970s the Root River was more active in many aspects compared to more recent decades. Channel migration rates have decreased in magnitude and are not concentrated in specific areas. Channel width adjustment prior to the 1970s alternated between widening and narrowing throughout the entire channel network, but this tendency has decreased significantly throughout the entire channel network, especially in the main stem of the river. The main stem of the Root River has been widening in a smaller but steadier manner than during decades prior to the 1970s. We attribute this change to an increase in vegetation and a reduction in sediment supply.

These results highlight the importance of other factors in lateral channel adjustment. More detailed studies of the influence of vegetation and changes in sediment supply need to be done in order to better understand the processes of lateral channel adjustment and what changes may or may not reflect significantly on the channel.

## **2.6 References**

- Andrews, E.D., 1982. Bank stability and channel width adjustment, East Fork River, Wyoming. *Water Resour. Res.* 18 (4): 1184-1192.
- Argabright, M.R., Helms, C.D., Pavelis, G., Sinclair, R., 1996. Historical changes in soil erosion, 1930-1992: The northern Mississippi valley loess hills. *Natural resour. Conservation Service, USDA. Historical note No 5.*
- Belmont, P., 2011. Floodplain width adjustments in response to rapid base level fall and knickpoint migration. *Geomorphology.* 128 (1-2): 92-102.
- Corenblit, D., Steiger, J., 2009. Vegetation as a major conductor of geomorphic changes on the Earth surface: toward evolutionary geomorphology. *ESPL.* 34: 891–896.

- Day, S.S., 2012. Anthropogenically-intensified erosion in incising river systems. Ph.D. Thesis, University of Minnesota. Minneapolis, Minnesota.
- Gulliver, J.S., Gake, L, Renaud, R., 1982. Feasibility of Hydropower Rehabilitation at the Lanesboro Dam, MN. University of Minnesota, project report No. 217.
- Huang, H.Q., Nanson, G.C., 1997. Vegetation and channel variation; a case study of four small streams in southeastern Australia. *Geomorphology*. 18: 237-249.
- Hughes, M.L., McDowell, P.F., Marcus, W.A., 2006. Accuracy assessment of georectified aerial photographs: Implications for measuring lateral channel movement in a GIS. *Geomorphology*. 74: 1-16.
- Knox, J.C., 2006. Floodplain sedimentation in the Upper Mississippi Valley: Natural versus human accelerated. *Geomorphology*, 79 (3-4): 286-310.
- Kondolf, M., Montgomery, D.R., Piégay, H., Schmitt, L., 2005. Geomorphic classification of rivers and streams, in *Tools in Fluvial Geomorphology*. John Wiley & Sons, Ltd, Chichester, UK.
- Lauer, J.W., Parker, G., 2008. Net local removal of floodplain sediment by river meander migration. *Geomorphology*. 96 (1-2): 123-149.
- Leopold, L.B., Wolman M.G., 1957. River Channel Patterns: Braided, Meandering and Straight. USGS Professional Paper 282-B: 39-103.
- Montgomery, D.R. and Buffington J.M., 1997. Channel-reach morphology in mountain drainage basins. *Geol. Soc. Am.* 109 (5): 596-611.
- Parker, G., Wilcock, P.R., Paola, C., Dietrich, W.E., and Pitlick, J., 2007. Physical basis for quasi-universal relations describing bankfull hydraulic geometry of single-thread gravel bed rivers. *J. of geophys. res.* 112, F04005.
- Simon, A. Collison, A.J.C., 2002. Quantifying the mechanical and hydrologic effects of riparian vegetation on streambank stability. *ESPL*. 27: 527-546.
- Stout, J.C., 2012. Identifying and quantifying sediment sources and sinks in the Root River, Southeastern Minnesota. All Graduate Theses and Dissertations. Paper 1304. <http://digitalcommons.usu.edu/etd/1304>.
- Stout, J.C., Belmont, P., Schottler, S.P., Willenbring, J.K., 2013. Identifying Sediment Sources and Sinks in the Root River, Southeastern Minnesota. *Annals Assoc. Am. Geographers*. 104(1): 20-39
- Strahler, A. N., 1957. Quantitative analysis of watershed geomorphology. *Trans. Am. Geophys. Union* 38 (6): 913-920.
- Trimble, S.W., 1999. Decreased Rates of Alluvial Sediment Storage in the Coon Creek Basin, Wisconsin, 1975-93. *Sci.* 285 (5431): 1244-1246.

Trimble, S.W., Lund, S.W., 1982. Soil conservation and the reduction of erosion and sedimentation in the Coon Creek basin, Wisconsin. USGS professional paper 1234. Washington, DC: Government printing office.

Table 2.1. Root River main stem planform geometry variables

Reach	Reach Length (km)	Ch. Width (m)	Valley Width (m)	Valley Length (m)	Valley Confinement	Sinuosity	Wave length (m)	Meander Amplitude (m)
1	10.5	65.1	1673	9.0	25.7	1.2	-	-
2	15.4	65.3	1476	13.4	22.6	1.1	-	-
3	8.7	56.7	1372	7.0	24.2	1.2	-	-
4	13.3	57.1	719	7.2	12.6	1.8	500	250
5	14.9	54.6	868	10.8	15.9	1.4	600	230
6	14.9	51.5	366	8.0	7.1	1.9	600	600
7	9.7	55.0	363	6.2	6.6	1.6	900	460
8	12.9	44.7	170	2.7	3.8	4.8	1600	1750
9	11.8	37.3	119	6.1	3.2	1.9	800	700
10	17.1	39.4	138	6.8	3.5	2.5	1800	980

Table 2.2. Photographs analyzed

Decade	Years
1930s	1937, 1938, 1939
1950s	1951, 1952
1970s	1974, 1976, 1977
1990s	1991
2000s	2003
2010s	2010

Table 2.3. Reach vegetation coverage

Reach	Side	Forested	Cultivated	Low Vegetation	Dominant Vegetation
1	Left	9.4 %	84.1 %	6.5 %	Cultivated
	Right	64.8 %	20.8 %	14.4 %	Forested
2	Left	10.8 %	68.5 %	20.7 %	Cultivated
	Right	16.3 %	64.9 %	18.9 %	Cultivated
3	Left	7 %	86.6 %	6.4 %	Cultivated
	Right	10.8 %	88.9 %	0.3 %	Cultivated
4	Left	24.7 %	73.3 %	2 %	Cultivated
	Right	38.6 %	61.0 %	0.4 %	Cultivated
5	Left	31.1 %	65.0 %	3.9 %	Cultivated
	Right	18.6 %	76.4 %	5 %	Cultivated
6	Left	47.7 %	47.2 %	5.1 %	Forested/Cultivated
	Right	65.2 %	32.1 %	2.7 %	Forested
7	Left	57.9 %	34.2 %	7.8 %	Forested
	Right	60.2 %	38.2 %	1.6 %	Forested
8	Left	77.4 %	20.3 %	2.3 %	Forested
	Right	84.3 %	13.9 %	1.8 %	Forested
9	Left	89.6 %	7.9 %	2.5 %	Forested
	Right	84.3 %	13.9 %	1.8 %	Forested
10	Left	60.2 %	29.7 %	10.2 %	Forested
	Right	62.1 %	23.8 %	14.1 %	Forested

Table 2.4. Root River channel migration per reach

Reach	2000-2010	1990-2000	1970-1990	1950-1970	1930-1950
	(m/yr)	(m/yr)	(m/yr)	(m/yr)	(m/yr)
1	0.43	0.05	0.49	0.64	0.92
2	0.39	0.22	0.18	0.58	0.82
3	0.47	0.39	0.31	0.71	1.11
4	1.39	0.96	1.76	1.34	2.03
5	1.12	0.76	0.61	1.16	1.32
6	1.08	0.61	0.49	0.65	1.01
7	0.86	0.67	0.53	0.74	2.03
8	0.86	0.46	0.37	1.15	1.95
9	0.46	0.23	0.18	0.66	1.14
10	0.50	0.29	0.24	0.80	1.05
Average	0.76	0.46	0.52	0.84	1.34

Table 2.5. Tributary migration rates

Tributary	Average Migration rates (m/yr)	
	1990s-2000s	2000s-2010s
South Fork	0.29	0.53
Rushford Creek	0.30	0.59
South Branch	0.41	0.49
North Branch	0.45	0.52
Money Creek	0.23	0.33
Middle Branch	0.50	0.46

Table 2.6. Width percent change per reach

Reach	2000-2010	1990-2000	1970-1990	1950-1970	1930-1950
1	9.2 %	0.9 %	2.5 %	0.2 %	9.4 %
2	0.7 %	-1.9 %	6.7 %	-8.0 %	30.0 %
3	0.5 %	0.9 %	11.1 %	-19.0 %	17.1 %
4	7.6 %	3.3 %	11.3 %	-17.3 %	8.4 %
5	6.9 %	14.2 %	-2.1 %	-21.6 %	32.3 %
6	9.5 %	7.8 %	18.6 %	-20.9 %	3.2 %
7	25.5 %	3.0 %	-15.4 %	-9.7 %	28.7 %
8	5.4 %	-5.9 %	26.4 %	-15.1 %	23.6 %
9	9.5 %	-11.9 %	0.8 %	-13.0 %	9.3 %
10	3.3 %	-1.6 %	11.5 %	-11.9 %	20.2 %

Table 2.7. Tributary average width per reach

<b>South Fork</b>								
Reach	Length (m)	Average Width (m)			Percent Change (%)		Delta width (m)	
		1991	2003	2010	1990s- 2000s	2000s- 2010s	1990s- 2000s	2000s- 2010s
reach5	15600	10.19	8.67	8.45	-0.15	-0.03	-1.52	-0.22
reach4	16250	14.25	13.99	14.03	-0.02	0.00	-0.26	0.04
reach3	16620	15.43	12.88	13.79	-0.17	0.07	-2.55	0.91
reach2	16800	16.26	14.23	14.65	-0.12	0.03	-2.03	0.42
reach1	9910	19.43	17.72	17.45	-0.09	-0.02	-1.71	-0.27
<b>Total</b>					<b>-0.11</b>	<b>0.01</b>	<b>-1.61</b>	<b>0.18</b>

<b>Rushford Creek</b>								
Reach	Length (m)	Average Width (m)			Percent Change (%)		Delta width (m)	
		1991	2003	2010	1990s- 2000s	2000s- 2010s	1990s- 2000s	2000s- 2010s
reach3	14420	9.97	6.48	9.27	-0.35	0.43	-3.49	2.79
reach2	15340	12.36	8.61	10.59	-0.30	0.23	-3.75	1.98
reach1	3410	16.52	13.87	15.94	-0.16	0.15	-2.65	2.07
<b>Total</b>					<b>-0.27</b>	<b>0.27</b>	<b>-3.30</b>	<b>2.28</b>

<b>South Branch</b>								
Reach	Length (m)	Average Width (m)			Percent Change (%)		Delta width (m)	
		1991	2003	2010	1990s- 2000s	2000s- 2010s	1990s- 2000s	2000s- 2010s
reach6	14700	14.9	10.82	11.38	-0.27	0.05	-4.08	0.56
reach5	14510	13.51	9.4	8.7	-0.30	-0.07	-4.11	-0.70
reach4	16240	14.56	10.28	10.89	-0.29	0.06	-4.28	0.61
reach3	16380	16.36	12.46	12.55	-0.24	0.01	-3.90	0.09
reach2	16080	18.86	14.48	17.94	-0.23	0.24	-4.38	3.46
reach1	8900	20.33	15.34	17.23	-0.25	0.12	-4.99	1.89
<b>Total</b>					<b>-0.26</b>	<b>0.07</b>	<b>-4.29</b>	<b>0.99</b>

<b>North Branch</b>								
Reach	Length (m)	Average Width (m)			Percent Change (%)		Delta width (m)	
		1991	2003	2010	1990s- 2000s	2000s- 2010s	1990s- 2000s	2000s- 2010s
reach6	13520	16.74	14.56	17.97	-0.13	0.23	-2.18	3.41
reach5	11840	42.05	16.03	21.23	-0.62	0.32	-26.02	5.20
reach4	13170	26.74	19.96	24.47	-0.25	0.23	-6.78	4.51
reach3	12470	24.31	19.16	23.39	-0.21	0.22	-5.15	4.23
reach2	12970	24.65	19.98	24.83	-0.19	0.24	-4.67	4.85

reach1	16290	26.49	20.73	25.37	-0.22	0.22	-5.76	4.64
<b>Total</b>					<b>-0.27</b>	<b>0.25</b>	<b>-8.43</b>	<b>4.47</b>

### Money Creek

Reach	Length (m)	Average Width (m)			Percent Change (%)		Delta width (m)	
		1991	2003	2010	1990s-2000s	2000s-2010s	1990s-2000s	2000s-2010s
reach2	10460	8.69	7.47	9.62	-0.14	0.29	-1.22	2.15
reach1	10120	10.21	8.21	11.14	-0.20	0.36	-2.00	2.93
<b>Total</b>					<b>-0.17</b>	<b>0.32</b>	<b>-1.61</b>	<b>2.54</b>

### Middle Branch

Reach	Length (m)	Average Width (m)			Percent Change (%)		Delta width (m)	
		1991	2003	2010	1990s-2000s	2000s-2010s	1990s-2000s	2000s-2010s
reach6	9830	9.61	7.32	9.88	-0.24	0.35	-2.29	2.56
reach5	12680	13.84	9.5	12.87	-0.31	0.35	-4.34	3.37
reach4	11820	16.4	13.12	17.49	-0.20	0.33	-3.28	4.37
reach3	12130	15.13	13.67	17.37	-0.10	0.27	-1.46	3.70
reach2	12340	20.08	17.25	20.7	-0.14	0.20	-2.83	3.45
reach1	14200	24.47	19.95	24.84	-0.18	0.25	-4.52	4.89
<b>Total</b>					<b>-0.20</b>	<b>0.29</b>	<b>-3.12</b>	<b>3.72</b>

Table 2.8. Highest peaks. USGS gage 05385000 near Houston

Year	Rank	Peak (cfs)	Return interval (years)	Exceedance Probability
2007	1	46000	91.0	0.01
1952	2	37000	45.5	0.02
2000	3	34600	30.3	0.03
1961	4	31400	22.8	0.04
1950	5	31000	18.2	0.05
1965	5	31000	18.2	0.05
1962	7	29500	13.0	0.08
1933	8	26600	11.4	0.09
1945	9	23900	10.1	0.10
2004	10	23800	9.1	0.11

Table 2.9. Lowest peaks. USGS gage 05385000 near Houston

Year	Rank	Peak (cfs)	Return interval (years)	Exceedance Probability (%)
1964	1	1110	1.0	0.99
1988	2	1600	1.0	0.98
1957	3	2230	1.0	0.97
1970	4	2250	1.0	0.96
1977	5	2290	1.1	0.95
1910	6	2500	1.1	0.93
2003	7	2650	1.1	0.92
1968	8	3210	1.1	0.91
1955	9	3760	1.1	0.90
2009	10	4070	1.1	0.89

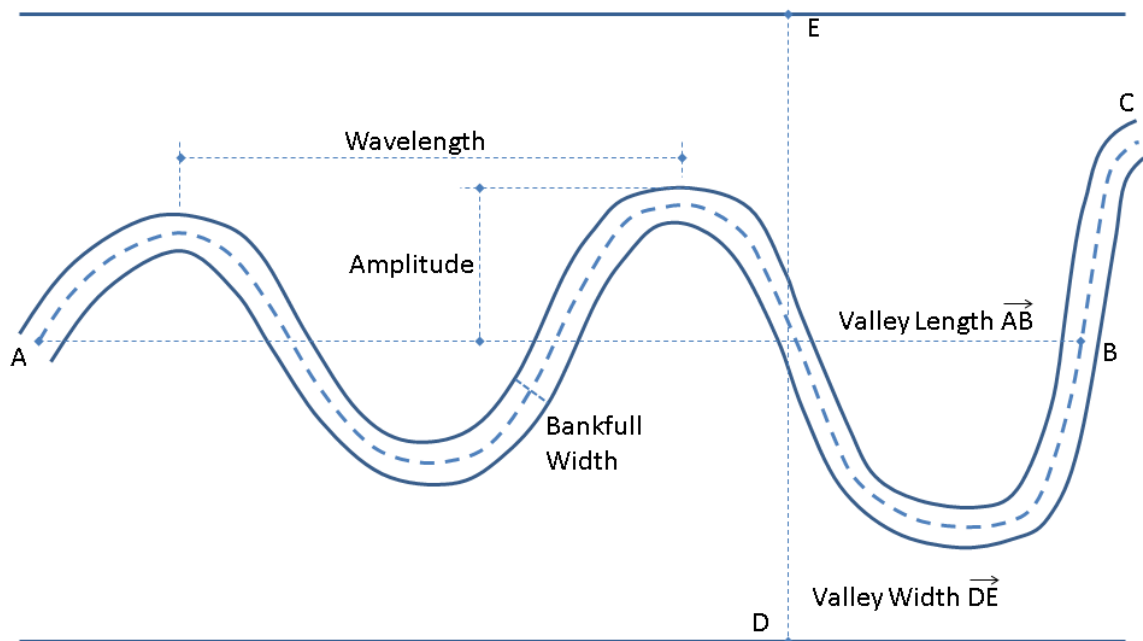


Figure 2.1. Planform geometry variables. Sinuosity is equal to the channel length divided by the distance between the starting and ending points, A and C in this case.

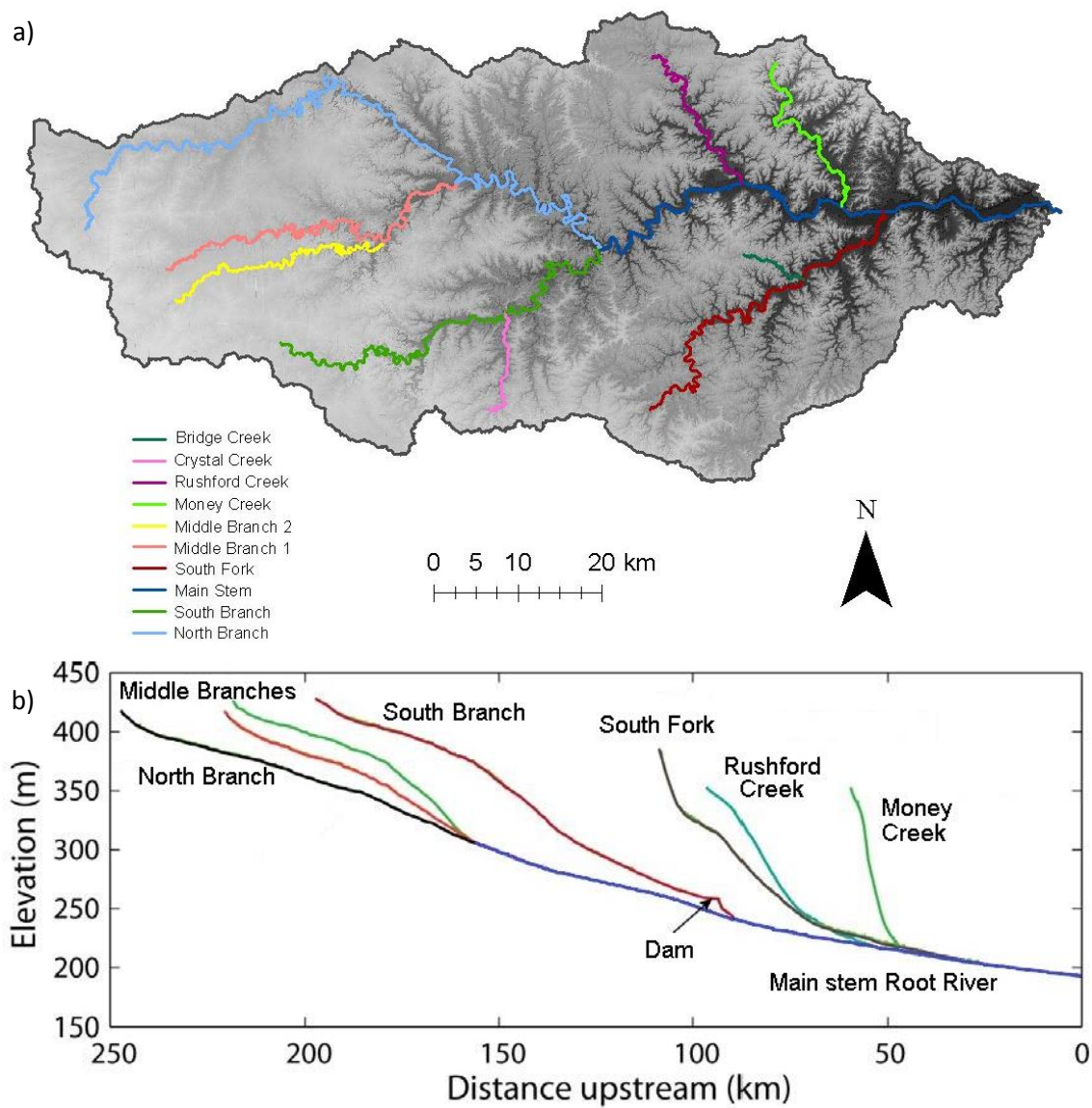


Figure 2.2. Root River channel network and longitudinal profiles. a) Root River channel network, b) longitudinal profiles of the main streams of the Root River (Stout, 2012).

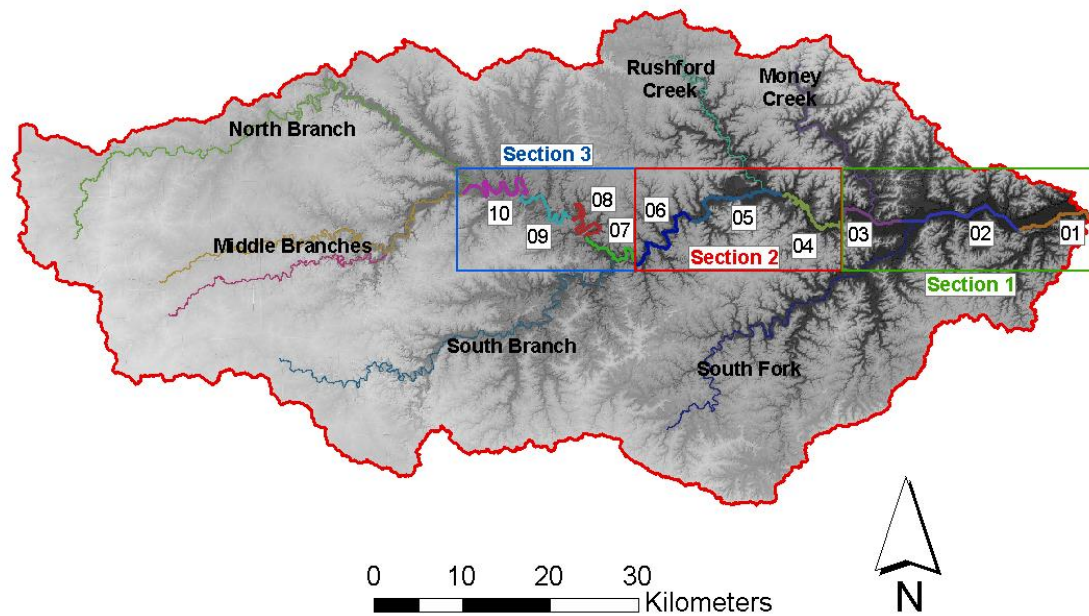


Figure 2.3. Reach division. Blue, red and green rectangles represent section 1, 2, and 3, respectively.



Figure 2.4. Old Lake Florence, close to the city of Stewartville in the county of Olmsted, MN. The dam that created the lake was removed in the early 1990s.

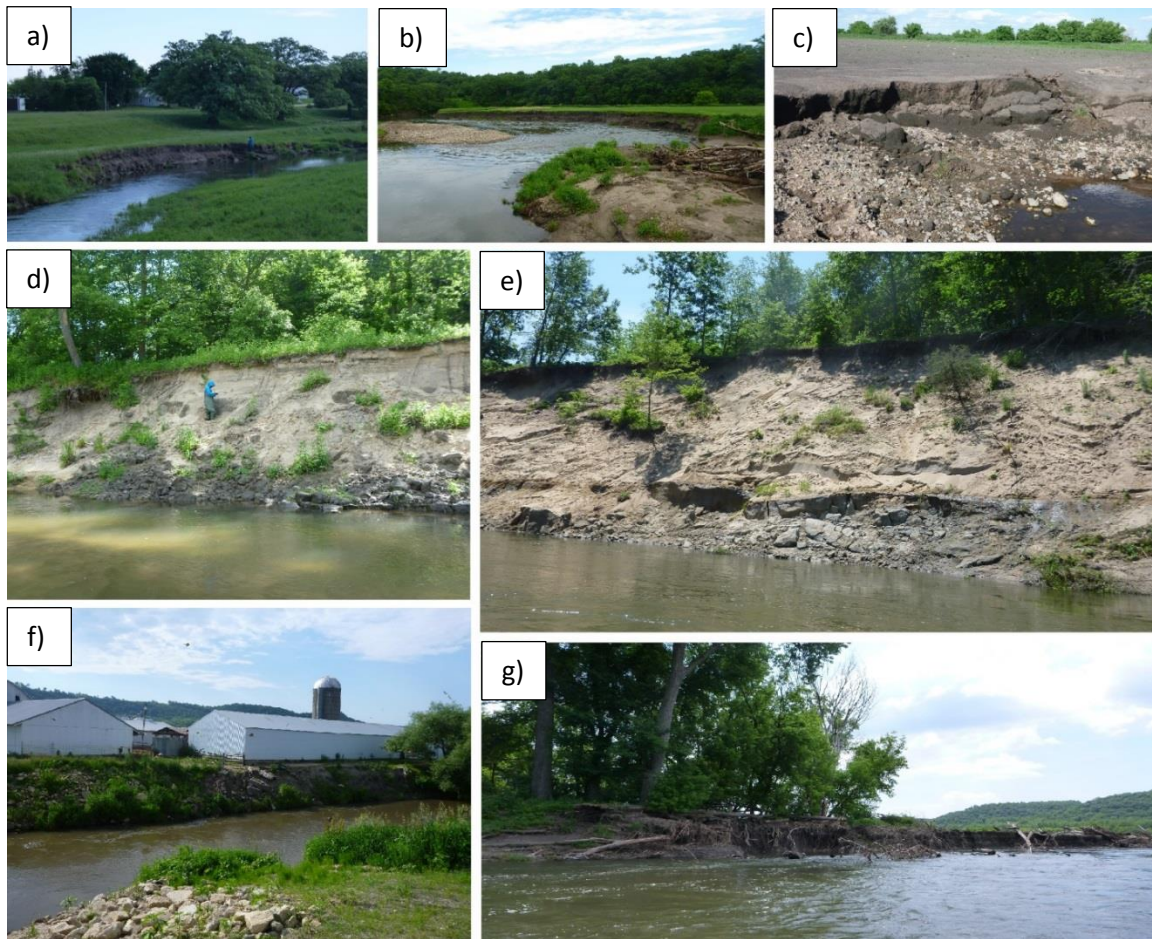


Figure 2.5. Different bank characteristics from channel network. a) North Branch, b) eroding bend at South Branch, c) eroding bank at one of the Middle Branches, d) sandy bank at Rushford Creek, e) paleo-channel at the main stem of the Root River, right after the confluence with Rushford Creek, f) Reinforced banks at South Fork, g) main stem of the Root River between the cities of Rushford and Houston.

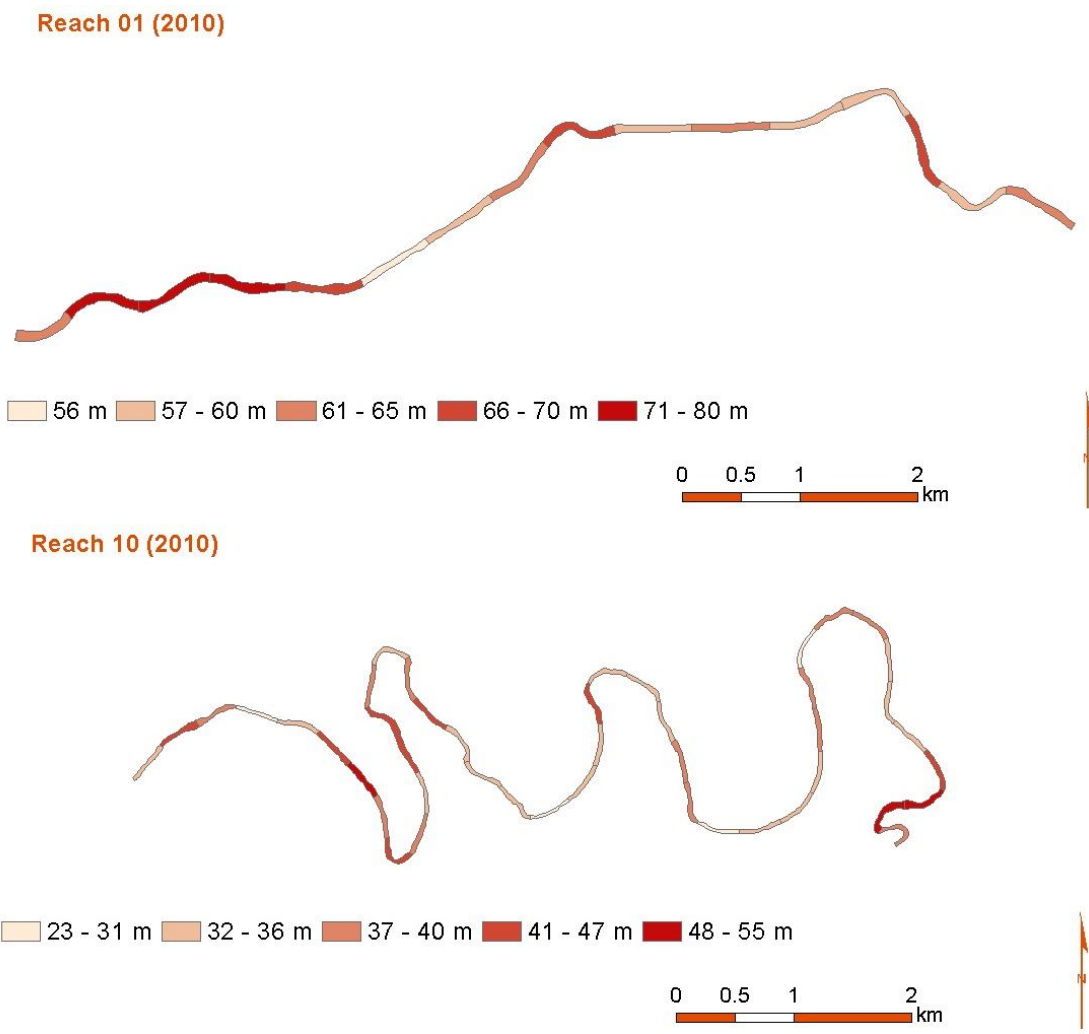


Figure 2.6. Sub-reach average width division example. Reaches 1 and 10 sub-reach average width 2003. Sub-polygons are about 10 times the average width of the whole reach.

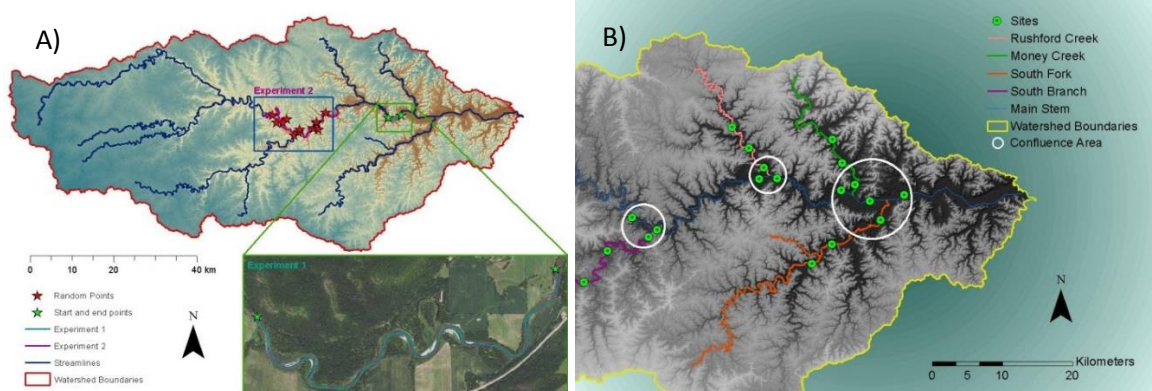


Figure 2.7. Error experiment locations and width validation sites. a) Error experiment Locations due to digitizer’s judgment, b) Width validation sites.

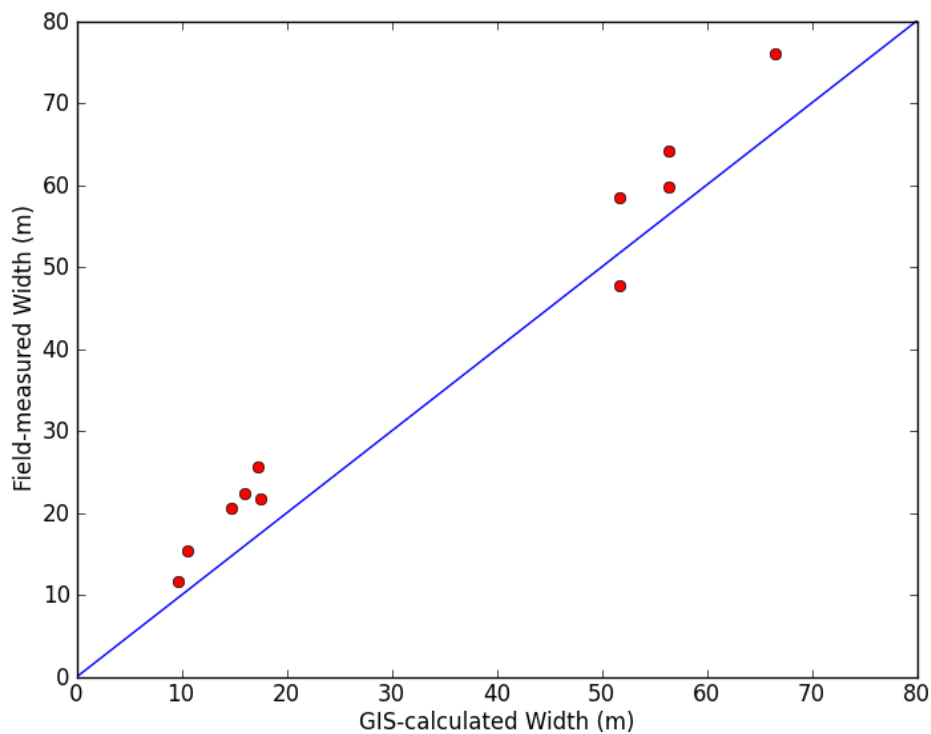


Figure 2.8. Average field-measured width 2013 versus average GIS-calculated width 2010. Blue line is a 1:1 line.

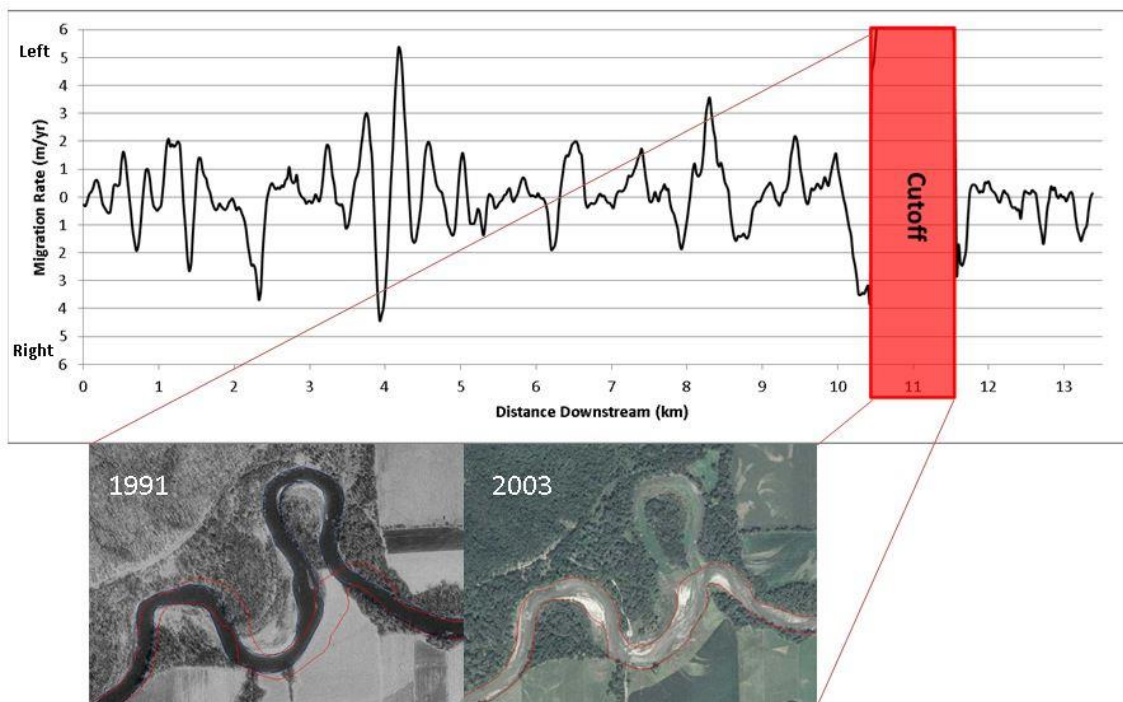


Figure 2.9. Aerial photographs of Root River main stem between Rushford and Houston for 1991 and 2003 with digitized banklines from 2003 overlain on the photos. Plot shows channel migration rates 1990s-2000s.

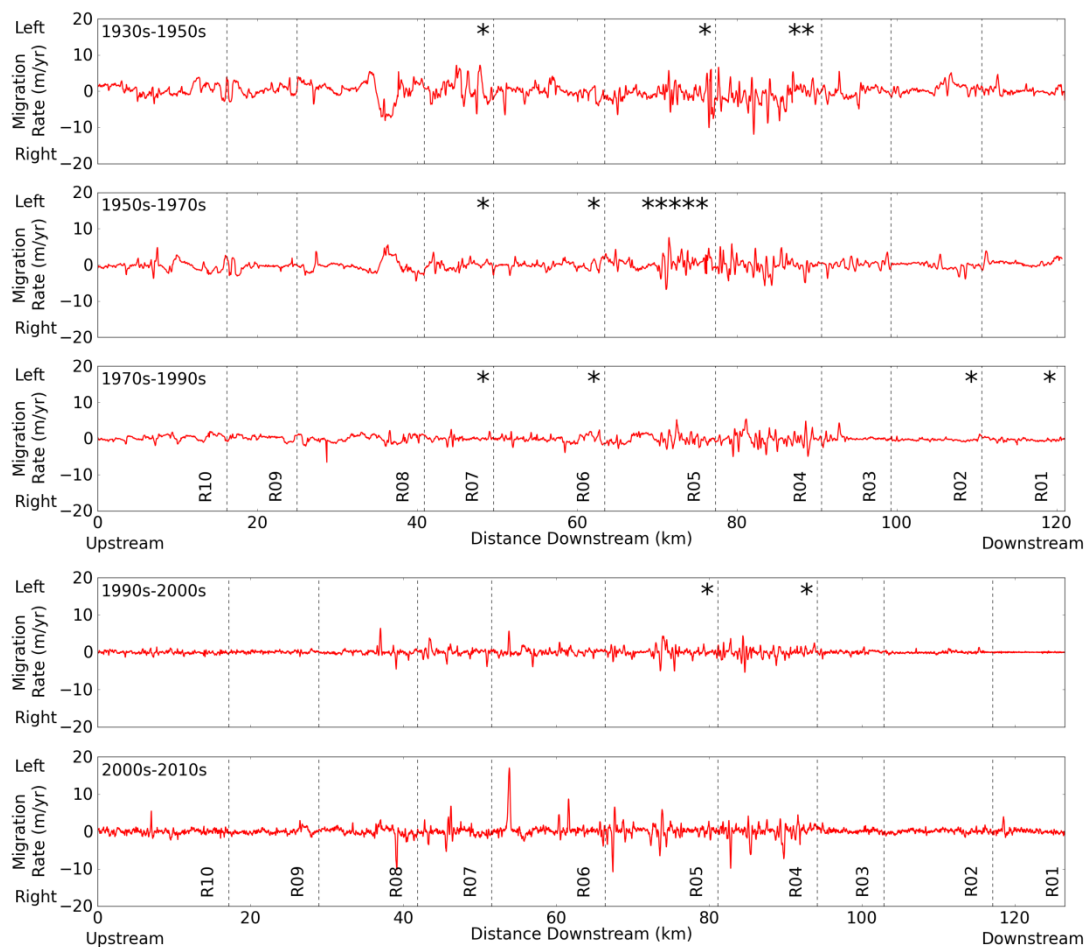


Figure 2.10. Migration rates main stem of the Root River from upstream to downstream. Migration to the left bank is positive; migration to the right bank is negative. Dashed lines are reach divisions. Starts on top of each reach area represent avulsions and abrupt changes in channel width.

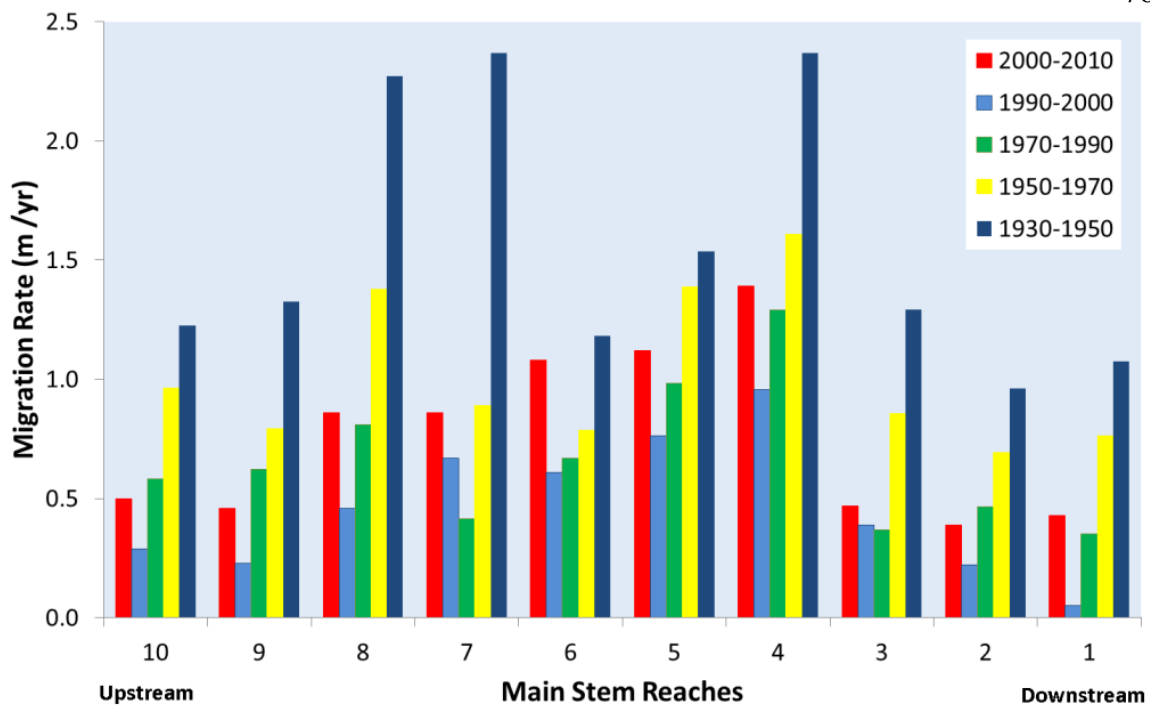


Figure 2.11. Average migration rates per reach, main stem of the Root River. Average migration rates have halved since the 1930s.

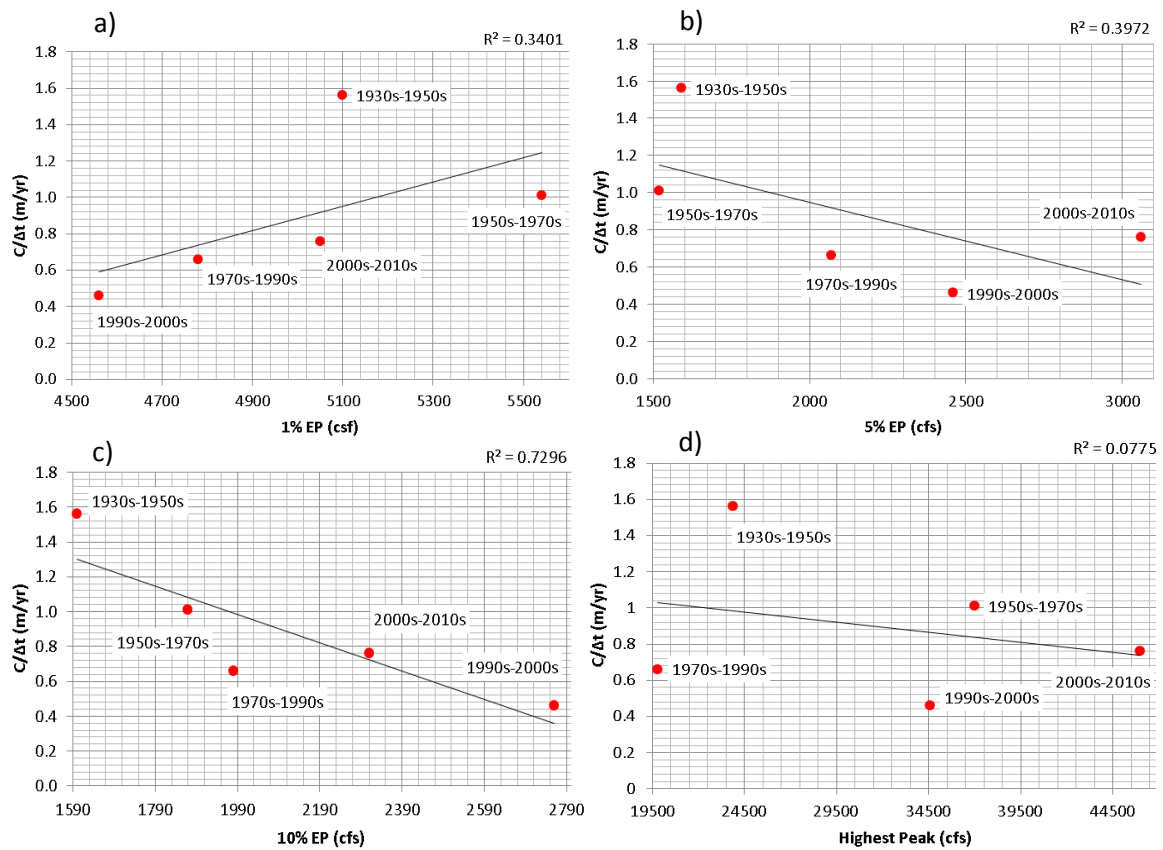


Figure 2.12. a) Average migration rates versus 1 % exceedance probability, b) average migration rates versus 5 % exceedance probability, c) average migration rates versus 10 % exceedance probability, d) average migration rates versus highest peak flow within the years of analysis. Channel migration is in meters per year. Exceedance probability and highest peak are in cubic meters per second.

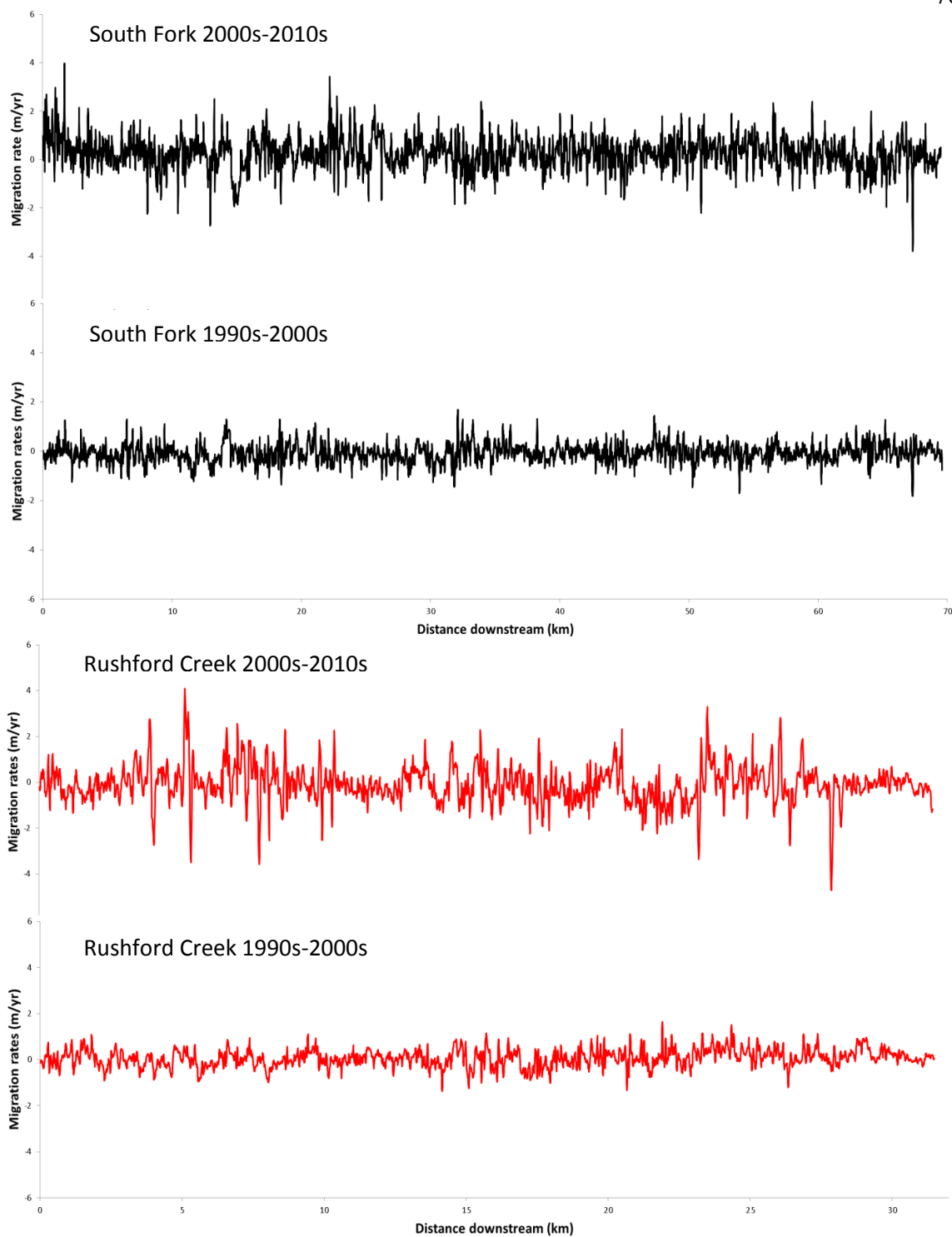


Figure 2.13. South Fork (in black) and Rushford Creek (in red) migration rates for the decades of 1990s-2000s and 2000s-2010s. The 1990s were notably less active than the 2000s.

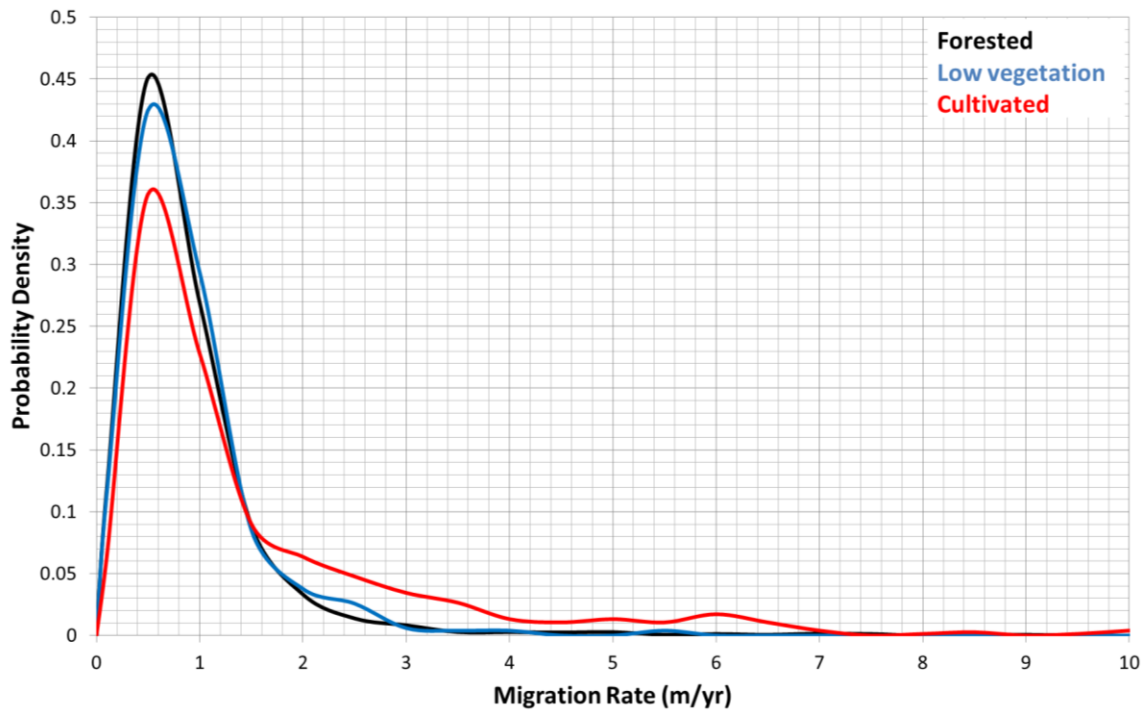
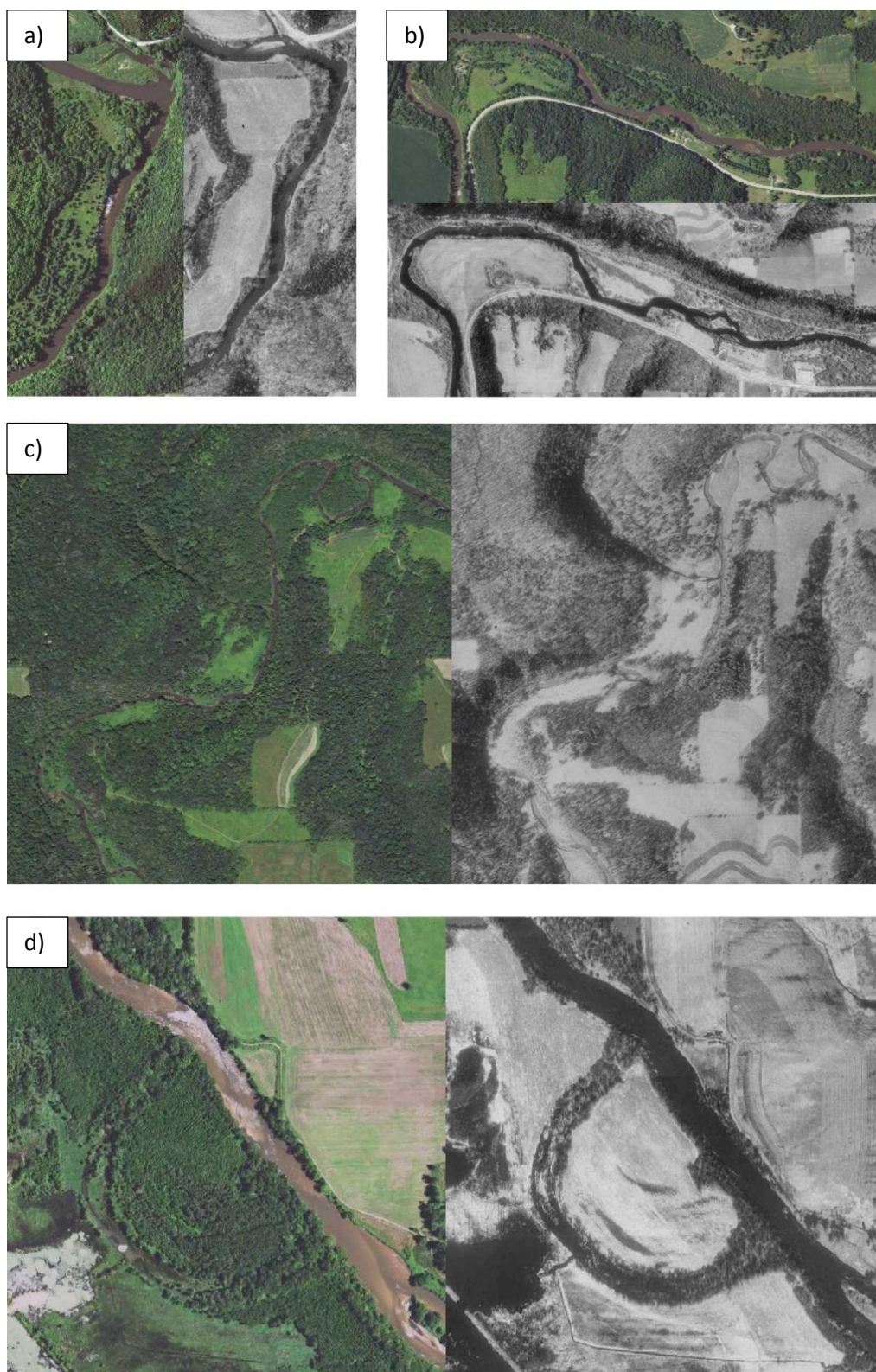


Figure 2.14. Probability distributions of the migration rates associated with different vegetation types. Solid line represents the migration rates of forested areas, dashed line represents the migration rates of low vegetation areas, and dash-dotted line represents the migration rates of cultivated areas.



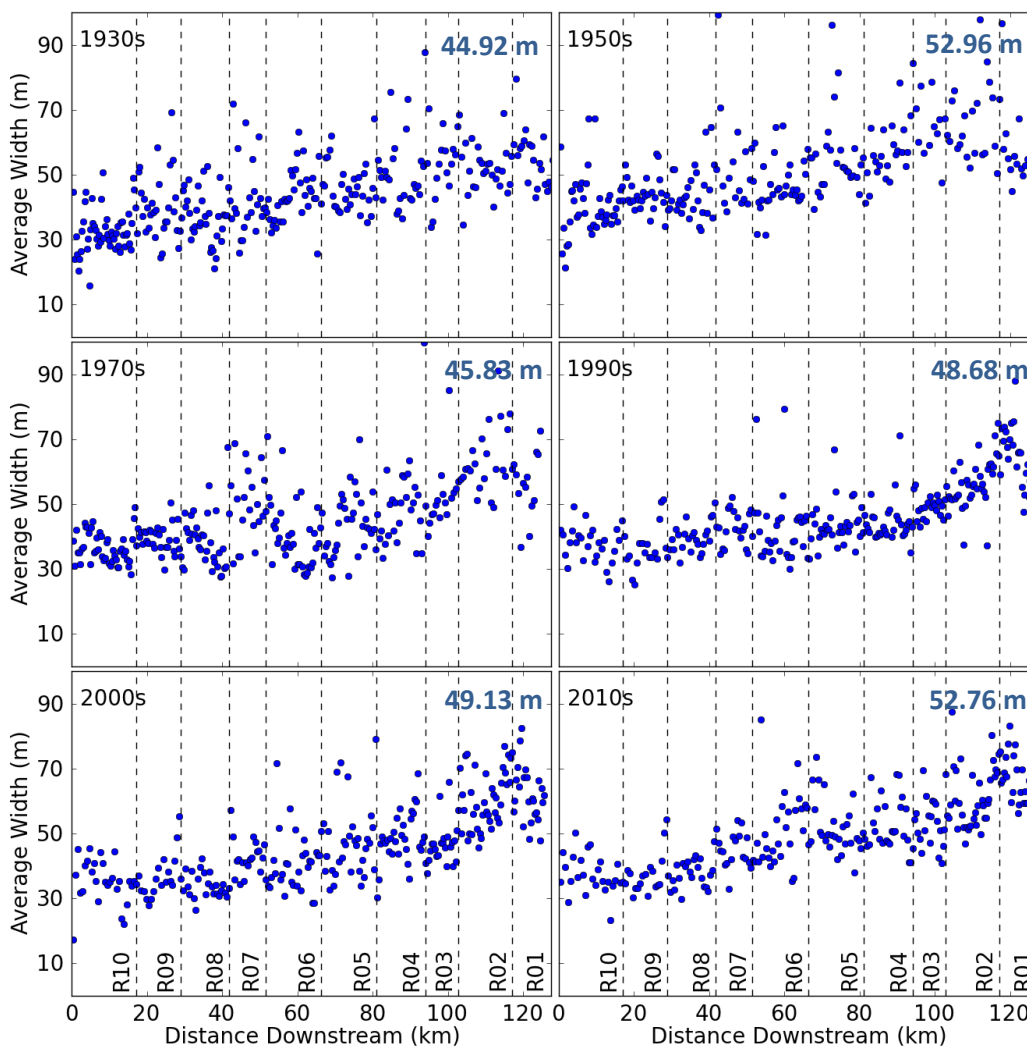


Figure 2.16. Sub-reach width, Root River. Each dot represents the average width of a sub-reach 10 times the average width of the reach. Blue number on top right is the average width for the entire main stem for that decade.

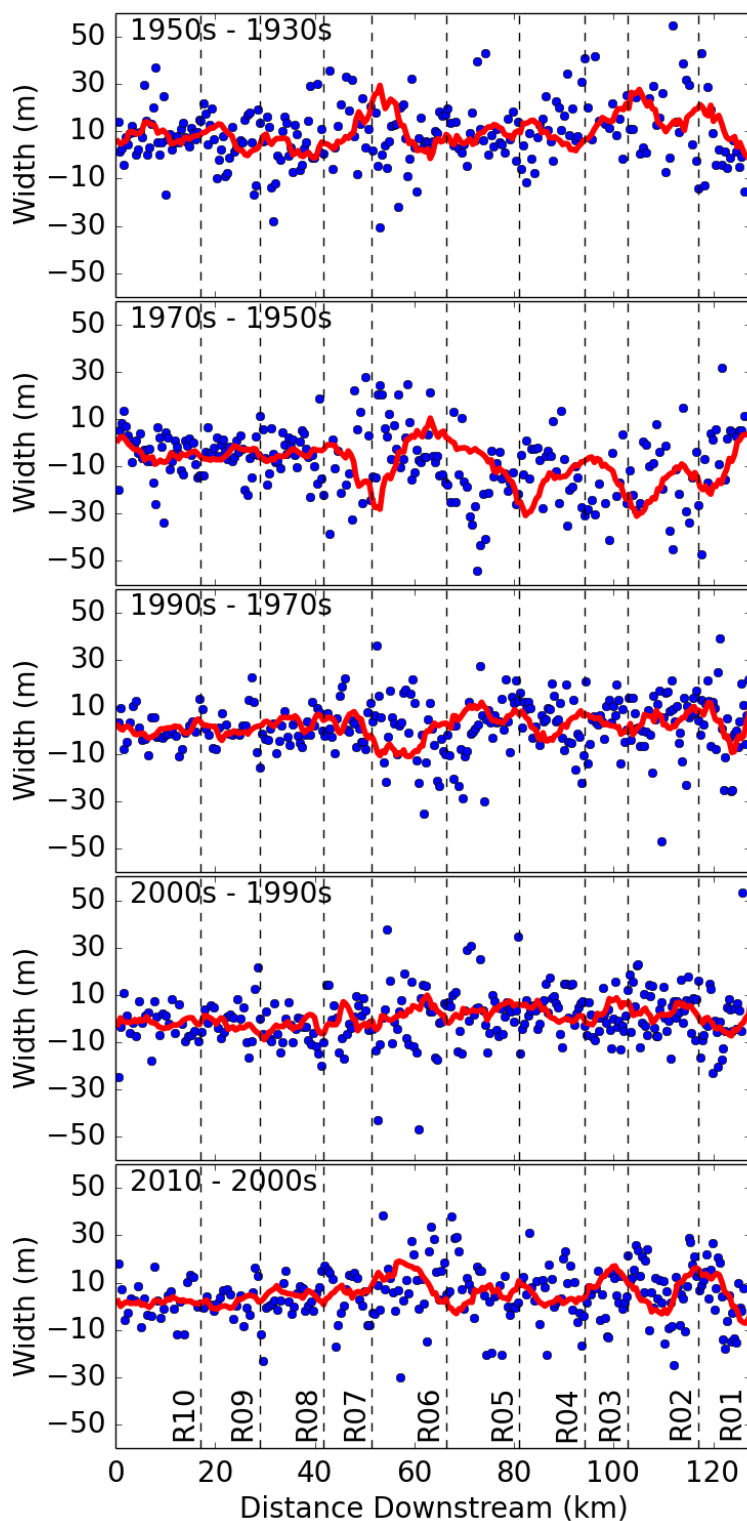


Figure 2.17. Delta sub-reach width, Root River. Each dot represents the difference between the average widths of a sub-reach 10 times the average width of the reach for two different decades. Red line represents the moving average of the blue dots.

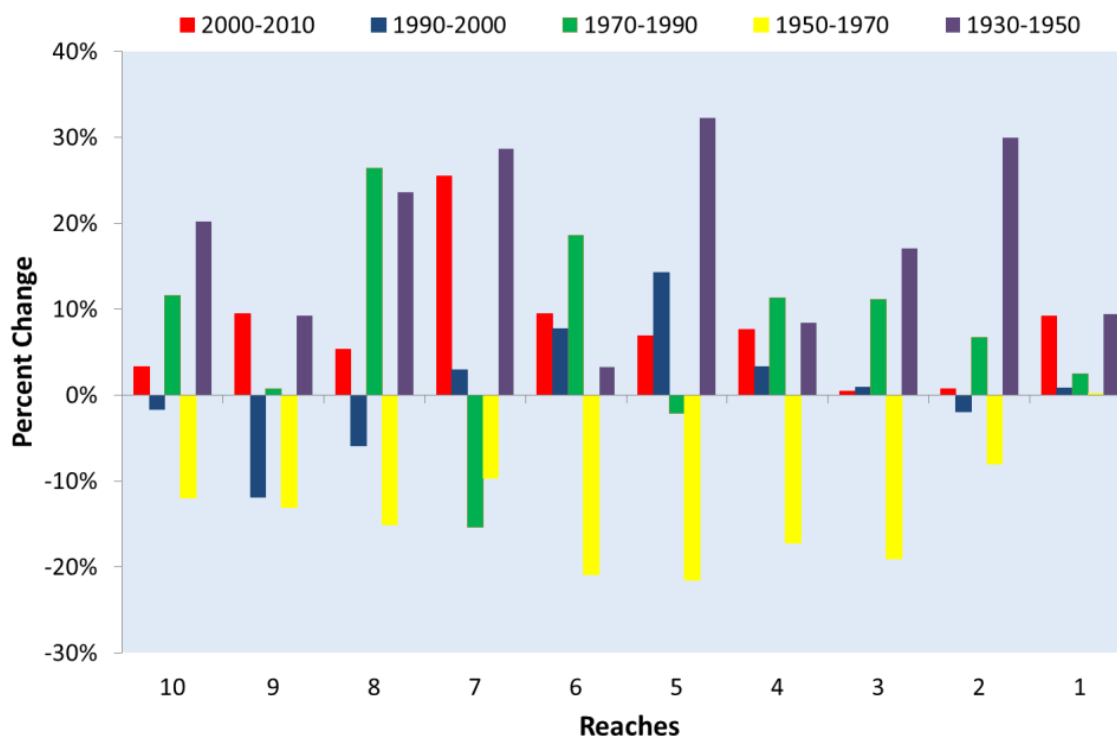


Figure 2.18. Percent width change per reach, Root River.

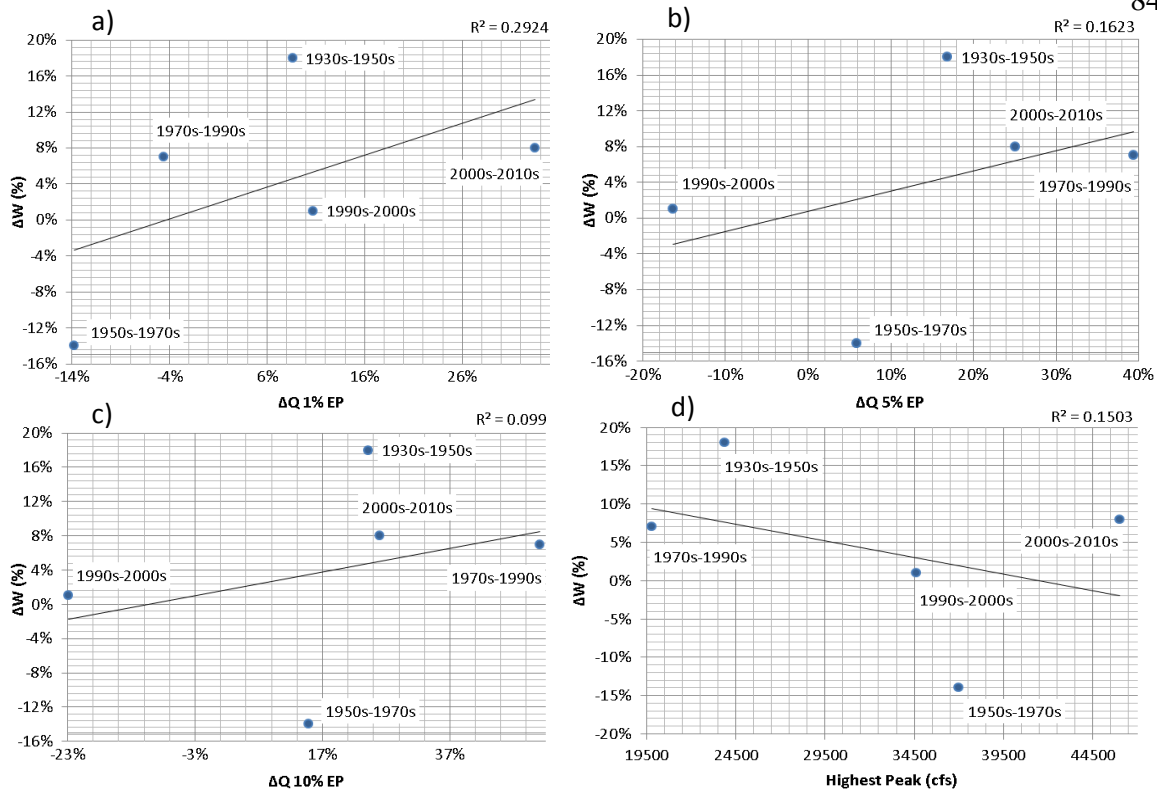


Figure 2.19. a) Average width percent change versus delta 1 % exceedance probability, b) Average width percent change versus delta 5 % exceedance probability, c) Average width percent change versus delta 10 % exceedance probability, d) average migration rates Average width percent change versus highest peak flow within the years of analysis. Average width percent change is in percent change, positive percent represents widening and negative percent represents narrowing. Delta Exceedance probability is the percentage that the 1, 5, or 10 % exceedance probability changed from one year to another.

## CHAPTER 3

CHANNEL-FLOODPLAIN SEDIMENT EXCHANGE IN THE ROOT RIVER,  
SOUTHEASTERN MINNESOTA**3.1 Introduction**

Understanding sediment fluxes at the watershed scale is important to constrain sediment budgets and to develop predictive models for river morphological changes. Naden (2010) describes fine sediment (<2 mm) as possibly the most important component of the sediment cascade due, among other things, to its cohesive characteristics and its ability to transport nutrients and contaminants. Furthermore, excess amounts of fine sediment alone can degrade aquatic habitats and water quality. This is because the portion of fine sediment smaller than 64  $\mu\text{m}$  (silt and clay) is chemically active, carrying with it many contaminants and nutrients. Excess amounts of fine sediment can cause turbidity problems in the water column as well (Owens et al., 2005).

Fine sediment in alluvial rivers is usually stored in its floodplains. Floodplains coevolve with their channels and can serve as sources of sediment from time to time depending on factors like climate, their morphology or ecological dynamics (Belmont, 2011). Geomorphic analysis in the Root River indicates that many reaches have easily accessible near-channel sources of sediment and that channel floodplain sediment interactions exert strong control on the flux of sediment in this river system (Stout et al., 2013). Currently, the Root River has a total of 104 reaches listed as impaired by the Minnesota Pollution Control Agency (MPCA) with 15 impaired by turbidity and 18 by

mercury, which is mainly transported by fine sediment

([http://cf.pca.state.mn.us/water/watershedweb/wdip/resultsList\\_impairments.cfm?huc=07040008](http://cf.pca.state.mn.us/water/watershedweb/wdip/resultsList_impairments.cfm?huc=07040008)). Another 50 reaches are simply listed as impaired for aquatic life, many of which are likely related to excessive amounts of fine sediment. In order to effectively respond to these impairments, we need to understand sediment sinks and sources throughout the watershed within the context of a sediment budget (see sediment budgets, chapter 1). The main goal of this chapter was to estimate the amount of sediment contributed to the channel from the floodplain to provide constraints for a sediment budget for the Root River watershed.

The processes of lateral channel adjustment can result in a net contribution of sediment to the channel. Sediment stored in floodplains is reworked as the channel moves laterally or changes its width. Channel widening results in a contribution of sediment from one or both banks. While less intuitive, the process of channel migration can also result in net contributions of sediment to the channel. Leopold and Wolman (1957) were among the first to document how the process of channel migration resulted in erosion of one bank and deposition on the other. Lauer and Parker (2008) developed a mathematical model to account for sediment sources and sinks related to channel migration at the channel cross section scale (see channel morphology, chapter 1).

Net contributions of fine sediment from the floodplain were estimated as follows. From a cross-sectional perspective, channel migration causes erosion and deposition in the outer and inner banks of the channel, respectively. One of the important assumptions of this model is that the outer bank is taller than the inner bank due to the fact that the inner bank is actively being built by sediment deposition and the outer bank is usually an

older floodplain. Wolman and Leopold (1957) noticed this tendency in meandering rivers and it has since been widely recognized. Lauer and Parker suggest that the net contribution of sediment at this specific location would be due to the difference in elevation between banks (see channel migration, chapter 1 and Figure 1.5). This method assumes that cross-sectional area remains the same throughout this process. Therefore, sediment fluxes due to changes in channel cross-sectional area (changes due to channel widening/narrowing) were estimated separately.

Lateral channel adjustment rates (quantified in chapter 2) and 2008 lidar data available for the entire watershed were combined to estimate the net volume of sediment from channel widening and migration. This analysis also included validation of lidar elevations, the effects of different vegetation types, and grain size distribution and bulk density analyses. A grain size distribution and bulk density campaign was conducted in summer 2013 to determine if and how floodplain/terrace grain size distributions vary throughout the Root River watershed and to estimate the sediment mass that is transported as washload (silt and clay). The net mass of fine sediment contributed to the channel was estimated from the combination of these datasets for the main stem of the Root River and its major tributaries.

### **3.2 Methods**

The net local mass of fine sediment contributed to the channel due to the processes of channel migration and widening was estimated by combining the channel adjustment analysis covered in chapter 2 with additional elevation data obtained from lidar, grain size distributions and bulk density measurements. The lidar analysis

consisted of the extraction of bank elevations from the 3 m resolution 2008 lidar data available for the entire watershed. The grain size and bulk density measurements were obtained from a sampling campaign of channel banks, floodplains and terraces throughout the entire watershed. The methods and procedures used in these analyses as well as the process of combining the three analyses (channel adjustment, lidar, and sediment distribution and bulk density analyses) into sediment mass and the uncertainty present in this analysis are detailed below.

### **3.2.1 Lidar Analysis**

To estimate the net, local contributions of fine sediment from channel migration one must know the channel migration rate and difference in elevation of opposing banks along the entire reach/river of interest (see Figure 1.5.d and associated text in chapter 1). Channel migration rates were measured in chapter 2. For the current analysis we used only the migration rates measured for the most recent two decades. The 2008 lidar topography data was used to measure the difference in elevation of opposing banks (referred to as “delta eta” or  $\Delta\eta$  following Lauer and Parker (2008)). We assumed that the delta eta values obtained from this year were representative for the most recent decades and that bank elevations have not changed appreciably in the past two decades. This assumption was based on the fact that the rates of lateral erosion in the Root River (see results, chapter 2) are quite slow (up to 2 m/yr) relative to the total width of its floodplains. These relatively small rates, compared to the wide floodplain they are destroying/creating suggest that it would take a long time for lateral adjustment processes

to rework an entire floodplain or even appreciably change the distribution of bank elevations at the scale of the entire channel network.

### **3.2.2 Extracting bank elevations**

A bank elevation extraction was conducted in order to calculate delta eta. To extract elevations along each bank, polygon boxes were automatically generated as a buffer along the manually digitized channel banklines using the Planform Statistics Toolbox developed by J. Wesley Lauer (<http://www.nced.umn.edu/content/stream-restoration-toolbox>) (see methods, chapter 1). A new set of banklines was created using the 2008 lidar (rather than the aerial photographs) so that the polygon boxes would exactly match the edge of the channel. Breaks in elevation were used as the main indicator of the edge of bank, but the 2010 aerial photographs were used as a backup to verify ambiguous areas where the rise in elevation was too gradual or difficult to identify. Polygon boxes were created using the Bank Buffer Tool of the Planform Statistics Toolbox. A range of polygon widths were tested in the main stem of the river (1, 2, 5 and 10 m) to quantify the sensitivity of delta eta measurements to polygon width. While 1, 2, and 5 yielded similar results, the 10 m polygon boxes yielded higher delta etas in general. Polygon boxes were chosen to be 2 m wide and 25 m long based on the length assigned to the migration polygons and a width wide enough to get a good estimate of the average elevation of the floodplain considering that average lateral channel adjustment rates did not exceed 2 m/yr.

A python script was used to calculate delta eta from opposing banks. The script extracted the elevations from the lidar using the Zonal Statistics as Table function from

the Arcpy module and then subtracting left and right arrays of data to obtain delta eta.

The output results from the script were comma-separated value (csv) files with average right and left elevations, delta eta and absolute value of delta eta.

### **3.2.3 Cross Sections**

Different locations throughout the watershed were surveyed to estimate average bankfull depth. Cross sections were collected in summer 2012 using a Nikon NPL-332 Total Station at 6 different locations (Figure 3.1). Each survey was between 150 and 200 m with a separation of approximately 15 m between cross sections. Historical cross sections near Houston obtained from the Minnesota Water Resources Division office of the USGS were also used. Average height was estimated for these sites and extrapolated to other reaches with the same stream order and similar channel width throughout the rest of the channel network. This data was used to estimate the volume of sediment contributed to the channel due to channel widening.

### **3.2.4 Grain Size Distribution**

A grain size sampling campaign was conducted in the Root River in summer 2013. This campaign consisted of collecting sediment samples from 20 bank sites throughout the Root River channel network (Figures 3.1, 3.2) to analyze sediment grain size distribution and bulk density. Sample locations were selected mainly based on floodplain height and local channel adjustment rates. Samples were generally collected from vertical, actively eroding banks, with 3 replicate samples collected at the each location.

Grain size distributions were measured using a Sequoia Scientific LISST-Portable particle size laser diffractometer (Sequoia, 2011). The analysis procedure consisted of placing a small, well-mixed portion of the sample into the 175 mL chamber of the instrument filled with deionized water where a laser detects the light scattering pattern of the sample. The instrument offers two methods that assume different particle shapes (spherical or random) for processing of the data. The random shape model was chosen for this analysis due to the fact that sediment particles in a river environment rarely present a perfect spherical shape. Agrawal et al. (2008) show that while smooth, rounded but random-shaped particles usually tend to behave like spheres, the scattering signature of particles that have large angles is recognizably different from sphere-like particles. Therefore, in this scenario a random shape model is more consistent with all particles.

The time that the instrument takes to measure light diffraction on each sample is selectable and ranges from 5 to 120 seconds. It is recommended that the duration is increased from the default (5 seconds) when low concentration samples are measured to reduce the influence of random noise in the results. The optimal concentration range for the instrument is determined as a function of percent transmission. Recommended transmission values range from 30 to 90 %. Stout et al. (2013) used 20 seconds for his grain size analysis of sediment collected from terraces of the Root River. A 20 second duration was also chosen for this analysis, making sure that the sample concentration was always between 30 and 70 % transmission. The chamber of the instrument was rinsed after analyzing the three samples for the same location to make sure that no particles from a previous location remained when analyzing another location. Results were exported into an ASCII file, which contains the processed data in a comma-separated

format. The ASCII files were imported into a template spreadsheet provided by the manufacturer to produce grain size distribution figures.

### 3.2.5 Bulk Density

Bulk density samples were collected at the same sample locations as the grain size samples. A metal cylinder with a volume of 114.5 cm<sup>3</sup> was used to collect the samples. The metal cylinder was inserted into the vertical bank, which was previously cleared of vegetation, and then excavated and scraped into a bag using a small trowel. Bulk density samples were collected at 17 out of the 20 sites selected. In the lab, samples were weighed before and after being oven-dried, using a Mettler Toledo balance model SB12001. This instrument had a readability of 0.1 g and a repeatability of 0.1 g. Samples were weighed twice to test the repeatability. Results were within 0.1g for all samples. Samples were dried at 120 °F for 48 hours using a Grieve oven model SA-400. Once the dried samples were weighed, bulk density for each sample was calculated as:

$$\rho = \frac{M}{V} \quad (Eq. 3.1)$$

where  $\rho$  is the bulk density,  $M$  is the dry weight, and  $V$  is the volume of the metal cylinder used to collect the samples.

Grain size distribution and bulk density results were averaged throughout the Root River. Values were averaged for most of the tributaries as well, with the exceptions of Rushford and the North Branch, where the distributions were coarser and in general seemed to be spatially related. The percent smaller than 67  $\mu\text{m}$  was used because the

percent of fine sediment comprised of silt and clay that usually goes as washload has a grain size distribution smaller than 64  $\mu\text{m}$ .

### 3.2.6 Sediment Mass

Fine sediment contributions from the floodplain to the channel were calculated for the more recent decades by multiplying the channel adjustment rate, bulk density and grain sizes, and difference in elevation between the two banks or total bank height depending on the mass calculated for channel migration or channel widening. Sediment contributions were calculated for each 25 m increment for channel migration and ten times the average reach width for channel widening. Sediment mass contributed to the channel due to channel migration and channel widening was calculated using the following formulas:

$$E_M = C \Delta\eta S D_{<67} \rho \quad (\text{Eq. 3.2. a})$$

$$E_W = W \left[ 2 \left( H_{bf} + \frac{\Delta\eta}{2} \right) \right] S D_{<67} \rho \quad (\text{Eq. 3.2. b})$$

where  $E_C$  is the net, local sediment mass contributed to the channel,  $C$  is the migration rate,  $\Delta\eta$  is delta eta,  $S$  is the length of the bank ( $S = 25$  m for channel migration;  $S = 10$  times the average width of the reach),  $D_{<67}$  is the percent of sediment smaller than 67  $\mu\text{m}$ ,  $\rho$  is the bulk density,  $E_W$  is the net, local sediment mass contributed to the channel due to channel widening,  $W$  is the channel widening/narrowing rate, and  $H_{bf}$  is the average bankfull height of the channel.

A python script was used to calculate the total sediment contributions due to channel migration by organizing the variables into numpy arrays and multiplying them all together. Results were output into comma-separated files. An excel spreadsheet was used to calculate the sediment volume contributions due to channel widening.

### **3.3 Error Analysis and Validation**

An error analysis to determine the accuracy of the elevations extracted from the 2008 lidar of the Root River was done using control points collected by county and contracted surveyors at the time of the lidar flight. More than 100 validation points were collected and used to verify the vertical accuracy of the lidar data. Accuracy assessments from these points were completed using RTK-GPS and techniques established by the National Standard for Spatial Data Accuracy (NSSDA). These conventional estimates of error for each county were: Fillmore 0.155 m, Houston 0.134 m, Mower 0.170 m, Olmsted 0.117 m, and Winona 0.161 m.

However, the general estimates of error provided above are not necessarily representative of error in the near-channel environment that is the focus of this study. The actual error in these near-channel environments may be lower in locations with minimal vegetation cover, or may be higher in locations with high density of vegetation. Control points from Houston and Fillmore counties, which include most of the main stem of the Root River, were used in combination with a land cover analysis of the floodplain area to determine the effects of different vegetation types on the difference between control points and lidar elevation (Figure 3.4) (see methods, chapter 2). This analysis helped us identify and distribute uncertainty based on the vegetation cover.

ArcMap was used to assign a vegetation class (cultivated, low vegetation, or forested) to the ground control points. Control points were scattered throughout the counties of Houston and Fillmore. Only the points that were in the valley area were used for the analysis, totaling 23 points. For each vegetation class, control point elevations were compared to elevation values extracted from the lidar topography data. The RMSE between control points and lidar elevations was calculated for each vegetation type.

A validation of the difference in elevation between opposing banks was also conducted. Following the logic of Lauer and Parker (2008), for the process of channel migration to result in a net contribution of sediment to the channel, the channel has to migrate towards its taller bank. It is normally accepted that this is how meandering rivers behave; however, there are exceptions. Therefore, a validation of delta eta values was conducted to make sure that net sediment contributions were only included in cases where the channel was migrating into its taller bank. A Python script implementing a series of “if” statements was used to eliminate locations where the channel appeared to be migrating toward the shorter of its bank or where bank heights were virtually the same. For example, from upstream to downstream if the channel migrated to the left and delta eta (left - right bank elevations) was negative, the value was deleted. Instances where the channel appeared to have migrated towards its shorter bank were excluded. The difference in sediment volume estimated with and without the cases when the channel appeared to be migrating into the shorter of its two banks for the decade of 2000-2010 was calculated to determine if this purge of values had a significant influence in the overall net sediment contribution to the channel due to channel migration.

### **3.3.1 Error Analysis Results**

The RMSE comparing the control point and lidar-derived elevations for the three floodplain vegetation classes were very similar to the county-average error. Errors for each vegetation type were 0.15 m for cultivated land, 0.12 m for low vegetation, and 0.12 m for forested land. Error in elevations considering the effects of vegetation did not offer strong results that distinguished the effects of different vegetation types on lidar elevation. This was probably due to the reduced number of points analyzed. An average of 7 points was used for each vegetation type. Since the errors could not be tight to vegetation cover and the values obtained for each vegetation type were still lower than the values obtained for each county, the error in lidar elevations was estimated to be 0.15 m by averaging the county error values showed above.

### **3.4 Results and Discussions**

The mass of fine sediment contributed from near-channel sources due to the processes of channel migration and channel widening was calculated for the Root River. Sediment mass results helped us better understand sediment dynamics in the Root River and the importance of near-channel sediment sources. These results will also be used to constrain a sediment budget for the Root River watershed. Based on prior work done in and near the Root River, we expected to see a fair amount of sediment coming from the floodplains. Results presented below show how the combination of factors used to estimate sediment mass varied over the entire channel network and the influence that these had in the sediment mass results.

### 3.4.1 Lidar Analysis

Lidar analysis consisted of the extraction of bank heights along the channel network of the Root River. These bank heights were used to calculate the difference in elevation between opposing banks (delta eta,  $\Delta\eta$ ). Figure 3.5 shows the absolute elevation of right and left banks as well as delta eta for all ten reaches of the main stem of the Root River. Average delta etas ranged from 0.13 m to 0.78 m in the Main stem. Reach 2 had the smallest difference in bank heights with an average of 0.13 m. Reach 10, upstream, had the greatest difference in bank heights with an average of 0.78 m. Average delta eta for the tributaries were 1.43, 0.89, 0.92, 1.58, 1.38, and 1.44 m for South Fork, Rushford Creek, South Branch, North Branch, Money Creek, and Middle Branch, respectively.

### 3.4.2 Grain Size Distribution and Bulk Density

Table 3.1 shows the grain size distributions for the samples collected in the Root River. Stout et al. (2013) measured the ratio of the percent of sediment smaller than 250  $\mu\text{m}$  and the percent larger than 250  $\mu\text{m}$  against terrace height and found what appeared to be a fining of grain size distributions as one goes from the taller terraces far from the channel to the younger and shorter floodplains closer to the channel (see methods, chapter 1). We wanted to determine if this fining pattern was apparent in the relatively low floodplains and terraces (<4 m tall) that comprise most of the banks throughout the channel network, in which case floodplain/terrace height could be used for extrapolation of grain size data throughout the watershed. Figure 3.6 shows different grain size distribution metrics (percent smaller than 67  $\mu\text{m}$ , median size, and the percent smaller

than 67  $\mu\text{m}$  divided by the percent greater than 67  $\mu\text{m}$ ) plotted against bank height. The percent of sediment smaller than 67  $\mu\text{m}$  was used because fine sediment (silt and clay) that leaves the system as washload is usually considered to be smaller than 64  $\mu\text{m}$ . The trends followed by each tributary and the main stem can be visualized in the figure. Outliers within the results of the same stream were easily identified; allowing us to evaluate these areas separately and determine why they did not follow the same trend than the other values in the same stream.

The grain size distributions of the banks did not appear to change systematically with respect to the bank heights. This is probably due to the relatively small range of heights along the channel network. Figure 3.7 shows the distributions of floodplain heights along the Root River channel network. About 90 % of the floodplains do not exceed 5 m. Rushford Creek has the coarsest distribution, followed by the North Branch; this makes sense because the Rushford Creek and the North Branch watersheds are underlain by very sandy soils. The main stem of the Root River has the finest distribution with the exception of one sample site, which was immediately after Rushford Creek and appeared to be a paleo-channel filled mostly with sand (see Figure 2.5.e).

All this information helped in the decision of extrapolating results to the entire watershed based on specific tributaries. This was done because no trends other than the spatial distribution of specific tributaries was found. From this, an average 73 % of the sediment eroded due to lateral channel adjustment was estimated to be smaller than 67  $\mu\text{m}$  for the main stem and its tributaries with the exceptions of Rushford Creek and the North Branch. Only a 54 % of the sediment eroded was considered to be smaller than 67

$\mu\text{m}$  due to the higher presence of sand in these tributaries. Standard error was estimated to be 17 %.

Table 3.2 shows the bulk density results for the samples collected. Results varied from 1.0 to 1.7  $\text{g}/\text{cm}^3$ . Standard error was calculated to be 0.1  $\text{g}/\text{cm}^3$  from the sample values collected, being the equivalent to a 7.7 % of the average 1.3  $\text{g}/\text{cm}^3$  bulk density assumed in the analysis for the entire watershed. Bulk density values were necessary to convert computed sediment volumes to mass.

Since average values were used to extrapolate grain size distributions and bulk density, the uncertainty added due to this extrapolation was estimated based on how much our averages departed from the values in our samples. The combined standard error due to the extrapolation of grain size distributions and bulk density was estimated to be 24.7 %.

### **3.4.3 Sediment Mass**

Sediment mass results are presented in Figure 3.8 and table 3.3. While most of the fine sediment is coming from the main stem of the Root River, tributaries are also an important source contributing more than half of the total sediment mass calculated. The total amount of fine sediment ( $<67 \mu\text{m}$ ) contributed to the Root River due to lateral channel adjustment for the last decade was estimated to be  $3.0 \times 10^5 \text{ Mg/yr}$ . The main stem contributes  $1.3 \times 10^5 \text{ Mg/yr}$ , followed by the North Branch with  $4.9 \times 10^4 \text{ Mg/yr}$ , the Middle Branch with  $5.1 \times 10^4 \text{ Mg/yr}$ , the South Branch with  $2.2 \times 10^4 \text{ Mg/yr}$ , South Fork with  $2.6 \times 10^4 \text{ Mg/yr}$ , Rushford Creek with  $9.8 \times 10^3 \text{ Mg/yr}$ , and Money Creek with  $9.8 \times 10^3 \text{ Mg/yr}$ . The total uncertainty in these calculations was estimated to be 60 % by

combining the different sources of error from chapters 2 and 3. In order to account for this uncertainty, channel adjustment and lidar values that were below their respective error thresholds were excluded from the calculations (see Error Analysis Results, chapter 2 and chapter 3) and final results were reduced by a 25 % to account for the uncertainty due to the extrapolation of grain size distribution and bulk density throughout the Root River watershed (see Grain Size Distribution and Bulk Density, chapter 3).

### 3.5 References

- Agrawal, Y.C., Whitmire, A., Mikkelsen, O.A., Pottsmith, H.C., 2008. Light scattering by random shaped particles and consequences on measuring suspended sediments by laser diffraction. *J. Geophys. Res.*, 113(C4), C04023.
- Belmont, P., 2011. Floodplain width adjustments in response to rapid base level fall and knickpoint migration. *Geomorphology*. 128 (1-2): 92-102.
- Day, S.S., 2012. Anthropogenically-intensified erosion in incising river systems. Ph.D. Thesis, University of Minnesota. Minneapolis, Minnesota.
- Lauer, J.W., Parker, G., 2008. Net local removal of floodplain sediment by river meander migration. *Geomorphology*, 96 (1-2): 123-149.
- Leopold, L.B. Wolman, M.G., 1957. River channel patterns: Braided, meandering and straight. USGS Professional Paper 282-B: 39-103.
- Naden, P.S., 2010. The Fine-Sediment Cascade, Sediment Cascades. In: Burt, T., Allison, R. (Eds.), *Sediment Cascades: An Integrated Approach*. John Wiley & Sons, Ltd. Centre for Ecology and Hydrology, UK, pp. 271-305.
- Owens, P.N., Batalla, r. j., Collins, A.J., a. j., Gomez, B., Hicks, D.M., Horowitz, A.J., Kondolf, G.M., Marden, M., Page, M.J., Peacock, D.H., Petticrew, E.L., Salomonsk, W., and Trustruml, N.A., 2005. Fine-grained sediment in river systems: environmental significance and management issues. *River Research and Applications*. 21: 693-717.
- Sequoia, 2011. LISST-Portable User's Guide Version 3.11. In: S.S. Inc.
- Stout, J.C., Belmont, P., Schottler, S.P., Willenbring, J.K., 2013. Identifying Sediment Sources and Sinks in the Root River, Southeastern Minnesota. *Annals Assoc. Am. Geographers*. 104(1): 20-39

Wolman, M.G. and Leopold, L.B., 1957. River flood plains: some observations on their formation. Washington, DC: USDA Geol. Survey. 282-C: 86-109.

Table 3.1. Root River grain size distribution

Sample Code	X	Y	Bank Height (m)	Lidar Elevation (m)	Percent <67 $\mu\text{m}$	D10 ( $\mu\text{m}$ )	D50 ( $\mu\text{m}$ )	D84 ( $\mu\text{m}$ )
MS05	634526	4848313	1.95	195.42	98.0 %	4.54	16.07	33.76
SF02	617741	4846940	2.6	207.11	67.3 %	8.4	46.12	162.68
MS04	608457	4847227	2.6	212.99	76.5 %	7.08	36.09	102.96
RC01	596903	4854994	0.72	227.83	38.4 %	16.31	118.17	246.89
SB01	568119	4834401	2.2	300.25	72.5 %	6.57	34.22	142.16
NB03	567092	4851140	3.09	285.16	80.1 %	5.46	23.42	89.56
NB02	562074	4855572	1.34	294.43	96.7 %	1.24	13.24	29.71
NB01	534166	4855820	2.26	377.30	19.5 %	27.06	175.88	280.43
MB101	534742	4837549	1.71	405.29	72.1 %	3.58	22.53	155.1
SF01	594811	4832811	2.8	220.95	72.2 %	9.16	38.38	111.39
MC01	604625	4858220	1.64	229.41	71.6 %	10.35	38.02	124.08
MS01	594318	4848770	2.76	226.94	69.4 %	8.51	41.72	152.95
SB02	572744	4829249	1.77	313.92	76.3 %	6.65	33.66	109.8
MS02	603406	4850602	0.89	215.93	89.6 %	4.91	21.29	54.39
RC02	598297	4854982	2.59	229.96	52.0 %	10.35	107.52	197.17
SB03	577723	4840198	3.76	268.92	68.8 %	11.09	51.16	139.47
SB04	583461	4842622	1.92	243.80	60.7 %	8.35	45.62	200.79
RC03	598729	4854543	2.55	224.85	49.1 %	91.06	136.98	182.02
MS02B	604983	4849155	2.94	216.13	86.8 %	5.08	22.07	63.66
MS03	605655	4849310	1.64	212.60	38.8 %	15.18	147.73	342.83

Table 3.2. Root River bulk density

Sample Code	X	Y	Dry Weight (g)	Bulk Density (g/cm <sup>3</sup> )
SF01	594811	4832811	127.2	1.1
SF02	617741	4846940	140.4	1.2
MS01	594318	4848770	129.7	1.1
MS02	603406	4850602	130.2	1.1
MS04	608457	4847227	143.1	1.3
MS05	634526	4848313	144.6	1.3
NB01	534166	4855820	175.5	1.5
NB02	562074	4855572	134.2	1.2
NB03	567092	4851140	149.7	1.3
SB01	568119	4834401	163.6	1.4
SB02	572744	4829249	161.4	1.4
SB03	577723	4840198	142.3	1.2
SB04	583461	4842622	128.6	1.1
RC01	596903	4854994	144.4	1.3
RC02	598297	4854982	192.3	1.7
MB101	534742	4837549	117.8	1.0
MC01	604625	4858220	119.1	1.0

Table 3.3. Average sediment volume and sediment mass results per tributary

Root River Main streams	Widening		Migration		Total		
	Volume (m <sup>3</sup> /yr)	Volume <67 µm (m <sup>3</sup> /yr)	Volume (m <sup>3</sup> /yr)	Volume <67 µm (m <sup>3</sup> /yr)	Volume (m <sup>3</sup> /yr)	Volume <67 µm (m <sup>3</sup> /yr)	Mass* (Mg/yr)
Main Stem	150389	109784	23715	17312	174104	127096	1.3 x 10 <sup>5</sup>
South Fork	2791	2037	33917	24759	36708	26797	2.6 x 10 <sup>4</sup>
Rushford Creek	9839	5510	7712	4319	17551	9829	9.8 x 10 <sup>3</sup>
South Branch	12490	9118	18407	13437	30897	22555	2.2 x 10 <sup>4</sup>
North Branch	68353	38278	20856	11679	89209	49957	4.9 x 10 <sup>4</sup>
Money Creek	8221	6002	5357	3910	13578	9912	9.8 x 10 <sup>3</sup>
Middle Branch	51200	37376	20060	14644	71260	52020	5.1 x 10 <sup>4</sup>
					433307	298165	3.0 x 10 <sup>5</sup>

\*25 % reduction applied to sediment mass results.

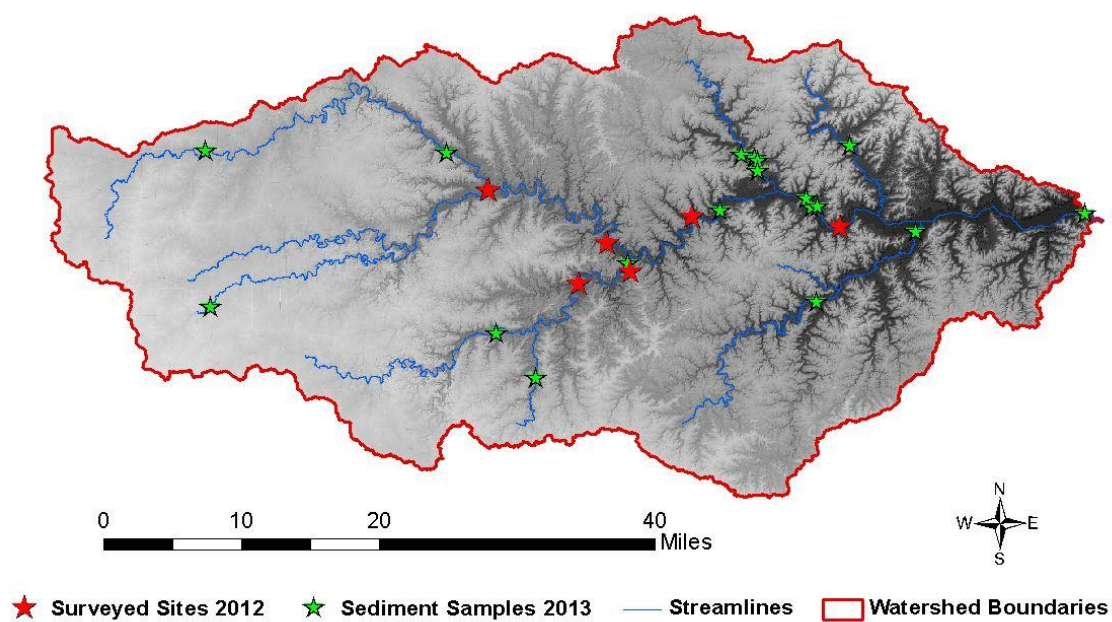


Figure 3.1. Surveyed sites (in red) collected in June, 2012 and sediment sample locations (in green) collected in June, 2013 for measurement of grain size and bulk density.



Figure 3.2. Grain size and bulk density campaign, summer 2013. a) banks upstream the North Branch, b) vertical bank from where grain size samples were collected, c) vertical bank after collecting bulk density sample, d) sandy banks at Rushford Creek.

a)



b)



Figure 3.3. a) LISST-Portable particle size laser diffractometer, b) Mettler Toledo balance model SB12001 and Grieve oven model SA-400.

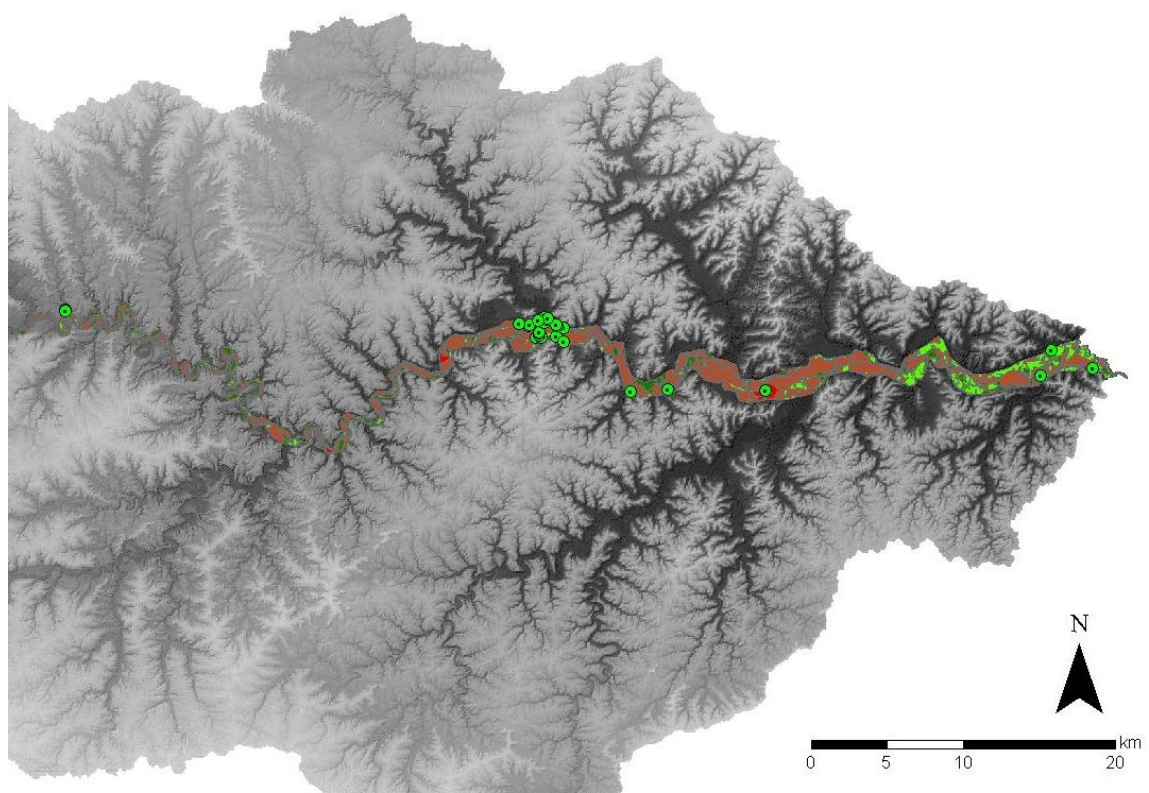
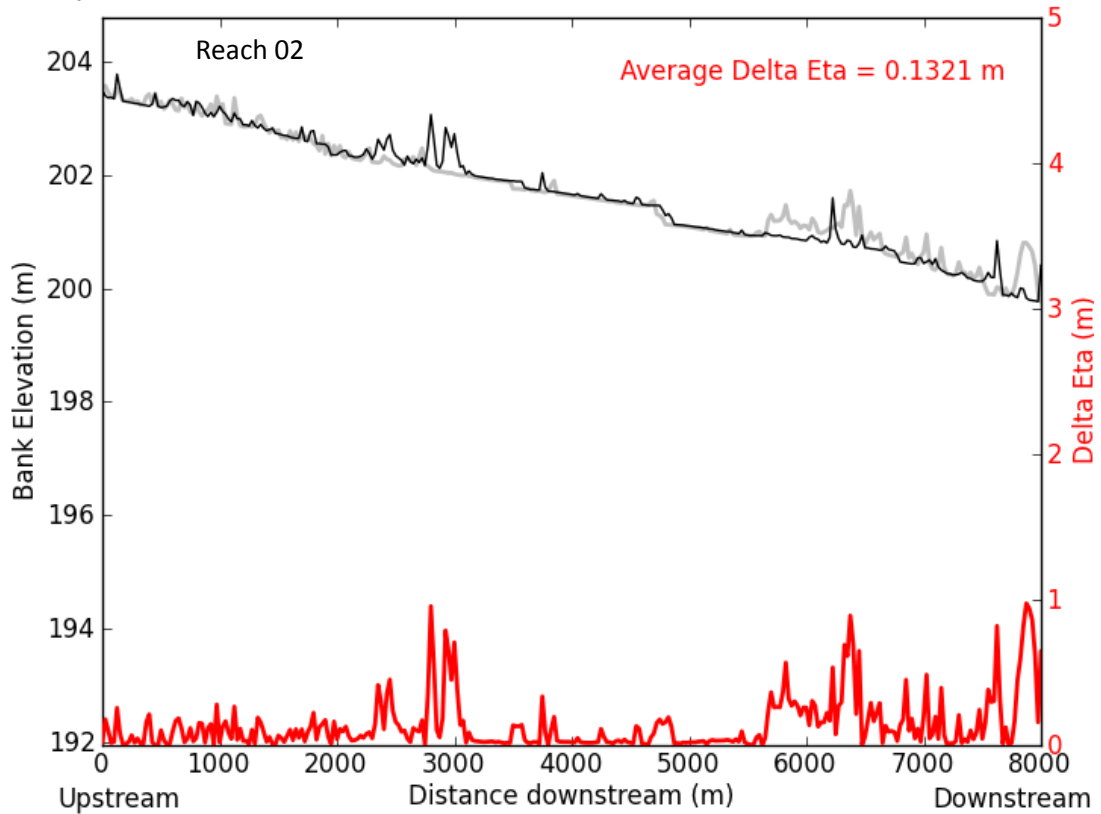
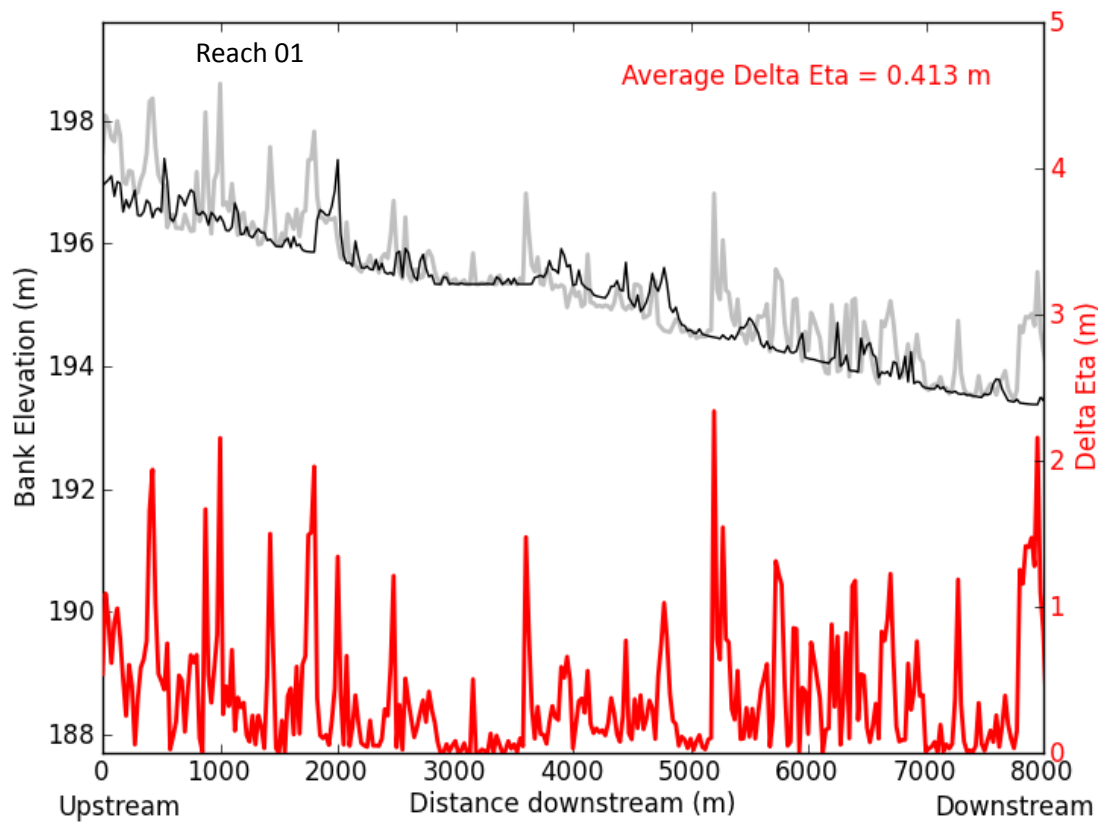
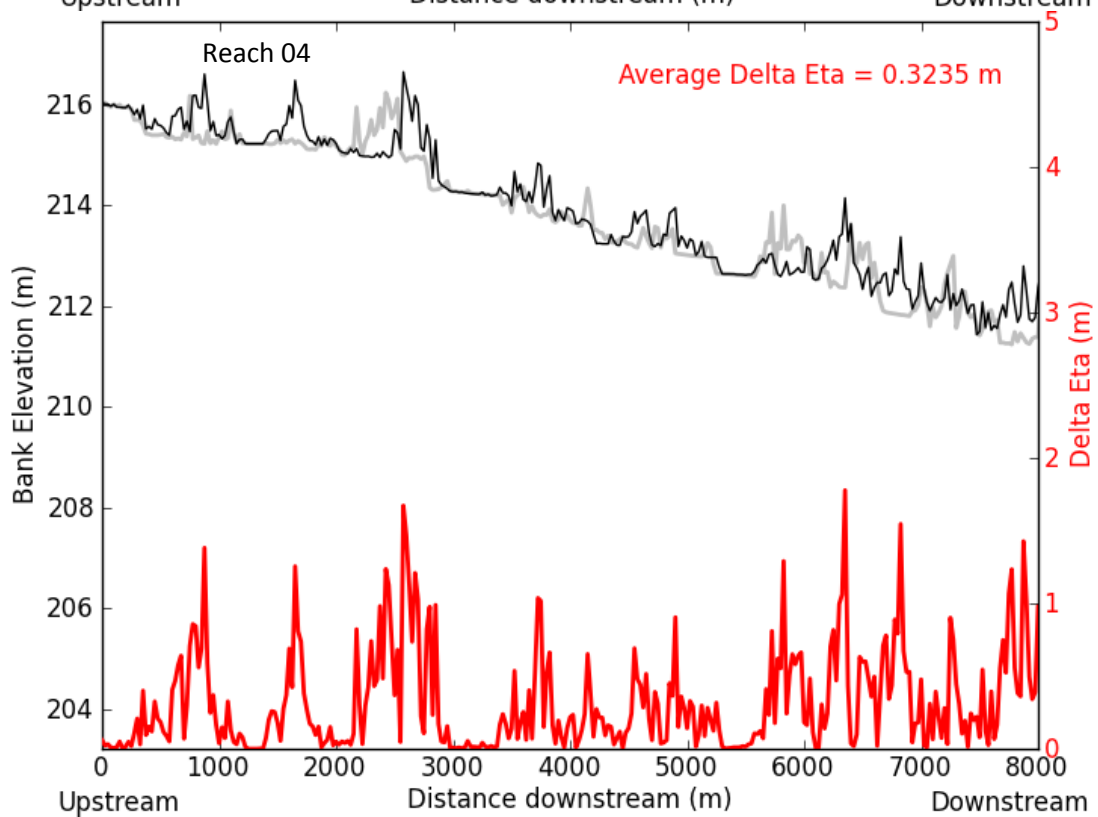
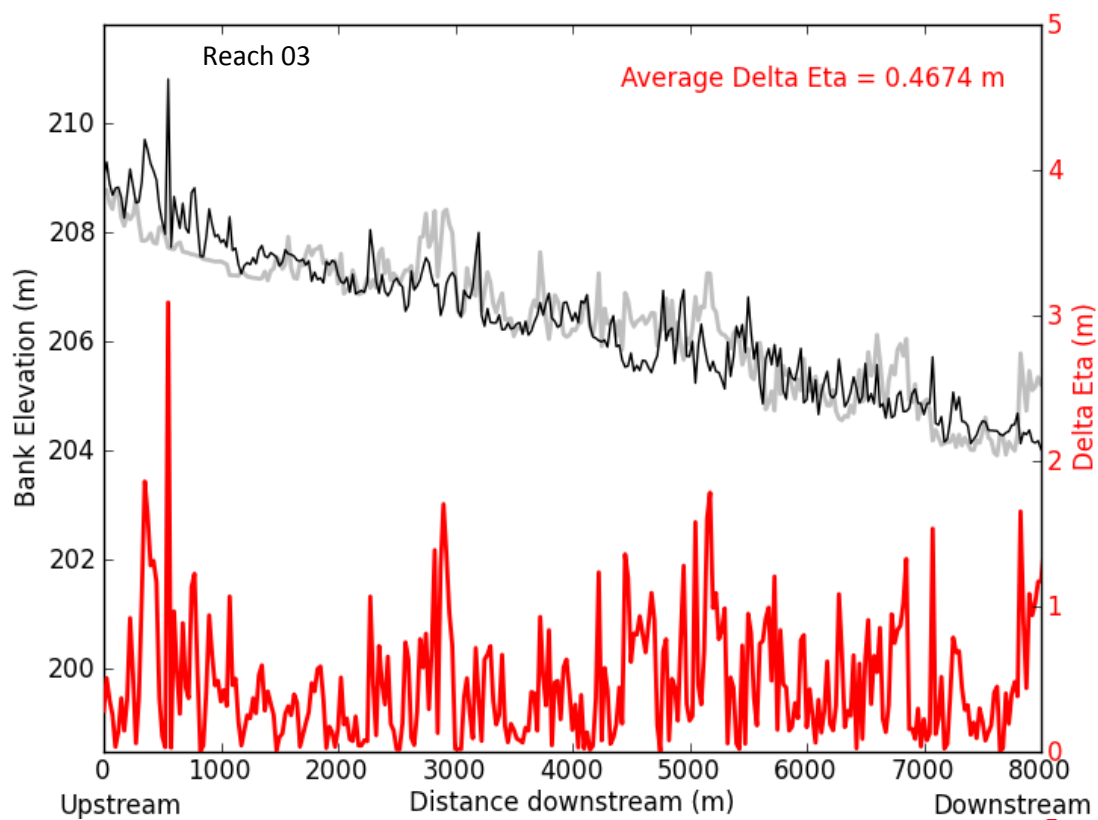
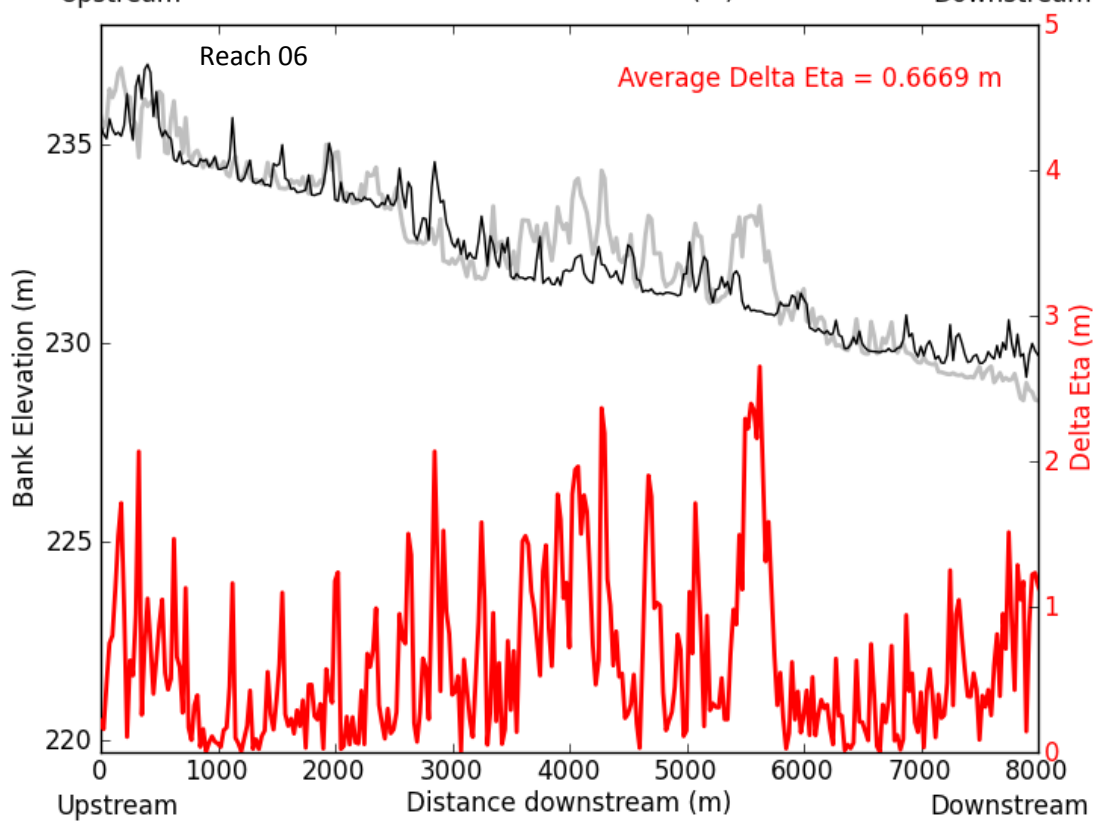
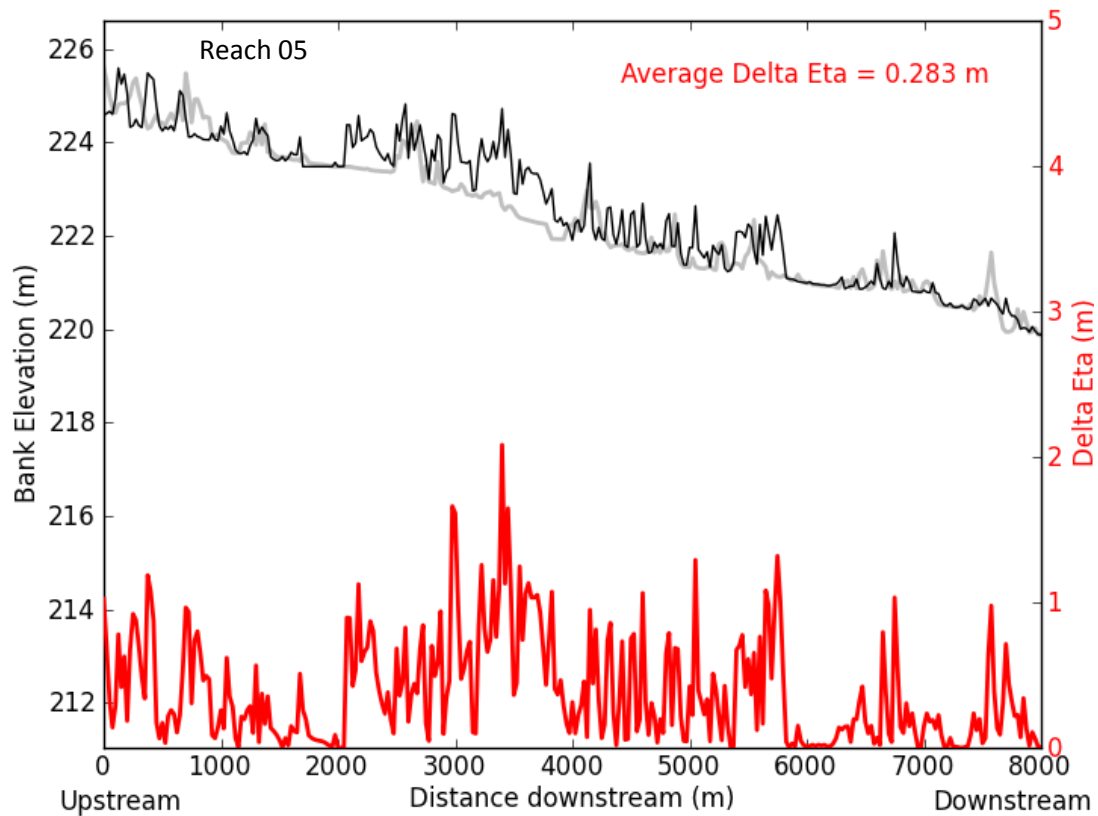
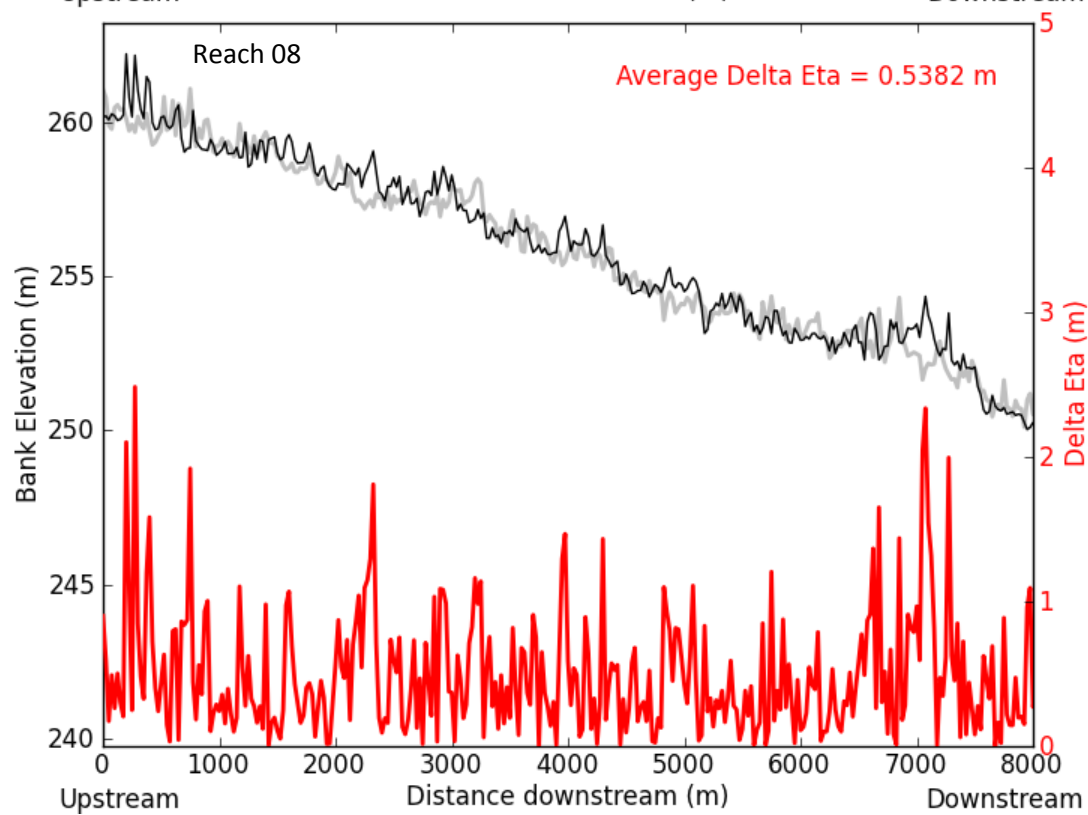
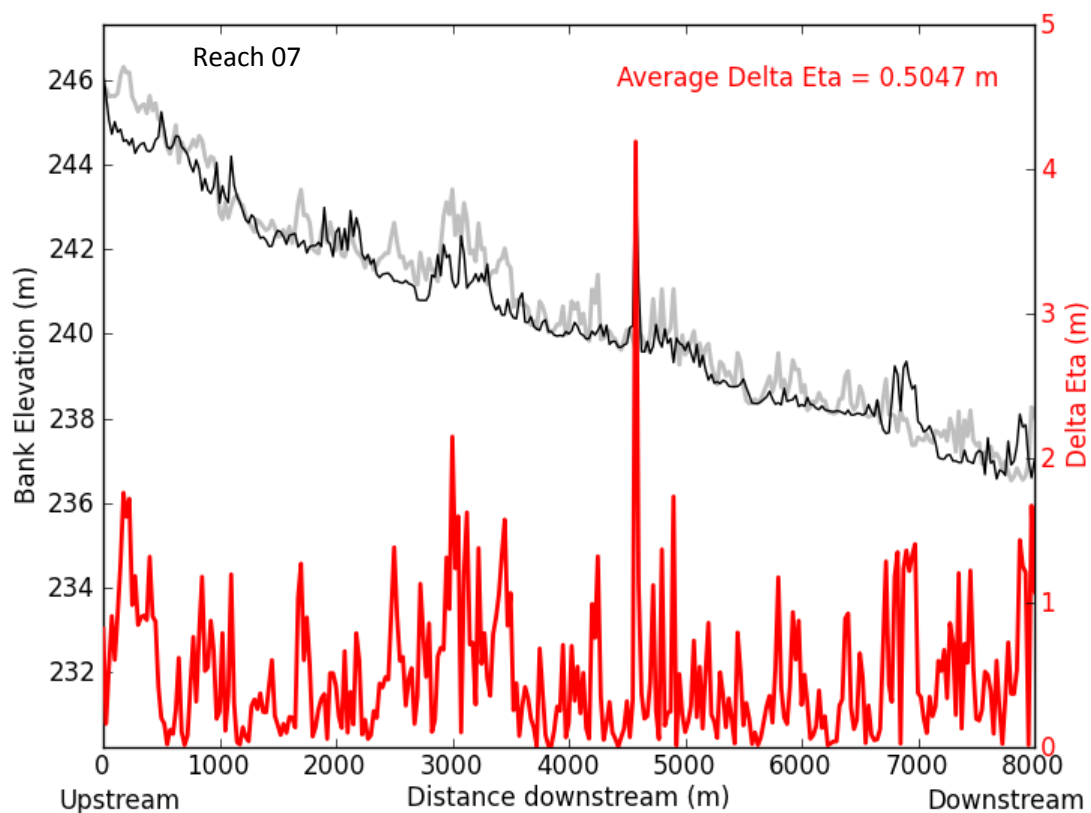


Figure 3.4. Root River main stem. Control points and vegetation cover: Cultivated land in brown, forested land in dark green, low vegetation in bright green and urban areas in red.









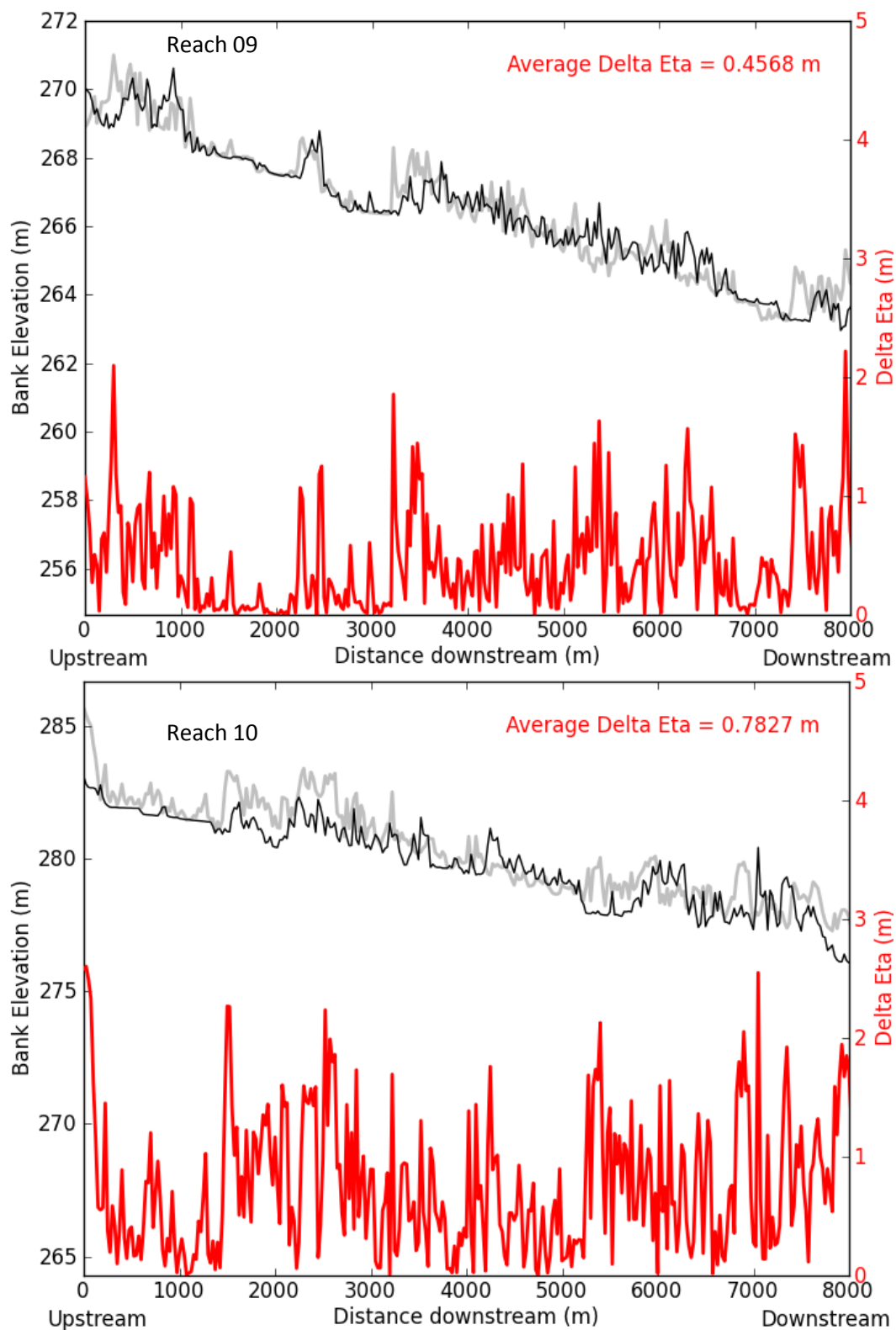


Figure 3.5. Right bank (black), left bank (gray) elevations, and Delta eta (red) extracted from 2008 lidar. First 8000 m of each reach of the main stem of the Root River.

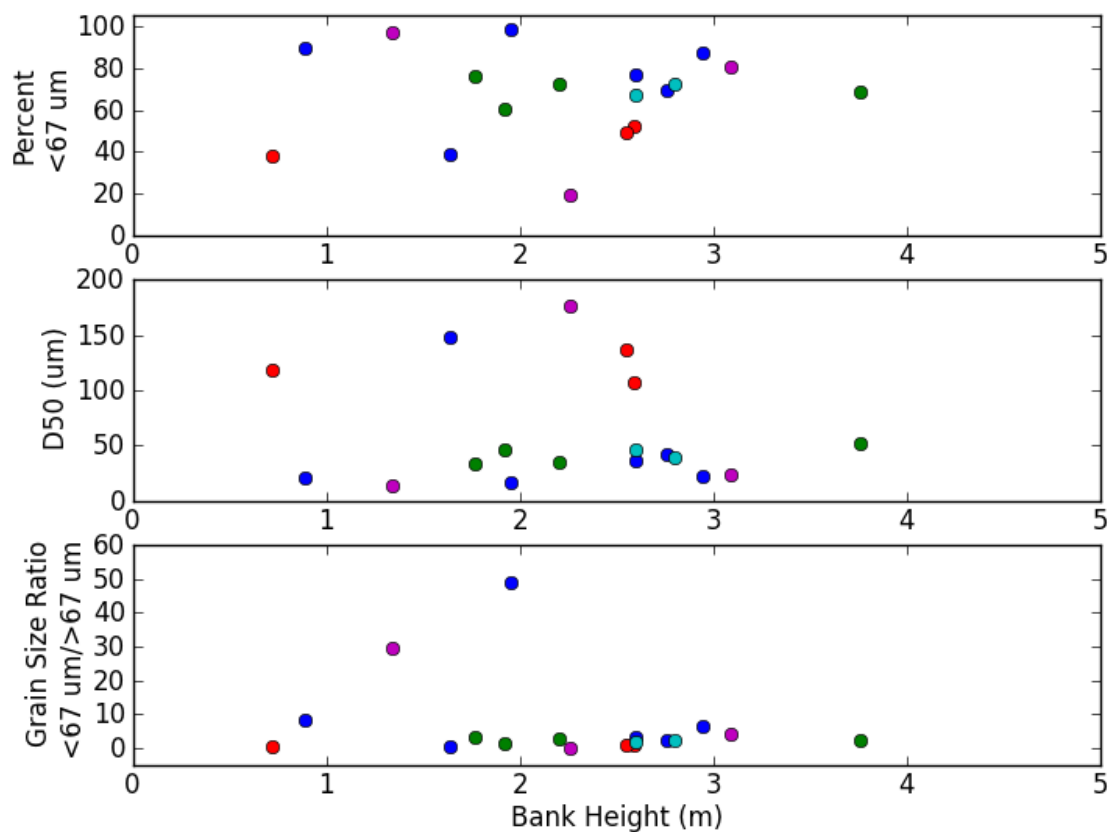


Figure 3.6. Grain size changes with bank height. a) Percent smaller than 67 microns, b) Median size and c) grain size ratio percent smaller than 67 microns and percent greater than 67 microns. Blue, red, green, magenta and cyan colors represent the main stem of the river, Rushford Creek, South Branch, North Branch and South Fork, respectively.

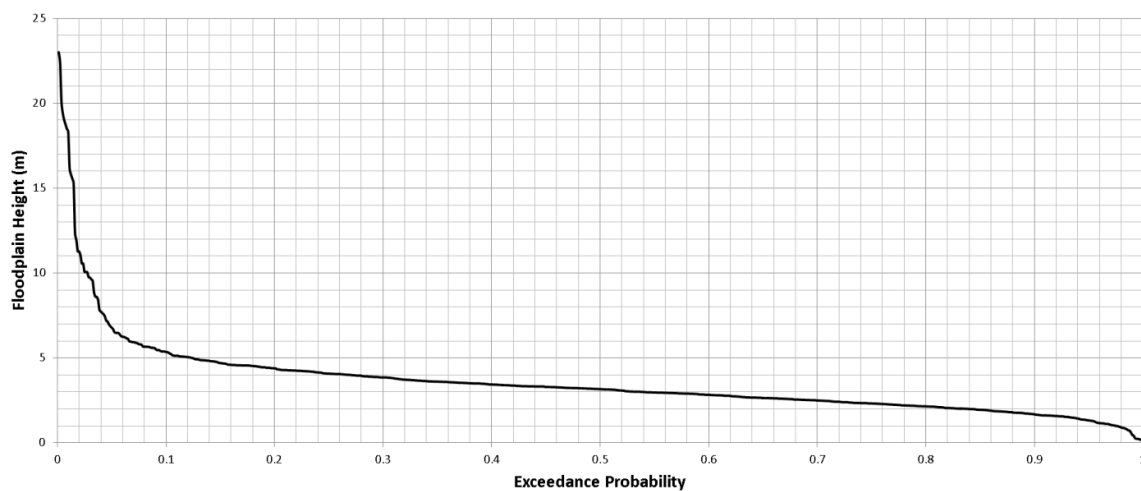


Figure 3.7. A cumulative exceedance probability distribution plot of floodplain and terrace heights along the Root River.

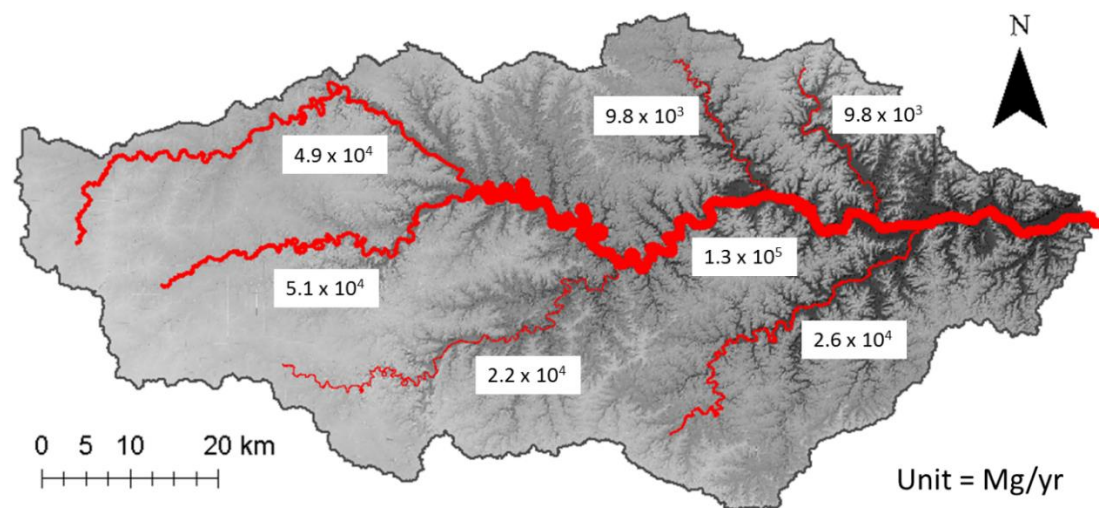


Figure 3.8. Fine sediment contributions (<math><67 \mu\text{m}</math>) due to lateral channel adjustment. Results are presented in annual averages.

## CHAPTER 4

## SUMMARY AND FUTURE WORK

**4.1 Summary**

Lateral channel adjustment depends on a combination of multiple factors. Changes in water supply do not necessarily result in changes in channel morphology as it is commonly assumed. There are many factors that contribute to lateral channel adjustment (Hassan et al., 2005). Factors like sediment fluxes and bank stability are very important to determine channel morphology and how a river evolves (Braudrick et al., 2009; Naden, 2010). In the case of the Root River, we found that even though high and low flows have increased substantially (Stout et al., 2013), lateral channel adjustment rates have decreased. We attributed this reduction in the rates to a reduction in sediment supply (Trimble and Lund, 1982; Argabright et al., 1996) and an increase in riparian vegetation.

Fine sediment contributions coming from near-channel sources due to lateral channel adjustment processes are an important source that must be accounted for in order to better understand sediment dynamics at the watershed scale. Trimble (1999) demonstrated how sediment yield at the watershed mouth does not offer information about the processes taking place within the watershed. Sediment sinks and sources within the watershed may change without having an effect in sediment yield. Sediment can be stored in floodplains for millennia or pass through the river in short time periods (Skalak and Pizzuto, 2010). Understanding where sediment comes from provides more detailed information that can be used to develop better practices and target the specific

problems more effectively. Near-channel sources of sediment in the Root River play a very important role. Floodplains can act as sinks or sources of sediment depending on sediment supply and water supply, and also depending in the timing of flow events.

A combination of GIS analyses, including aerial photograph and lidar analysis, was used to determine the amount of fine sediment ( $<67 \mu\text{m}$ ) contributed to the Root River from near-channel sources due to lateral channel adjustment.

We found that lateral channel adjustment and fine sediment contributions have significantly change since the 1970s in the Root River. The reduction experienced in lateral adjustment in the Root River helped us understand current trends and facilitated the selection of the most recent decades to estimate fine sediment contributions in a more accurate way.

In general, these findings demonstrate that water supply is not always the main factor influencing lateral channel adjustment and that other factors like sediment supply and vegetation need to be studied in more detail in order to better understand sediment dynamics in the Root River.

## **4.2 Future Work**

The main purpose of this thesis was to quantify the amount of fine sediment added to the channel due to channel migration and channel widening. Since the increases in high and low flows in the Root River did not result in increases in channel migration and channel widening rates, during the development of this study more questions originated related to the factors that are involved in lateral channel adjustment. Factors like riparian vegetation effects and bank resistance in general were addressed in this

thesis, but a more detailed analysis of the land cover evolution of the Root River and the effects of riparian vegetation on bank resistance is needed. A more detailed hydrologic analysis to determine the effects of the flow increases at the watershed scale would also be helpful.

The results offered in this thesis will be used to constrain a sediment budget for the entire Root River Watershed. One of the key elements in a sediment budget is to use multiple lines of evidence. Therefore, other approaches to quantify near-channel sediment contributions and sediment dynamics in general in the Root River should be pursued in order to verify these results.

The importance of bed load material in channel morphology and the relation between bed load and wash load is another important area that should be considered for future work.

Lastly, an analysis of the best management practices that would work the best with the results should be conducted. Understanding sediment dynamics should ultimately translate into best management practices to improve water quality and should also provide useful and practical information.

#### **4.3 References**

- Argabright, M.R., Helms, C.D., Pavelis, G., Sinclair, R., 1996. Historical changes in soil erosion, 1930-1992: The northern Mississippi valley loess hills. Natural Resour. Conservation Service, USDA. Historical note No 5.
- Braudrick, C.A., Dietrich, W.T., Leverich, G.T., Sklarb, L.S., 2009. Experimental evidence for the conditions necessary to sustain meandering in coarse-bedded rivers. *Proceedings of the National Academy of Sciences USA*. 106 (40): 16936-16941.

- Hassan, M.A., Church, M., Lisle, T.E., Brardinoni, F., Benda, L., Grant, G. E., 2005. Sediment transport and channel morphology of small, forested streams. *Jawra journal of the american water resources association*. 41: 85-876.
- Naden, P.S., 2010. The Fine-Sediment Cascade, *Sediment Cascades*. In: Burt, T., Allison, R. (Eds.), *Sediment Cascades: An Integrated Approach*. John Wiley & Sons, Ltd. Centre for Ecology and Hydrology, UK, pp. 271-305.
- Skalak, K. Pizzuto, J., 2010. The distribution and residence time of suspended sediment stored within the channel margins of a gravel-bed bedrock river. *Earth Surface Processes and Landforms*, 35: 435-446.
- Stout, J.C., Belmont, P., Schottler, S.P., Willenbring, J.K., 2013. Identifying Sediment Sources and Sinks in the Root River, Southeastern Minnesota. *Annals Assoc. Am. Geographers*.
- Trimble, S.W., 1999. Decreased Rates of Alluvial Sediment Storage in the Coon Creek Basin, Wisconsin, 1975-93. *Science*. 285 (5431): 1244-1246.
- Trimble, S.W., Lund, S.W., 1982. Soil conservation and the reduction of erosion and sedimentation in the Coon Creek basin, Wisconsin. USGS professional paper 1234. Washington DC: Government printing office.

APPENDICES

**Channel migration figures:**

```

# imports modules
import arcpy
import numpy as np
import os
import matplotlib.pyplot as plt
import matplotlib.pyplot as py

# defines parameters
arcpy.env.overwriteOutput = True
workspace = r'C:\Users\Schumm\Documents\Belmont Lab\GIS_root\migration'
arcpy.env.workspace = workspace
decade_3050 = r'C:\Users\Schumm\Documents\Belmont
    Lab\GIS_root\migration\migr1938-1950s'
decade_5070 = r'C:\Users\Schumm\Documents\Belmont
    Lab\GIS_root\migration\migr1950s-1970s'
decade_7090 = r'C:\Users\Schumm\Documents\Belmont
    Lab\GIS_root\migration\migr1970s-1991'

# gets migration 1930s-1950s from shapefiles
# appends migration values to Y list
arcpy.env.workspace = decade_3050
y = []
for reaches in arcpy.ListFeatureClasses('migration*', 'Polygon'):
    with arcpy.da.SearchCursor(reaches, 'Mig_myr') as rows:
        for row in rows:
            y.append(-row[0])

# creates x list depending on Y length every 25 m
# x_np = range(0, len(y)*25, 25) **note: use this instead of the next two lines for x-axis to
# be in meters**
x_np = np.arange(0, len(y)*0.025, 0.025)
x = x_np.tolist()

# sets the separation between the ticks and the axes
py.rcParams['xtick.major.pad'] = '10'
py.rcParams['ytick.major.pad'] = '10'

# creates figure, sets size
fig = plt.figure(1, figsize=(32, 18))

# sets space at the bottom of the figure for xlabel
fig.subplots_adjust(bottom=0.2)

```

```

# creates the first subfigure 1 of 3 top plot
ax1 = fig.add_subplot(311)

# plots migration vs distance downstream
ax1.plot(x,y,'r-',lw=2)

# plots reach dashed lines
ax1.plot([16.150,16.150],[-20,20],'k--')
ax1.plot([24.950,24.950],[-20,20],'k--')
ax1.plot([40.850,40.850],[-20,20],'k--')
ax1.plot([49.530,49.530],[-20,20],'k--')
ax1.plot([63.410,63.410],[-20,20],'k--')
ax1.plot([77.290,77.290],[-20,20],'k--')
ax1.plot([90.560,90.560],[-20,20],'k--')
ax1.plot([99.260,99.260],[-20,20],'k--')
ax1.plot([110.610,110.610],[-20,20],'k--')

# sets ylabel to specified string
ax1.set_ylabel('Migration\nRate (m/yr)\n\n',horizontalalignment='center')

# makes xticks invisible
plt.setp(ax1.get_xticklabels(), visible=False)

#sets x and y limits
ax1.set_xlim(0,121)
ax1.set_ylim(-20,20)

# specifies what ticks to show in the y-axis
ax1.set_yticks([-20,-10,0,10,20])

# adds text to the plots at specified locations
ax1.annotate('Right', xy=(0,-19), xycoords='data',xytext=(-150,0), textcoords='offset
points',size=30)
ax1.annotate('Left', xy=(0,16), xycoords='data',xytext=(-150,0), textcoords='offset
points',size=30)
ax1.annotate('1930s-1950s', xy=(0,15), xycoords='data',xytext=(10,-1), textcoords='offset
points',size=30)
ax1.annotate('*', xy=(49.530,13), xycoords='data',xytext=(-30,1), textcoords='offset
points',size=50)
ax1.annotate('*', xy=(77.290,13), xycoords='data',xytext=(-30,1), textcoords='offset
points',size=50)
ax1.annotate('**', xy=(90.560,13), xycoords='data',xytext=(-60,1), textcoords='offset
points',size=50)

```

```

# sets the fontsize of the subplot to specified size
for item in ([ax1.xaxis.label, ax1.yaxis.label] + ax1.get_xticklabels() +
             ax1.get_yticklabels()):
    item.set_fontsize(30)

# gets migration 1950s-1970s from shapefiles
arcpy.env.workspace = decade_5070
y = []
for reaches in arcpy.ListFeatureClasses('migration*', 'Polygon'):
    with arcpy.da.SearchCursor(reaches, 'Mig_myr') as rows:
        for row in rows:
            y.append(-row[0])

#x = range(0, len(y)*25, 25) **note: use this instead of the next two lines for x-axis to be
    in meters**
x_np = np.arange(0, len(y)*0.025, 0.025)
x = x_np.tolist()

# creates the second subfigure 2 of 3 **middle plot**
ax2 = fig.add_subplot(312)

# plots migration vs distance downstream
ax2.plot(x, y, 'r-', lw=2)

# plots reach dashed lines
ax2.plot([16.150, 16.150], [-20, 20], 'k--')
ax2.plot([24.950, 24.950], [-20, 20], 'k--')
ax2.plot([40.850, 40.850], [-20, 20], 'k--')
ax2.plot([49.530, 49.530], [-20, 20], 'k--')
ax2.plot([63.410, 63.410], [-20, 20], 'k--')
ax2.plot([77.290, 77.290], [-20, 20], 'k--')
ax2.plot([90.560, 90.560], [-20, 20], 'k--')
ax2.plot([99.260, 99.260], [-20, 20], 'k--')
ax2.plot([110.610, 110.610], [-20, 20], 'k--')

# sets ylabel to specified string
ax2.set_ylabel('Migration\nRate (m/yr)\n\n', horizontalalignment='center')

# makes xticks invisible
plt.setp(ax2.get_xticklabels(), visible=False)

#sets x and y limits
ax2.set_xlim(0, 121)
ax2.set_ylim(-20, 20)

```

```

# specifies what ticks to show in the y-axis
ax2.set_yticks([-20,-10,0,10,20])

# adds text to the plots at specified locations
ax2.annotate('Right', xy=(0,-19), xycoords='data',xytext=(-150,0), textcoords='offset
    points',size=30)
ax2.annotate('Left', xy=(0,16), xycoords='data',xytext=(-150,0), textcoords='offset
    points',size=30)
ax2.annotate('1950s-1970s', xy=(0,15), xycoords='data',xytext=(10,-1), textcoords='offset
    points',size=30)
ax2.annotate('*', xy=(49.530,13), xycoords='data',xytext=(-30,1), textcoords='offset
    points',size=50)
ax2.annotate('*', xy=(63.410,13), xycoords='data',xytext=(-30,1), textcoords='offset
    points',size=50)
ax2.annotate('*****', xy=(77.290,13), xycoords='data',xytext=(-135,1),
    textcoords='offset points',size=50)

# sets the fontsize of the subplot to specified size
for item in ([ax2.xaxis.label, ax2.yaxis.label] + ax2.get_xticklabels() +
    ax2.get_yticklabels()):
    item.set_fontsize(30)

# gets migration 1930s-1950s from shapefiles
arcpy.env.workspace = decade_7090
y = []
for reaches in arcpy.ListFeatureClasses('migration*', 'Polygon'):
    with arcpy.da.SearchCursor(reaches, 'Mig_myr') as rows:
        for row in rows:
            y.append(-row[0])

#x = range(0,len(y)*25,25)
x_np = np.arange(0,len(y)*0.025,0.025)
x = x_np.tolist()

# creates the third subfigure 3 of 3 **bottom plot**
ax = fig.add_subplot(313)

# plots migration vs distance downstream
ax.plot(x,y,'r-',lw=2)

# plots reach dashed lines
ax.plot([16.150,16.150],[-20,20],'k--')
ax.plot([24.950,24.950],[-20,20],'k--')
ax.plot([40.850,40.850],[-20,20],'k--')
ax.plot([49.530,49.530],[-20,20],'k--')

```

```

ax.plot([63.410,63.410],[-20,20],'k--')
ax.plot([77.290,77.290],[-20,20],'k--')
ax.plot([90.560,90.560],[-20,20],'k--')
ax.plot([99.260,99.260],[-20,20],'k--')
ax.plot([110.610,110.610],[-20,20],'k--')

# sets x and ylabels to specified strings
ax.set_ylabel('Migration\nRate (m/yr)\n\n',horizontalalignment='center')
ax.set_xlabel('Distance Downstream (km)')

#sets x and y limits
ax.set_xlim(0,121)
ax.set_ylim(-20,20)

# specifies what ticks to show in the y-axis
ax.set_yticks([-20,-10,0,10,20])

# adds text to the plots at specified locations
ax.annotate('Upstream',xy=(0,-20), xycoords='data',xytext=(-20,-70), textcoords='offset
points',size=30)
ax.annotate('Downstream', xy=(121,-20), xycoords='data',xytext=(-150,-70),
textcoords='offset points',size=30)
ax.annotate('Right', xy=(0,-19), xycoords='data',xytext=(-150,0), textcoords='offset
points',size=30)
ax.annotate('Left', xy=(0,16), xycoords='data',xytext=(-150,0), textcoords='offset
points',size=30)
ax.annotate('1970s-1990s', xy=(0,15), xycoords='data',xytext=(10,-1), textcoords='offset
points',size=30)
ax.annotate('*', xy=(49.530,13), xycoords='data',xytext=(-30,1), textcoords='offset
points',size=50)
ax.annotate('*', xy=(63.410,13), xycoords='data',xytext=(-30,1), textcoords='offset
points',size=50)
ax.annotate('*', xy=(110.610,13), xycoords='data',xytext=(-30,1), textcoords='offset
points',size=50)
ax.annotate('*', xy=(110.610,13), xycoords='data',xytext=(115,1), textcoords='offset
points',size=50)
ax.annotate('R10', xy=(16.150,-20), xycoords='data',xytext=(-50,50), textcoords='offset
points',size=30).set_rotation('vertical')
ax.annotate('R09', xy=(24.950,-20), xycoords='data',xytext=(-50,50), textcoords='offset
points',size=30).set_rotation('vertical')
ax.annotate('R08', xy=(40.850,-20), xycoords='data',xytext=(-50,50), textcoords='offset
points',size=30).set_rotation('vertical')
ax.annotate('R07', xy=(49.530,-20), xycoords='data',xytext=(-50,50), textcoords='offset
points',size=30).set_rotation('vertical')

```

```

ax.annotate('R06', xy=(63.410,-20), xycoords='data',xytext=(-50,50), textcoords='offset
    points',size=30).set_rotation('vertical')
ax.annotate('R05', xy=(77.290,-20), xycoords='data',xytext=(-50,50), textcoords='offset
    points',size=30).set_rotation('vertical')
ax.annotate('R04', xy=(90.560,-20), xycoords='data',xytext=(-50,50), textcoords='offset
    points',size=30).set_rotation('vertical')
ax.annotate('R03', xy=(99.260,-20), xycoords='data',xytext=(-50,50), textcoords='offset
    points',size=30).set_rotation('vertical')
ax.annotate('R02', xy=(110.610,-20), xycoords='data',xytext=(-50,50), textcoords='offset
    points',size=30).set_rotation('vertical')
ax.annotate('R01', xy=(110.610,-20), xycoords='data',xytext=(100,50), textcoords='offset
    points',size=30).set_rotation('vertical')

# sets the fontsize of the subplot to specified size
for item in ([ax.xaxis.label, ax.yaxis.label] + ax.get_xticklabels() + ax.get_yticklabels()):
    item.set_fontsize(30)

# saves figure to specified location
plt.savefig(workspace + '\mig_older.png',format='png')

# clears figure
plt.clf()

```

### **Channel width figures:**

```

# imports modules
import arcpy
import numpy as np
import os
import matplotlib.pyplot as plt
import matplotlib.pyplot as py

# defines parameters
arcpy.env.overwriteOutput = True
workspace = r'D:\Belmont Lab\GIS_root\polygons'
arcpy.env.workspace = workspace
decades = arcpy.ListWorkspaces('sub_*','Folder')
decade_30 = r'D:\Belmont Lab\GIS_root\polygons\sub_reaches_1930s'
decade_50 = r'D:\Belmont Lab\GIS_root\polygons\sub_reaches_1950s'
decade_70 = r'D:\Belmont Lab\GIS_root\polygons\sub_reaches_1970s'
decade_90 = r'D:\Belmont Lab\GIS_root\polygons\sub_reaches_1991'
decade_00 = r'D:\Belmont Lab\GIS_root\polygons\sub_reaches_2003'
decade_10 = r'D:\Belmont Lab\GIS_root\polygons\sub_reaches_2010'

```

```

# creates width figures "average sub-width vs distance downstream" for each decade
# note: the most recent polygons FID goes from dwnstream to upstream, while the FID
      of the older ones goes from upstream to downstream

# extracts sub-width from shapefiles
arcpy.env.workspace = decade_30
y = []
x_sub = []
y1=[];y2=[];y3=[];y4=[];y5=[];y6=[];y7=[];y8=[];y9=[];y10=[]
x_sub1=[];x_sub2=[];x_sub3=[];x_sub4=[];x_sub5=[];x_sub6=[];x_sub7=[];x_sub8=[];x
      _sub9=[];x_sub10=[]
for reaches in arcpy.ListFeatureClasses('reach01*', 'Polygon'):
    with arcpy.da.SearchCursor(reaches, ('av_w_sub', 'av_width_m')) as rows:
        for row in rows:
            y1.append(row[0])
            x_sub1.append((row[1]*10)/1000)
for reaches in arcpy.ListFeatureClasses('reach02*', 'Polygon'):
    with arcpy.da.SearchCursor(reaches, ('av_w_sub', 'av_width_m')) as rows:
        for row in rows:
            y2.append(row[0])
            x_sub2.append((row[1]*10)/1000)
for reaches in arcpy.ListFeatureClasses('reach03*', 'Polygon'):
    with arcpy.da.SearchCursor(reaches, ('av_w_sub', 'av_width_m')) as rows:
        for row in rows:
            y3.append(row[0])
            x_sub3.append((row[1]*10)/1000)
for reaches in arcpy.ListFeatureClasses('reach04*', 'Polygon'):
    with arcpy.da.SearchCursor(reaches, ('av_w_sub', 'av_width_m')) as rows:
        for row in rows:
            y4.append(row[0])
            x_sub4.append((row[1]*10)/1000)
for reaches in arcpy.ListFeatureClasses('reach05*', 'Polygon'):
    with arcpy.da.SearchCursor(reaches, ('av_w_sub', 'av_width_m')) as rows:
        for row in rows:
            y5.append(row[0])
            x_sub5.append((row[1]*10)/1000)
for reaches in arcpy.ListFeatureClasses('reach06*', 'Polygon'):
    with arcpy.da.SearchCursor(reaches, ('av_w_sub', 'av_width_m')) as rows:
        for row in rows:
            y6.append(row[0])
            x_sub6.append((row[1]*10)/1000)
for reaches in arcpy.ListFeatureClasses('reach07*', 'Polygon'):
    with arcpy.da.SearchCursor(reaches, ('av_w_sub', 'av_width_m')) as rows:
        for row in rows:

```

```

        y7.append(row[0])
        x_sub7.append((row[1]*10)/1000)
for reaches in arcpy.ListFeatureClasses('reach08*', 'Polygon'):
    with arcpy.da.SearchCursor(reaches, ('av_w_sub', 'av_width_m')) as rows:
        for row in rows:
            y8.append(row[0])
            x_sub8.append((row[1]*10)/1000)
for reaches in arcpy.ListFeatureClasses('reach09*', 'Polygon'):
    with arcpy.da.SearchCursor(reaches, ('av_w_sub', 'av_width_m')) as rows:
        for row in rows:
            y9.append(row[0])
            x_sub9.append((row[1]*10)/1000)
for reaches in arcpy.ListFeatureClasses('reach10*', 'Polygon'):
    with arcpy.da.SearchCursor(reaches, ('av_w_sub', 'av_width_m')) as rows:
        for row in rows:
            y10.append(row[0])
            x_sub10.append((row[1]*10)/1000)

y1.reverse();y2.reverse();y3.reverse();y4.reverse();y5.reverse();y6.reverse();y7.reverse();
y8.reverse();y9.reverse();y10.reverse()

y = y1 + y2 + y3 + y4 + y5 + y6 + y7 + y8 + y9 + y10
x_sub = x_sub1 + x_sub2 + x_sub3 + x_sub4 + x_sub5 + x_sub6 + x_sub7 + x_sub8 +
        x_sub9 + x_sub10
y.reverse()
x_sub.reverse()

# calculates x
x = [0.5177]
for v in x_sub:
    v = x[-1]+v
    x.append(v)

x.remove(x[-1])

# sets the separation between the ticks and the axes
py.rcParams['xtick.major.pad']='8'
py.rcParams['ytick.major.pad']='8'

# creates figure, sets size
fig = plt.figure(1,figsize=(16,18))

# sets space at the bottom of the figure for xlabel
fig.subplots_adjust(bottom=0.2)

```

```

# creates the first subfigure 1 of 2 top plot
ax1 = fig.add_subplot(321)

# plots average sub-width vs distance downstream
ax1.plot(x,y,'bo',lw=2)

# plots reach dashed lines
ax1.plot([17.150,17.150],[0,100],'k--')
ax1.plot([28.920,28.920],[0,100],'k--')
ax1.plot([41.820,41.820],[0,100],'k--')
ax1.plot([51.500,51.500],[0,100],'k--')
ax1.plot([66.380,66.380],[0,100],'k--')
ax1.plot([81.110,81.110],[0,100],'k--')
ax1.plot([94.110,94.110],[0,100],'k--')
ax1.plot([102.810,102.810],[0,100],'k--')
ax1.plot([117.060,117.060],[0,100],'k--')

# sets ylabel to specified string
ax1.set_ylabel('Average Width (m)')

# makes xticks invisible
plt.setp(ax1.get_xticklabels(), visible=False)

#sets x and y limits
ax1.set_xlim(0,127.5)
ax1.set_ylim(0,100)

# specifies what ticks to show in the y-axis
ax1.set_yticks([10,30,50,70,90])

# adds text to the plots at specified locations
ax1.annotate('1930s', xy=(0,90), xycoords='data',xytext=(10,-2), textcoords='offset
points',size=20)

# sets the fontsize of the subplot to specified size
for item in ([ax1.xaxis.label, ax1.yaxis.label] + ax1.get_xticklabels() +
ax1.get_yticklabels()):
    item.set_fontsize(20)

# extracts sub-width from shapefiles
arcpy.env.workspace = decade_50
y = []
x_sub = []
y1=[];y2=[];y3=[];y4=[];y5=[];y6=[];y7=[];y8=[];y9=[];y10=[]

```

```

x_sub1=[];x_sub2=[];x_sub3=[];x_sub4=[];x_sub5=[];x_sub6=[];x_sub7=[];x_sub8=[];x
_sub9=[];x_sub10=[]
for reaches in arcpy.ListFeatureClasses('reach01*', 'Polygon'):
    with arcpy.da.SearchCursor(reaches,('av_w_sub','av_width_m')) as rows:
        for row in rows:
            y1.append(row[0])
            x_sub1.append((row[1]*10)/1000)
for reaches in arcpy.ListFeatureClasses('reach02*', 'Polygon'):
    with arcpy.da.SearchCursor(reaches,('av_w_sub','av_width_m')) as rows:
        for row in rows:
            y2.append(row[0])
            x_sub2.append((row[1]*10)/1000)
for reaches in arcpy.ListFeatureClasses('reach03*', 'Polygon'):
    with arcpy.da.SearchCursor(reaches,('av_w_sub','av_width_m')) as rows:
        for row in rows:
            y3.append(row[0])
            x_sub3.append((row[1]*10)/1000)
for reaches in arcpy.ListFeatureClasses('reach04*', 'Polygon'):
    with arcpy.da.SearchCursor(reaches,('av_w_sub','av_width_m')) as rows:
        for row in rows:
            y4.append(row[0])
            x_sub4.append((row[1]*10)/1000)
for reaches in arcpy.ListFeatureClasses('reach05*', 'Polygon'):
    with arcpy.da.SearchCursor(reaches,('av_w_sub','av_width_m')) as rows:
        for row in rows:
            y5.append(row[0])
            x_sub5.append((row[1]*10)/1000)
for reaches in arcpy.ListFeatureClasses('reach06*', 'Polygon'):
    with arcpy.da.SearchCursor(reaches,('av_w_sub','av_width_m')) as rows:
        for row in rows:
            y6.append(row[0])
            x_sub6.append((row[1]*10)/1000)
for reaches in arcpy.ListFeatureClasses('reach07*', 'Polygon'):
    with arcpy.da.SearchCursor(reaches,('av_w_sub','av_width_m')) as rows:
        for row in rows:
            y7.append(row[0])
            x_sub7.append((row[1]*10)/1000)
for reaches in arcpy.ListFeatureClasses('reach08*', 'Polygon'):
    with arcpy.da.SearchCursor(reaches,('av_w_sub','av_width_m')) as rows:
        for row in rows:
            y8.append(row[0])
            x_sub8.append((row[1]*10)/1000)
for reaches in arcpy.ListFeatureClasses('reach09*', 'Polygon'):
    with arcpy.da.SearchCursor(reaches,('av_w_sub','av_width_m')) as rows:
        for row in rows:

```

```

        y9.append(row[0])
        x_sub9.append((row[1]*10)/1000)
for reaches in arcpy.ListFeatureClasses('reach10*', 'Polygon'):
    with arcpy.da.SearchCursor(reaches, ('av_w_sub', 'av_width_m')) as rows:
        for row in rows:
            y10.append(row[0])
            x_sub10.append((row[1]*10)/1000)

y1.reverse();y2.reverse();y3.reverse();y4.reverse();y5.reverse();y6.reverse();y7.reverse();
y8.reverse();y9.reverse();y10.reverse()

y = y1 + y2 + y3 + y4 + y5 + y6 + y7 + y8 + y9 + y10
x_sub = x_sub1 + x_sub2 + x_sub3 + x_sub4 + x_sub5 + x_sub6 + x_sub7 + x_sub8 +
        x_sub9 + x_sub10
y.reverse()
x_sub.reverse()

# calculates x
x = [0.5177]
for v in x_sub:
    v = x[-1]+v
    x.append(v)

x.remove(x[-1])

# creates the first subfigure 1 of 2 top plot
ax2 = fig.add_subplot(322)

# plots average sub-width vs distance downstream
ax2.plot(x,y,'bo',lw=2)

# plots reach dashed lines
ax2.plot([17.150,17.150],[0,100],'k--')
ax2.plot([28.920,28.920],[0,100],'k--')
ax2.plot([41.820,41.820],[0,100],'k--')
ax2.plot([51.500,51.500],[0,100],'k--')
ax2.plot([66.380,66.380],[0,100],'k--')
ax2.plot([81.110,81.110],[0,100],'k--')
ax2.plot([94.110,94.110],[0,100],'k--')
ax2.plot([102.810,102.810],[0,100],'k--')
ax2.plot([117.060,117.060],[0,100],'k--')

# makes xticks and yticks invisible
plt.setp(ax2.get_xticklabels(), visible=False)
plt.setp(ax2.get_yticklabels(), visible=False)

```

```

#sets x and y limits
ax2.set_xlim(0,127.5)
ax2.set_ylim(0,100)

# specifies what ticks to show in the y-axis
ax2.set_yticks([10,30,50,70,90])

# adds text to the plots at specified locations
ax2.annotate('1950s', xy=(0,90), xycoords='data',xytext=(10,-2), textcoords='offset
           points',size=20)

# sets the fontsize of the subplot to specified size
for item in ([ax2.xaxis.label, ax2.yaxis.label] + ax2.get_xticklabels() +
           ax2.get_yticklabels()):
    item.set_fontsize(20)

# extracts sub-width from shapefiles
arcpy.env.workspace = decade_70
y = []
x_sub = []
y1=[];y2=[];y3=[];y4=[];y5=[];y6=[];y7=[];y8=[];y9=[];y10=[]
x_sub1=[];x_sub2=[];x_sub3=[];x_sub4=[];x_sub5=[];x_sub6=[];x_sub7=[];x_sub8=[];x
    _sub9=[];x_sub10=[]
for reaches in arcpy.ListFeatureClasses('reach01*', 'Polygon'):
    with arcpy.da.SearchCursor(reaches,('av_w_sub','av_width_m')) as rows:
        for row in rows:
            y1.append(row[0])
            x_sub1.append((row[1]*10)/1000)
for reaches in arcpy.ListFeatureClasses('reach02*', 'Polygon'):
    with arcpy.da.SearchCursor(reaches,('av_w_sub','av_width_m')) as rows:
        for row in rows:
            y2.append(row[0])
            x_sub2.append((row[1]*10)/1000)
for reaches in arcpy.ListFeatureClasses('reach03*', 'Polygon'):
    with arcpy.da.SearchCursor(reaches,('av_w_sub','av_width_m')) as rows:
        for row in rows:
            y3.append(row[0])
            x_sub3.append((row[1]*10)/1000)
for reaches in arcpy.ListFeatureClasses('reach04*', 'Polygon'):
    with arcpy.da.SearchCursor(reaches,('av_w_sub','av_width_m')) as rows:
        for row in rows:
            y4.append(row[0])
            x_sub4.append((row[1]*10)/1000)
for reaches in arcpy.ListFeatureClasses('reach05*', 'Polygon'):

```

```

with arcpy.da.SearchCursor(reaches,('av_w_sub','av_width_m')) as rows:
    for row in rows:
        y5.append(row[0])
        x_sub5.append((row[1]*10)/1000)
for reaches in arcpy.ListFeatureClasses('reach06*', 'Polygon'):
    with arcpy.da.SearchCursor(reaches,('av_w_sub','av_width_m')) as rows:
        for row in rows:
            y6.append(row[0])
            x_sub6.append((row[1]*10)/1000)
for reaches in arcpy.ListFeatureClasses('reach07*', 'Polygon'):
    with arcpy.da.SearchCursor(reaches,('av_w_sub','av_width_m')) as rows:
        for row in rows:
            y7.append(row[0])
            x_sub7.append((row[1]*10)/1000)
for reaches in arcpy.ListFeatureClasses('reach08*', 'Polygon'):
    with arcpy.da.SearchCursor(reaches,('av_w_sub','av_width_m')) as rows:
        for row in rows:
            y8.append(row[0])
            x_sub8.append((row[1]*10)/1000)
for reaches in arcpy.ListFeatureClasses('reach09*', 'Polygon'):
    with arcpy.da.SearchCursor(reaches,('av_w_sub','av_width_m')) as rows:
        for row in rows:
            y9.append(row[0])
            x_sub9.append((row[1]*10)/1000)
for reaches in arcpy.ListFeatureClasses('reach10*', 'Polygon'):
    with arcpy.da.SearchCursor(reaches,('av_w_sub','av_width_m')) as rows:
        for row in rows:
            y10.append(row[0])
            x_sub10.append((row[1]*10)/1000)

y1.reverse();y2.reverse();y3.reverse();y4.reverse();y5.reverse();y6.reverse();y7.reverse();
y8.reverse();y9.reverse();y10.reverse()

y = y1 + y2 + y3 + y4 + y5 + y6 + y7 + y8 + y9 + y10
x_sub = x_sub1 + x_sub2 + x_sub3 + x_sub4 + x_sub5 + x_sub6 + x_sub7 + x_sub8 +
        x_sub9 + x_sub10
y.reverse()
x_sub.reverse()

# calculates x
x = [0.5177]
for v in x_sub:
    v = x[-1]+v
    x.append(v)

```

```

x.remove(x[-1])

# creates the first subfigure 1 of 2 **top plot**
ax3 = fig.add_subplot(323)

# plots average sub-width vs distance downstream
ax3.plot(x,y,'bo',lw=2)

# plots reach dashed lines
ax3.plot([17.150,17.150],[0,100],'k--')
ax3.plot([28.920,28.920],[0,100],'k--')
ax3.plot([41.820,41.820],[0,100],'k--')
ax3.plot([51.500,51.500],[0,100],'k--')
ax3.plot([66.380,66.380],[0,100],'k--')
ax3.plot([81.110,81.110],[0,100],'k--')
ax3.plot([94.110,94.110],[0,100],'k--')
ax3.plot([102.810,102.810],[0,100],'k--')
ax3.plot([117.060,117.060],[0,100],'k--')

# sets ylabel to specified string
ax3.set_ylabel('Average Width (m)')

# makes xticks invisible
plt.setp(ax3.get_xticklabels(), visible=False)

#sets x and y limits
ax3.set_xlim(0,127.5)
ax3.set_ylim(0,100)

# specifies what ticks to show in the y-axis
ax3.set_yticks([10,30,50,70,90])

# adds text to the plots at specified locations
ax3.annotate('1970s', xy=(0,90), xycoords='data',xytext=(10,-2), textcoords='offset
           points',size=20)

# sets the fontsize of the subplot to specified size
for item in ([ax3.xaxis.label, ax3.yaxis.label] + ax3.get_xticklabels() +
           ax3.get_yticklabels()):
    item.set_fontsize(20)

# extracts sub-width from shapefiles
arcpy.env.workspace = decade_90
y = []
x_sub = []

```

```

for reaches in arcpy.ListFeatureClasses('reach*', 'Polygon'):
    with arcpy.da.SearchCursor(reaches, ('av_w_sub', 'av_width_m')) as rows:
        for row in rows:
            y.append(row[0])
            x_sub.append((row[1]*10)/1000)
y.reverse()

# calculates x
x = [0.5177]
for v in x_sub:
    v = x[-1]+v
    x.append(v)

x.remove(x[-1])

# creates the first subfigure 1 of 2 **top plot**
ax4 = fig.add_subplot(324)

# plots average sub-width vs distance downstream
ax4.plot(x,y,'bo',lw=2)

# plots reach dashed lines
ax4.plot([17.150,17.150],[0,100],'k--')
ax4.plot([28.920,28.920],[0,100],'k--')
ax4.plot([41.820,41.820],[0,100],'k--')
ax4.plot([51.500,51.500],[0,100],'k--')
ax4.plot([66.380,66.380],[0,100],'k--')
ax4.plot([81.110,81.110],[0,100],'k--')
ax4.plot([94.110,94.110],[0,100],'k--')
ax4.plot([102.810,102.810],[0,100],'k--')
ax4.plot([117.060,117.060],[0,100],'k--')

# makes xticks and yticks invisible
plt.setp(ax4.get_xticklabels(), visible=False)
plt.setp(ax4.get_yticklabels(), visible=False)

#sets x and y limits
ax4.set_xlim(0,127.5)
ax4.set_ylim(0,100)

# specifies what ticks to show in the y-axis
ax4.set_yticks([10,30,50,70,90])

# adds text to the plots at specified locations

```

```

ax4.annotate('1990s', xy=(0,90), xycoords='data',xytext=(10,-2), textcoords='offset
    points',size=20)

# sets the fontsize of the subplot to specified size
for item in ([ax4.xaxis.label, ax4.yaxis.label] + ax4.get_xticklabels() +
    ax4.get_yticklabels()):
    item.set_fontsize(20)

# extracts sub-width from shapefiles
arcpy.env.workspace = decade_00
y = []
x_sub = []

for reaches in arcpy.ListFeatureClasses('reach*', 'Polygon'):
    with arcpy.da.SearchCursor(reaches, ('av_w_sub', 'av_width_m')) as rows:
        for row in rows:
            y.append(row[0])
            x_sub.append((row[1]*10)/1000)
y.reverse()

# calculates x
x = [0.5177]
for v in x_sub:
    v = x[-1]+v
    x.append(v)

x.remove(x[-1])

# creates the first subfigure 1 of 2 top plot
ax5 = fig.add_subplot(325)

# plots average sub-width vs distance downstream
ax5.plot(x,y,'bo',lw=2)

# plots reach dashed lines
ax5.plot([17.150,17.150],[0,100],'k--')
ax5.plot([28.920,28.920],[0,100],'k--')
ax5.plot([41.820,41.820],[0,100],'k--')
ax5.plot([51.500,51.500],[0,100],'k--')
ax5.plot([66.380,66.380],[0,100],'k--')
ax5.plot([81.110,81.110],[0,100],'k--')
ax5.plot([94.110,94.110],[0,100],'k--')
ax5.plot([102.810,102.810],[0,100],'k--')
ax5.plot([117.060,117.060],[0,100],'k--')

```

```

# sets xlabel and ylabel to specified string
ax5.set_ylabel('Average Width (m)')
ax5.set_xlabel('Distance Downstream (km)')

#sets x and y limits
ax5.set_xlim(0,127.5)
ax5.set_ylim(0,100)

# specifies what ticks to show in the y-axis
ax5.set_yticks([10,30,50,70,90])

# adds text to the plots at specified locations
ax5.annotate('2000s', xy=(0,90), xycoords='data',xytext=(10,-2), textcoords='offset
    points',size=20)
ax5.annotate('R10', xy=(17.150,0), xycoords='data',xytext=(-20,25), textcoords='offset
    points',size=20).set_rotation('vertical')
ax5.annotate('R09', xy=(28.920,0), xycoords='data',xytext=(-20,25), textcoords='offset
    points',size=20).set_rotation('vertical')
ax5.annotate('R08', xy=(41.820,0), xycoords='data',xytext=(-20,25), textcoords='offset
    points',size=20).set_rotation('vertical')
ax5.annotate('R07', xy=(51.500,0), xycoords='data',xytext=(-20,25), textcoords='offset
    points',size=20).set_rotation('vertical')
ax5.annotate('R06', xy=(66.380,0), xycoords='data',xytext=(-20,25), textcoords='offset
    points',size=20).set_rotation('vertical')
ax5.annotate('R05', xy=(81.110,0), xycoords='data',xytext=(-20,25), textcoords='offset
    points',size=20).set_rotation('vertical')
ax5.annotate('R04', xy=(94.110,0), xycoords='data',xytext=(-20,25), textcoords='offset
    points',size=20).set_rotation('vertical')
ax5.annotate('R03', xy=(102.810,0), xycoords='data',xytext=(-20,25), textcoords='offset
    points',size=20).set_rotation('vertical')
ax5.annotate('R02', xy=(117.060,0), xycoords='data',xytext=(-20,25), textcoords='offset
    points',size=20).set_rotation('vertical')
ax5.annotate('R01', xy=(117.060,0), xycoords='data',xytext=(15,25), textcoords='offset
    points',size=20).set_rotation('vertical')

# sets the fontsize of the subplot to specified size
for item in ([ax5.xaxis.label, ax5.yaxis.label] + ax5.get_xticklabels() +
    ax5.get_yticklabels()):
    item.set_fontsize(20)

# extracts sub-width from shapefiles
arcpy.env.workspace = decade_10
y = []
x_sub = []

```

```

for reaches in arcpy.ListFeatureClasses('reach*', 'Polygon'):
    with arcpy.da.SearchCursor(reaches, ('av_w_sub', 'av_width_m')) as rows:
        for row in rows:
            y.append(row[0])
            x_sub.append((row[1]*10)/1000)
y.reverse()

# calculates x
x = [0.5177]
for v in x_sub:
    v = x[-1]+v
    x.append(v)

x.remove(x[-1])

# creates the first subfigure 1 of 2 top plot
ax6 = fig.add_subplot(326)

# plots average sub-width vs distance downstream
ax6.plot(x,y,'bo',lw=2)

# plots reach dashed lines
ax6.plot([17.150,17.150],[0,100],'k--')
ax6.plot([28.920,28.920],[0,100],'k--')
ax6.plot([41.820,41.820],[0,100],'k--')
ax6.plot([51.500,51.500],[0,100],'k--')
ax6.plot([66.380,66.380],[0,100],'k--')
ax6.plot([81.110,81.110],[0,100],'k--')
ax6.plot([94.110,94.110],[0,100],'k--')
ax6.plot([102.810,102.810],[0,100],'k--')
ax6.plot([117.060,117.060],[0,100],'k--')

# sets xlabel to specified string
ax6.set_xlabel('Distance Downstream (km)')

# makes yticks invisible
plt.setp(ax6.get_yticklabels(), visible=False)

#sets x and y limits
ax6.set_xlim(0,127.5)
ax6.set_ylim(0,100)

# specifies what ticks to show in the y-axis
ax6.set_yticks([10,30,50,70,90])

```

```

# adds text to the plots at specified locations
ax6.annotate('2010s', xy=(0,90), xycoords='data',xytext=(10,-2), textcoords='offset
    points',size=20)
ax6.annotate('R10', xy=(17.150,0), xycoords='data',xytext=(-20,25), textcoords='offset
    points',size=20).set_rotation('vertical')
ax6.annotate('R09', xy=(28.920,0), xycoords='data',xytext=(-20,25), textcoords='offset
    points',size=20).set_rotation('vertical')
ax6.annotate('R08', xy=(41.820,0), xycoords='data',xytext=(-20,25), textcoords='offset
    points',size=20).set_rotation('vertical')
ax6.annotate('R07', xy=(51.500,0), xycoords='data',xytext=(-20,25), textcoords='offset
    points',size=20).set_rotation('vertical')
ax6.annotate('R06', xy=(66.380,0), xycoords='data',xytext=(-20,25), textcoords='offset
    points',size=20).set_rotation('vertical')
ax6.annotate('R05', xy=(81.110,0), xycoords='data',xytext=(-20,25), textcoords='offset
    points',size=20).set_rotation('vertical')
ax6.annotate('R04', xy=(94.110,0), xycoords='data',xytext=(-20,25), textcoords='offset
    points',size=20).set_rotation('vertical')
ax6.annotate('R03', xy=(102.810,0), xycoords='data',xytext=(-20,25), textcoords='offset
    points',size=20).set_rotation('vertical')
ax6.annotate('R02', xy=(117.060,0), xycoords='data',xytext=(-20,25), textcoords='offset
    points',size=20).set_rotation('vertical')
ax6.annotate('R01', xy=(117.060,0), xycoords='data',xytext=(15,25), textcoords='offset
    points',size=20).set_rotation('vertical')

# sets the fontsize of the subplot to specified size
for item in ([ax6.xaxis.label, ax6.yaxis.label] + ax6.get_xticklabels() +
    ax6.get_yticklabels()):
    item.set_fontsize(20)

# sets space between subplots
plt.subplots_adjust(hspace = 0.015)
plt.subplots_adjust(wspace = 0.015)

# saves figure to specified location
plt.savefig(workspace + '\sub-width_per_reach.png',format='png')

# clears figure
plt.clf()

```

**Delta width figure:**

```

# imports modules
import arcpy
import numpy as np
import os
import matplotlib.pyplot as plt
import matplotlib.pyplot as py

# defines parameters
arcpy.env.overwriteOutput = True
workspace = r'F:\Belmont Lab\GIS_root\polygons'
arcpy.env.workspace = workspace
decades = arcpy.ListWorkspaces('sub_*','Folder')
decade_30 = r'F:\Belmont Lab\GIS_root\polygons\sub_reaches_1930s'
decade_50 = r'F:\Belmont Lab\GIS_root\polygons\sub_reaches_1950s'
decade_70 = r'F:\Belmont Lab\GIS_root\polygons\sub_reaches_1970s'
decade_90 = r'F:\Belmont Lab\GIS_root\polygons\sub_reaches_1991'
decade_00 = r'F:\Belmont Lab\GIS_root\polygons\sub_reaches_2003'
decade_10 = r'F:\Belmont Lab\GIS_root\polygons\sub_reaches_2010'

# creates width figures "average sub-width vs distance downstream" for each decade
# note: the most recent polygons FID goes from downstream to upstream, while the FID
      of the older ones goes from upstream to downstream

# extracts sub-width from shapefiles
arcpy.env.workspace = decade_30
y_30 = []
x_sub = []
y1=[];y2=[];y3=[];y4=[];y5=[];y6=[];y7=[];y8=[];y9=[];y10=[]
x_sub1=[];x_sub2=[];x_sub3=[];x_sub4=[];x_sub5=[];x_sub6=[];x_sub7=[];x_sub8=[];x
      _sub9=[];x_sub10=[]
for reaches in arcpy.ListFeatureClasses('reach01*','Polygon'):
    with arcpy.da.SearchCursor(reaches,('av_w_sub','av_width_m')) as rows:
        for row in rows:
            y1.append(row[0])
            x_sub1.append((row[1]*10)/1000)
for reaches in arcpy.ListFeatureClasses('reach02*','Polygon'):
    with arcpy.da.SearchCursor(reaches,('av_w_sub','av_width_m')) as rows:
        for row in rows:
            y2.append(row[0])
            x_sub2.append((row[1]*10)/1000)
for reaches in arcpy.ListFeatureClasses('reach03*','Polygon'):
    with arcpy.da.SearchCursor(reaches,('av_w_sub','av_width_m')) as rows:
        for row in rows:
            y3.append(row[0])

```

```

    x_sub3.append((row[1]*10)/1000)
for reaches in arcpy.ListFeatureClasses('reach04*', 'Polygon'):
    with arcpy.da.SearchCursor(reaches, ('av_w_sub', 'av_width_m')) as rows:
        for row in rows:
            y4.append(row[0])
            x_sub4.append((row[1]*10)/1000)
for reaches in arcpy.ListFeatureClasses('reach05*', 'Polygon'):
    with arcpy.da.SearchCursor(reaches, ('av_w_sub', 'av_width_m')) as rows:
        for row in rows:
            y5.append(row[0])
            x_sub5.append((row[1]*10)/1000)
for reaches in arcpy.ListFeatureClasses('reach06*', 'Polygon'):
    with arcpy.da.SearchCursor(reaches, ('av_w_sub', 'av_width_m')) as rows:
        for row in rows:
            y6.append(row[0])
            x_sub6.append((row[1]*10)/1000)
for reaches in arcpy.ListFeatureClasses('reach07*', 'Polygon'):
    with arcpy.da.SearchCursor(reaches, ('av_w_sub', 'av_width_m')) as rows:
        for row in rows:
            y7.append(row[0])
            x_sub7.append((row[1]*10)/1000)
for reaches in arcpy.ListFeatureClasses('reach08*', 'Polygon'):
    with arcpy.da.SearchCursor(reaches, ('av_w_sub', 'av_width_m')) as rows:
        for row in rows:
            y8.append(row[0])
            x_sub8.append((row[1]*10)/1000)
for reaches in arcpy.ListFeatureClasses('reach09*', 'Polygon'):
    with arcpy.da.SearchCursor(reaches, ('av_w_sub', 'av_width_m')) as rows:
        for row in rows:
            y9.append(row[0])
            x_sub9.append((row[1]*10)/1000)
for reaches in arcpy.ListFeatureClasses('reach10*', 'Polygon'):
    with arcpy.da.SearchCursor(reaches, ('av_w_sub', 'av_width_m')) as rows:
        for row in rows:
            y10.append(row[0])
            x_sub10.append((row[1]*10)/1000)

y1.reverse();y2.reverse();y3.reverse();y4.reverse();y5.reverse();y6.reverse();y7.reverse();
y8.reverse();y9.reverse();y10.reverse()

y_30 = y1 + y2 + y3 + y4 + y5 + y6 + y7 + y8 + y9 + y10
x_sub = x_sub1 + x_sub2 + x_sub3 + x_sub4 + x_sub5 + x_sub6 + x_sub7 + x_sub8 +
x_sub9 + x_sub10
y_30.reverse()
x_sub.reverse()

```

```

# calculates x
x_30 = [0.5177]
for v in x_sub:
    v = x_30[-1]+v
    x_30.append(v)

x_30.remove(x_30[-1])

# extracts sub-width from shapefiles
arcpy.env.workspace = decade_50
y_50 = []
x_sub = []
y1=[];y2=[];y3=[];y4=[];y5=[];y6=[];y7=[];y8=[];y9=[];y10=[]
x_sub1=[];x_sub2=[];x_sub3=[];x_sub4=[];x_sub5=[];x_sub6=[];x_sub7=[];x_sub8=[];x
_sub9=[];x_sub10=[]
for reaches in arcpy.ListFeatureClasses('reach01*', 'Polygon'):
    with arcpy.da.SearchCursor(reaches, ('av_w_sub', 'av_width_m')) as rows:
        for row in rows:
            y1.append(row[0])
            x_sub1.append((row[1]*10)/1000)
for reaches in arcpy.ListFeatureClasses('reach02*', 'Polygon'):
    with arcpy.da.SearchCursor(reaches, ('av_w_sub', 'av_width_m')) as rows:
        for row in rows:
            y2.append(row[0])
            x_sub2.append((row[1]*10)/1000)
for reaches in arcpy.ListFeatureClasses('reach03*', 'Polygon'):
    with arcpy.da.SearchCursor(reaches, ('av_w_sub', 'av_width_m')) as rows:
        for row in rows:
            y3.append(row[0])
            x_sub3.append((row[1]*10)/1000)
for reaches in arcpy.ListFeatureClasses('reach04*', 'Polygon'):
    with arcpy.da.SearchCursor(reaches, ('av_w_sub', 'av_width_m')) as rows:
        for row in rows:
            y4.append(row[0])
            x_sub4.append((row[1]*10)/1000)
for reaches in arcpy.ListFeatureClasses('reach05*', 'Polygon'):
    with arcpy.da.SearchCursor(reaches, ('av_w_sub', 'av_width_m')) as rows:
        for row in rows:
            y5.append(row[0])
            x_sub5.append((row[1]*10)/1000)
for reaches in arcpy.ListFeatureClasses('reach06*', 'Polygon'):
    with arcpy.da.SearchCursor(reaches, ('av_w_sub', 'av_width_m')) as rows:
        for row in rows:
            y6.append(row[0])

```

```

    x_sub6.append((row[1]*10)/1000)
for reaches in arcpy.ListFeatureClasses('reach07*', 'Polygon'):
    with arcpy.da.SearchCursor(reaches, ('av_w_sub', 'av_width_m')) as rows:
        for row in rows:
            y7.append(row[0])
            x_sub7.append((row[1]*10)/1000)
for reaches in arcpy.ListFeatureClasses('reach08*', 'Polygon'):
    with arcpy.da.SearchCursor(reaches, ('av_w_sub', 'av_width_m')) as rows:
        for row in rows:
            y8.append(row[0])
            x_sub8.append((row[1]*10)/1000)
for reaches in arcpy.ListFeatureClasses('reach09*', 'Polygon'):
    with arcpy.da.SearchCursor(reaches, ('av_w_sub', 'av_width_m')) as rows:
        for row in rows:
            y9.append(row[0])
            x_sub9.append((row[1]*10)/1000)
for reaches in arcpy.ListFeatureClasses('reach10*', 'Polygon'):
    with arcpy.da.SearchCursor(reaches, ('av_w_sub', 'av_width_m')) as rows:
        for row in rows:
            y10.append(row[0])
            x_sub10.append((row[1]*10)/1000)

y1.reverse();y2.reverse();y3.reverse();y4.reverse();y5.reverse();y6.reverse();y7.reverse();
y8.reverse();y9.reverse();y10.reverse()

y_50 = y1 + y2 + y3 + y4 + y5 + y6 + y7 + y8 + y9 + y10
x_sub = x_sub1 + x_sub2 + x_sub3 + x_sub4 + x_sub5 + x_sub6 + x_sub7 + x_sub8 +
        x_sub9 + x_sub10
y_50.reverse()
x_sub.reverse()

# calculates x
x_50 = [0.5177]
for v in x_sub:
    v = x_50[-1]+v
    x_50.append(v)

x_50.remove(x_50[-1])

y_30_array = np.array(y_30)
y_50_array = np.array(y_50)

if y_30_array.size > y_50_array.size:
    y_30_array.resize(y_50_array.shape)
    x = x_50

```

```

elif y_50_array.size > y_30_array.size:
    y_50_array.resize(y_30_array.shape)
    x = x_30

y_array = y_50_array - y_30_array
y = y_array.tolist()

# calculates moving average for Y
weights = np.repeat(1.0,10)/10
m_av = np.convolve(y,weights,'valid').tolist()

# creates x for moving average
step = 127.5/len(m_av)
x_av = np.arange(0.5177,127.5,step).tolist()

# sets the separation between the ticks and the axes
py.rcParams['xtick.major.pad']='8'
py.rcParams['ytick.major.pad']='8'

# creates figure, sets size
fig = plt.figure(1,figsize=(8,20))

# sets space at the bottom of the figure for xlabel
fig.subplots_adjust(bottom=0.2)

# creates the first subfigure 1 of 2 top plot
ax1 = fig.add_subplot(511)

# plots delta average sub-width vs distance downstream
ax1.plot(x,y,'bo',lw=2)

# plots moving average
ax1.plot(x_av,m_av,'r-',lw=4)

# plots reach dashed lines
ax1.plot([17.150,17.150],[-60,100],'k--')
ax1.plot([28.920,28.920],[-60,100],'k--')
ax1.plot([41.820,41.820],[-60,100],'k--')
ax1.plot([51.500,51.500],[-60,100],'k--')
ax1.plot([66.380,66.380],[-60,100],'k--')
ax1.plot([81.110,81.110],[-60,100],'k--')
ax1.plot([94.110,94.110],[-60,100],'k--')
ax1.plot([102.810,102.810],[-60,100],'k--')
ax1.plot([117.060,117.060],[-60,100],'k--')

```

```

# sets ylabel to specified string
ax1.set_ylabel('Width (m)')

# makes xticks invisible
plt.setp(ax1.get_xticklabels(), visible=False)

#sets x and y limits
ax1.set_xlim(0,127.5)
ax1.set_ylim(-60,60)

# specifies what ticks to show in the y-axis
ax1.set_yticks([-50,-30,-10,10,30,50])

# adds text to the plots at specified locations
ax1.annotate('1950s - 1930s', xy=(0,50), xycoords='data',xytext=(10,-2),
            textcoords='offset points',size=20)

# sets the fontsize of the subplot to specified size
for item in ([ax1.xaxis.label, ax1.yaxis.label] + ax1.get_xticklabels() +
            ax1.get_yticklabels()):
    item.set_fontsize(20)

# extracts sub-width from shapefiles
arcpy.env.workspace = decade_50
y_50 = []
x_sub = []
y1=[];y2=[];y3=[];y4=[];y5=[];y6=[];y7=[];y8=[];y9=[];y10=[]
x_sub1=[];x_sub2=[];x_sub3=[];x_sub4=[];x_sub5=[];x_sub6=[];x_sub7=[];x_sub8=[];x
    _sub9=[];x_sub10=[]
for reaches in arcpy.ListFeatureClasses('reach01*', 'Polygon'):
    with arcpy.da.SearchCursor(reaches,('av_w_sub','av_width_m')) as rows:
        for row in rows:
            y1.append(row[0])
            x_sub1.append((row[1]*10)/1000)
for reaches in arcpy.ListFeatureClasses('reach02*', 'Polygon'):
    with arcpy.da.SearchCursor(reaches,('av_w_sub','av_width_m')) as rows:
        for row in rows:
            y2.append(row[0])
            x_sub2.append((row[1]*10)/1000)
for reaches in arcpy.ListFeatureClasses('reach03*', 'Polygon'):
    with arcpy.da.SearchCursor(reaches,('av_w_sub','av_width_m')) as rows:
        for row in rows:
            y3.append(row[0])
            x_sub3.append((row[1]*10)/1000)
for reaches in arcpy.ListFeatureClasses('reach04*', 'Polygon'):

```

```

with arcpy.da.SearchCursor(reaches,('av_w_sub','av_width_m')) as rows:
    for row in rows:
        y4.append(row[0])
        x_sub4.append((row[1]*10)/1000)
for reaches in arcpy.ListFeatureClasses('reach05*', 'Polygon'):
    with arcpy.da.SearchCursor(reaches,('av_w_sub','av_width_m')) as rows:
        for row in rows:
            y5.append(row[0])
            x_sub5.append((row[1]*10)/1000)
for reaches in arcpy.ListFeatureClasses('reach06*', 'Polygon'):
    with arcpy.da.SearchCursor(reaches,('av_w_sub','av_width_m')) as rows:
        for row in rows:
            y6.append(row[0])
            x_sub6.append((row[1]*10)/1000)
for reaches in arcpy.ListFeatureClasses('reach07*', 'Polygon'):
    with arcpy.da.SearchCursor(reaches,('av_w_sub','av_width_m')) as rows:
        for row in rows:
            y7.append(row[0])
            x_sub7.append((row[1]*10)/1000)
for reaches in arcpy.ListFeatureClasses('reach08*', 'Polygon'):
    with arcpy.da.SearchCursor(reaches,('av_w_sub','av_width_m')) as rows:
        for row in rows:
            y8.append(row[0])
            x_sub8.append((row[1]*10)/1000)
for reaches in arcpy.ListFeatureClasses('reach09*', 'Polygon'):
    with arcpy.da.SearchCursor(reaches,('av_w_sub','av_width_m')) as rows:
        for row in rows:
            y9.append(row[0])
            x_sub9.append((row[1]*10)/1000)
for reaches in arcpy.ListFeatureClasses('reach10*', 'Polygon'):
    with arcpy.da.SearchCursor(reaches,('av_w_sub','av_width_m')) as rows:
        for row in rows:
            y10.append(row[0])
            x_sub10.append((row[1]*10)/1000)

y1.reverse();y2.reverse();y3.reverse();y4.reverse();y5.reverse();y6.reverse();y7.reverse();
y8.reverse();y9.reverse();y10.reverse()

y_50 = y1 + y2 + y3 + y4 + y5 + y6 + y7 + y8 + y9 + y10
x_sub = x_sub1 + x_sub2 + x_sub3 + x_sub4 + x_sub5 + x_sub6 + x_sub7 + x_sub8 +
        x_sub9 + x_sub10
y_50.reverse()
x_sub.reverse()

# calculates x

```

```

x_50 = [0.5177]
for v in x_sub:
    v = x_50[-1]+v
    x_50.append(v)

x_50.remove(x_50[-1])

# extracts sub-width from shapefiles
arcpy.env.workspace = decade_70
y_70 = []
x_sub = []
y1=[];y2=[];y3=[];y4=[];y5=[];y6=[];y7=[];y8=[];y9=[];y10=[]
x_sub1=[];x_sub2=[];x_sub3=[];x_sub4=[];x_sub5=[];x_sub6=[];x_sub7=[];x_sub8=[];x
    _sub9=[];x_sub10=[]
for reaches in arcpy.ListFeatureClasses('reach01*', 'Polygon'):
    with arcpy.da.SearchCursor(reaches,('av_w_sub','av_width_m')) as rows:
        for row in rows:
            y1.append(row[0])
            x_sub1.append((row[1]*10)/1000)
for reaches in arcpy.ListFeatureClasses('reach02*', 'Polygon'):
    with arcpy.da.SearchCursor(reaches,('av_w_sub','av_width_m')) as rows:
        for row in rows:
            y2.append(row[0])
            x_sub2.append((row[1]*10)/1000)
for reaches in arcpy.ListFeatureClasses('reach03*', 'Polygon'):
    with arcpy.da.SearchCursor(reaches,('av_w_sub','av_width_m')) as rows:
        for row in rows:
            y3.append(row[0])
            x_sub3.append((row[1]*10)/1000)
for reaches in arcpy.ListFeatureClasses('reach04*', 'Polygon'):
    with arcpy.da.SearchCursor(reaches,('av_w_sub','av_width_m')) as rows:
        for row in rows:
            y4.append(row[0])
            x_sub4.append((row[1]*10)/1000)
for reaches in arcpy.ListFeatureClasses('reach05*', 'Polygon'):
    with arcpy.da.SearchCursor(reaches,('av_w_sub','av_width_m')) as rows:
        for row in rows:
            y5.append(row[0])
            x_sub5.append((row[1]*10)/1000)
for reaches in arcpy.ListFeatureClasses('reach06*', 'Polygon'):
    with arcpy.da.SearchCursor(reaches,('av_w_sub','av_width_m')) as rows:
        for row in rows:
            y6.append(row[0])
            x_sub6.append((row[1]*10)/1000)
for reaches in arcpy.ListFeatureClasses('reach07*', 'Polygon'):

```

```

with arcpy.da.SearchCursor(reaches,('av_w_sub','av_width_m')) as rows:
    for row in rows:
        y7.append(row[0])
        x_sub7.append((row[1]*10)/1000)
for reaches in arcpy.ListFeatureClasses('reach08*', 'Polygon'):
    with arcpy.da.SearchCursor(reaches,('av_w_sub','av_width_m')) as rows:
        for row in rows:
            y8.append(row[0])
            x_sub8.append((row[1]*10)/1000)
for reaches in arcpy.ListFeatureClasses('reach09*', 'Polygon'):
    with arcpy.da.SearchCursor(reaches,('av_w_sub','av_width_m')) as rows:
        for row in rows:
            y9.append(row[0])
            x_sub9.append((row[1]*10)/1000)
for reaches in arcpy.ListFeatureClasses('reach10*', 'Polygon'):
    with arcpy.da.SearchCursor(reaches,('av_w_sub','av_width_m')) as rows:
        for row in rows:
            y10.append(row[0])
            x_sub10.append((row[1]*10)/1000)

y1.reverse();y2.reverse();y3.reverse();y4.reverse();y5.reverse();y6.reverse();y7.reverse();
y8.reverse();y9.reverse();y10.reverse()

y_70 = y1 + y2 + y3 + y4 + y5 + y6 + y7 + y8 + y9 + y10
x_sub = x_sub1 + x_sub2 + x_sub3 + x_sub4 + x_sub5 + x_sub6 + x_sub7 + x_sub8 +
        x_sub9 + x_sub10
y_70.reverse()
x_sub.reverse()

# calculates x
x_70 = [0.5177]
for v in x_sub:
    v = x_70[-1]+v
    x_70.append(v)

x_70.remove(x_70[-1])

y_50_array = np.array(y_50)
y_70_array = np.array(y_70)

if y_50_array.size > y_70_array.size:
    y_50_array.resize(y_70_array.shape)
    x = x_70
elif y_70_array.size > y_50_array.size:
    y_70_array.resize(y_50_array.shape)

```

```

x = x_50

y_array = y_70_array - y_50_array
y = y_array.tolist()

# calculates moving average for Y
weights = np.repeat(1.0,10)/10
m_av = np.convolve(y,weights,'valid').tolist()

# creates x for moving average
step = 127.5/len(m_av)
x_av = np.arange(0.5177,127.5,step).tolist()

# creates the first subfigure 1 of 2 **top plot**
ax2 = fig.add_subplot(512)

# plots average sub-width vs distance downstream
ax2.plot(x,y,'bo',lw=2)

# plots moving average
ax2.plot(x_av,m_av,'r-',lw=4)

# plots reach dashed lines
ax2.plot([17.150,17.150],[-60,100],'k--')
ax2.plot([28.920,28.920],[-60,100],'k--')
ax2.plot([41.820,41.820],[-60,100],'k--')
ax2.plot([51.500,51.500],[-60,100],'k--')
ax2.plot([66.380,66.380],[-60,100],'k--')
ax2.plot([81.110,81.110],[-60,100],'k--')
ax2.plot([94.110,94.110],[-60,100],'k--')
ax2.plot([102.810,102.810],[-60,100],'k--')
ax2.plot([117.060,117.060],[-60,100],'k--')

# sets ylabel to specified string
ax2.set_ylabel('Width (m)')

# makes xticks and yticks invisible
plt.setp(ax2.get_xticklabels(), visible=False)

#sets x and y limits
ax2.set_xlim(0,127.5)
ax2.set_ylim(-60,60)

# specifies what ticks to show in the y-axis
ax2.set_yticks([-50,-30,-10,10,30,50])

```

```

# adds text to the plots at specified locations
ax2.annotate('1970s - 1950s', xy=(0,50), xycoords='data',xytext=(10,-2),
             textcoords='offset points',size=20)

# sets the fontsize of the subplot to specified size
for item in ([ax2.xaxis.label, ax2.yaxis.label] + ax2.get_xticklabels() +
             ax2.get_yticklabels()):
    item.set_fontsize(20)

# extracts sub-width from shapefiles
arcpy.env.workspace = decade_70
y_70 = []
x_sub = []
y1=[];y2=[];y3=[];y4=[];y5=[];y6=[];y7=[];y8=[];y9=[];y10=[]
x_sub1=[];x_sub2=[];x_sub3=[];x_sub4=[];x_sub5=[];x_sub6=[];x_sub7=[];x_sub8=[];x
    _sub9=[];x_sub10=[]
for reaches in arcpy.ListFeatureClasses('reach01*', 'Polygon'):
    with arcpy.da.SearchCursor(reaches,('av_w_sub','av_width_m')) as rows:
        for row in rows:
            y1.append(row[0])
            x_sub1.append((row[1]*10)/1000)
for reaches in arcpy.ListFeatureClasses('reach02*', 'Polygon'):
    with arcpy.da.SearchCursor(reaches,('av_w_sub','av_width_m')) as rows:
        for row in rows:
            y2.append(row[0])
            x_sub2.append((row[1]*10)/1000)
for reaches in arcpy.ListFeatureClasses('reach03*', 'Polygon'):
    with arcpy.da.SearchCursor(reaches,('av_w_sub','av_width_m')) as rows:
        for row in rows:
            y3.append(row[0])
            x_sub3.append((row[1]*10)/1000)
for reaches in arcpy.ListFeatureClasses('reach04*', 'Polygon'):
    with arcpy.da.SearchCursor(reaches,('av_w_sub','av_width_m')) as rows:
        for row in rows:
            y4.append(row[0])
            x_sub4.append((row[1]*10)/1000)
for reaches in arcpy.ListFeatureClasses('reach05*', 'Polygon'):
    with arcpy.da.SearchCursor(reaches,('av_w_sub','av_width_m')) as rows:
        for row in rows:
            y5.append(row[0])
            x_sub5.append((row[1]*10)/1000)
for reaches in arcpy.ListFeatureClasses('reach06*', 'Polygon'):
    with arcpy.da.SearchCursor(reaches,('av_w_sub','av_width_m')) as rows:
        for row in rows:

```

```

        y6.append(row[0])
        x_sub6.append((row[1]*10)/1000)
for reaches in arcpy.ListFeatureClasses('reach07*', 'Polygon'):
    with arcpy.da.SearchCursor(reaches, ('av_w_sub', 'av_width_m')) as rows:
        for row in rows:
            y7.append(row[0])
            x_sub7.append((row[1]*10)/1000)
for reaches in arcpy.ListFeatureClasses('reach08*', 'Polygon'):
    with arcpy.da.SearchCursor(reaches, ('av_w_sub', 'av_width_m')) as rows:
        for row in rows:
            y8.append(row[0])
            x_sub8.append((row[1]*10)/1000)
for reaches in arcpy.ListFeatureClasses('reach09*', 'Polygon'):
    with arcpy.da.SearchCursor(reaches, ('av_w_sub', 'av_width_m')) as rows:
        for row in rows:
            y9.append(row[0])
            x_sub9.append((row[1]*10)/1000)
for reaches in arcpy.ListFeatureClasses('reach10*', 'Polygon'):
    with arcpy.da.SearchCursor(reaches, ('av_w_sub', 'av_width_m')) as rows:
        for row in rows:
            y10.append(row[0])
            x_sub10.append((row[1]*10)/1000)

y1.reverse();y2.reverse();y3.reverse();y4.reverse();y5.reverse();y6.reverse();y7.reverse();
y8.reverse();y9.reverse();y10.reverse()

y_70 = y1 + y2 + y3 + y4 + y5 + y6 + y7 + y8 + y9 + y10
x_sub = x_sub1 + x_sub2 + x_sub3 + x_sub4 + x_sub5 + x_sub6 + x_sub7 + x_sub8 +
        x_sub9 + x_sub10
y_70.reverse()
x_sub.reverse()

# calculates x
x_70 = [0.5177]
for v in x_sub:
    v = x_70[-1]+v
    x_70.append(v)

x_70.remove(x_70[-1])

# extracts sub-width from shapefiles
arcpy.env.workspace = decade_90
y_90 = []
x_sub = []

```

```

for reaches in arcpy.ListFeatureClasses('reach*', 'Polygon'):
    with arcpy.da.SearchCursor(reaches, ('av_w_sub', 'av_width_m')) as rows:
        for row in rows:
            y_90.append(row[0])
            x_sub.append((row[1]*10)/1000)
y_90.reverse()

# calculates x
x_90 = [0.5177]
for v in x_sub:
    v = x_90[-1]+v
    x_90.append(v)

x_90.remove(x_90[-1])

y_70_array = np.array(y_70)
y_90_array = np.array(y_90)

if y_70_array.size > y_90_array.size:
    y_70_array.resize(y_90_array.shape)
    x = x_90
elif y_90_array.size > y_70_array.size:
    y_90_array.resize(y_70_array.shape)
    x = x_70

y_array = y_90_array - y_70_array
y = y_array.tolist()

# calculates moving average for Y
weights = np.repeat(1.0,10)/10
m_av = np.convolve(y,weights,'valid').tolist()

# creates x for moving average
step = 127.5/len(m_av)
x_av = np.arange(0.5177,127.5,step).tolist()
x_av.append(x_av[-1]+step)

# creates the first subfigure 1 of 2 **top plot**
ax3 = fig.add_subplot(513)

# plots average sub-width vs distance downstream
ax3.plot(x,y,'bo',lw=2)

# plots moving average
ax3.plot(x_av,m_av,'r-',lw=4)

```

```

# plots reach dashed lines
ax3.plot([17.150,17.150],[-60,100],'k--')
ax3.plot([28.920,28.920],[-60,100],'k--')
ax3.plot([41.820,41.820],[-60,100],'k--')
ax3.plot([51.500,51.500],[-60,100],'k--')
ax3.plot([66.380,66.380],[-60,100],'k--')
ax3.plot([81.110,81.110],[-60,100],'k--')
ax3.plot([94.110,94.110],[-60,100],'k--')
ax3.plot([102.810,102.810],[-60,100],'k--')
ax3.plot([117.060,117.060],[-60,100],'k--')

# sets ylabel to specified string
ax3.set_ylabel('Width (m)')

# makes xticks invisible
plt.setp(ax3.get_xticklabels(), visible=False)

#sets x and y limits
ax3.set_xlim(0,127.5)
ax3.set_ylim(-60,60)

# specifies what ticks to show in the y-axis
ax3.set_yticks([-50,-30,-10,10,30,50])

# adds text to the plots at specified locations
ax3.annotate('1990s - 1970s', xy=(0,50), xycoords='data',xytext=(10,-2),
            textcoords='offset points',size=20)

# sets the fontsize of the subplot to specified size
for item in ([ax3.xaxis.label, ax3.yaxis.label] + ax3.get_xticklabels() +
            ax3.get_yticklabels()):
    item.set_fontsize(20)

# extracts sub-width from shapefiles
arcpy.env.workspace = decade_90
y_90 = []
x_sub = []

for reaches in arcpy.ListFeatureClasses('reach*', 'Polygon'):
    with arcpy.da.SearchCursor(reaches,('av_w_sub','av_width_m')) as rows:
        for row in rows:
            y_90.append(row[0])
            x_sub.append((row[1]*10)/1000)
y_90.reverse()

```

```

# calculates x
x_90 = [0.5177]
for v in x_sub:
    v = x_90[-1]+v
    x_90.append(v)

x_90.remove(x_90[-1])

# extracts sub-width from shapefiles
arcpy.env.workspace = decade_00
y_00 = []
x_sub = []

for reaches in arcpy.ListFeatureClasses('reach*', 'Polygon'):
    with arcpy.da.SearchCursor(reaches, ('av_w_sub', 'av_width_m')) as rows:
        for row in rows:
            y_00.append(row[0])
            x_sub.append((row[1]*10)/1000)
y_00.reverse()

# calculates x
x_00 = [0.5177]
for v in x_sub:
    v = x_00[-1]+v
    x_00.append(v)

x_00.remove(x_00[-1])

y_90_array = np.array(y_90)
y_00_array = np.array(y_00)

if y_90_array.size > y_00_array.size:
    y_90_array.resize(y_00_array.shape)
    x = x_00
elif y_00_array.size > y_90_array.size:
    y_00_array.resize(y_90_array.shape)
    x = x_90

y_array = y_00_array - y_90_array
y = y_array.tolist()

# calculates moving average for Y
weights = np.repeat(1.0, 10)/10
m_av = np.convolve(y, weights, 'valid').tolist()

```

```

# creates x for moving average
step = 127.5/len(m_av)
x_av = np.arange(0.5177,127.5,step).tolist()
x_av.append(x_av[-1]+step)
print len(x_av)
print len(m_av)

# creates the first subfigure 1 of 2 top plot
ax4 = fig.add_subplot(514)

# plots average sub-width vs distance downstream
ax4.plot(x,y,'bo',lw=2)

# plots moving average
ax4.plot(x_av,m_av,'r-',lw=4)

# plots reach dashed lines
ax4.plot([17.150,17.150],[-60,100],'k--')
ax4.plot([28.920,28.920],[-60,100],'k--')
ax4.plot([41.820,41.820],[-60,100],'k--')
ax4.plot([51.500,51.500],[-60,100],'k--')
ax4.plot([66.380,66.380],[-60,100],'k--')
ax4.plot([81.110,81.110],[-60,100],'k--')
ax4.plot([94.110,94.110],[-60,100],'k--')
ax4.plot([102.810,102.810],[-60,100],'k--')
ax4.plot([117.060,117.060],[-60,100],'k--')

# sets ylabel to specified string
ax4.set_ylabel('Width (m)')

# makes xticks and yticks invisible
plt.setp(ax4.get_xticklabels(), visible=False)

#sets x and y limits
ax4.set_xlim(0,127.5)
ax4.set_ylim(-60,60)

# specifies what ticks to show in the y-axis
ax4.set_yticks([-50,-30,-10,10,30,50])

# adds text to the plots at specified locations
ax4.annotate('2000s - 1990s', xy=(0,50), xycoords='data',xytext=(10,-2),
            textcoords='offset points',size=20)

```

```

# sets the fontsize of the subplot to specified size
for item in ([ax4.xaxis.label, ax4.yaxis.label] + ax4.get_xticklabels() +
            ax4.get_yticklabels()):
    item.set_fontsize(20)

# extracts sub-width from shapefiles
arcpy.env.workspace = decade_00
y_00 = []
x_sub = []

for reaches in arcpy.ListFeatureClasses('reach*', 'Polygon'):
    with arcpy.da.SearchCursor(reaches, ('av_w_sub', 'av_width_m')) as rows:
        for row in rows:
            y_00.append(row[0])
            x_sub.append((row[1]*10)/1000)
y_00.reverse()

# calculates x
x_00 = [0.5177]
for v in x_sub:
    v = x_00[-1]+v
    x_00.append(v)

x_00.remove(x_00[-1])

# extracts sub-width from shapefiles
arcpy.env.workspace = decade_10
y_10 = []
x_sub = []

for reaches in arcpy.ListFeatureClasses('reach*', 'Polygon'):
    with arcpy.da.SearchCursor(reaches, ('av_w_sub', 'av_width_m')) as rows:
        for row in rows:
            y_10.append(row[0])
            x_sub.append((row[1]*10)/1000)
y_10.reverse()

# calculates x
x_10 = [0.5177]
for v in x_sub:
    v = x_10[-1]+v
    x_10.append(v)

x_10.remove(x_10[-1])

```

```

y_00_array = np.array(y_00)
y_10_array = np.array(y_10)

if y_00_array.size > y_10_array.size:
    y_00_array.resize(y_10_array.shape)
    x = x_10
elif y_10_array.size > y_00_array.size:
    y_10_array.resize(y_00_array.shape)
    x = x_00

y_array = y_10_array - y_00_array
y = y_array.tolist()

# calculates moving average for Y
weights = np.repeat(1.0,10)/10
m_av = np.convolve(y,weights,'valid').tolist()

# creates x for moving average
step = 127.5/len(m_av)
x_av = np.arange(0.5177,127.5,step).tolist()

# creates the first subfigure 1 of 2 top plot
ax5 = fig.add_subplot(515)

# plots average sub-width vs distance downstream
ax5.plot(x,y,'bo',lw=2)

# plots moving average
ax5.plot(x_av,m_av,'r-',lw=4)

# plots reach dashed lines
ax5.plot([17.150,17.150],[-60,100],'k--')
ax5.plot([28.920,28.920],[-60,100],'k--')
ax5.plot([41.820,41.820],[-60,100],'k--')
ax5.plot([51.500,51.500],[-60,100],'k--')
ax5.plot([66.380,66.380],[-60,100],'k--')
ax5.plot([81.110,81.110],[-60,100],'k--')
ax5.plot([94.110,94.110],[-60,100],'k--')
ax5.plot([102.810,102.810],[-60,100],'k--')
ax5.plot([117.060,117.060],[-60,100],'k--')

# sets xlabel and ylabel to specified string
ax5.set_ylabel('Width (m)')
ax5.set_xlabel('Distance Downstream (km)')

```

```

#sets x and y limits
ax5.set_xlim(0,127.5)
ax5.set_ylim(-60,60)

# specifies what ticks to show in the y-axis
ax5.set_yticks([-50,-30,-10,10,30,50])

# adds text to the plots at specified locations
ax5.annotate('2010 - 2000s', xy=(0,50), xycoords='data',xytext=(10,-2), textcoords='offset
points',size=20)
ax5.annotate('R10', xy=(17.150,-60), xycoords='data',xytext=(-20,25), textcoords='offset
points',size=20).set_rotation('vertical')
ax5.annotate('R09', xy=(28.920,-60), xycoords='data',xytext=(-20,25), textcoords='offset
points',size=20).set_rotation('vertical')
ax5.annotate('R08', xy=(41.820,-60), xycoords='data',xytext=(-20,25), textcoords='offset
points',size=20).set_rotation('vertical')
ax5.annotate('R07', xy=(51.500,-60), xycoords='data',xytext=(-20,25), textcoords='offset
points',size=20).set_rotation('vertical')
ax5.annotate('R06', xy=(66.380,-60), xycoords='data',xytext=(-20,25), textcoords='offset
points',size=20).set_rotation('vertical')
ax5.annotate('R05', xy=(81.110,-60), xycoords='data',xytext=(-20,25), textcoords='offset
points',size=20).set_rotation('vertical')
ax5.annotate('R04', xy=(94.110,-60), xycoords='data',xytext=(-20,25), textcoords='offset
points',size=20).set_rotation('vertical')
ax5.annotate('R03', xy=(102.810,-60), xycoords='data',xytext=(-20,25),
textcoords='offset points',size=20).set_rotation('vertical')
ax5.annotate('R02', xy=(117.060,-60), xycoords='data',xytext=(-20,25),
textcoords='offset points',size=20).set_rotation('vertical')
ax5.annotate('R01', xy=(117.060,-60), xycoords='data',xytext=(15,25), textcoords='offset
points',size=20).set_rotation('vertical')

# sets the fontsize of the subplot to specified size
for item in ([ax5.xaxis.label, ax5.yaxis.label] + ax5.get_xticklabels() +
ax5.get_yticklabels()):
    item.set_fontsize(20)

# sets space between subplots
plt.subplots_adjust(hspace = 0.015)
plt.subplots_adjust(wspace = 0.015)

# saves figure to specified location
plt.savefig(workspace + '\delta_sub-width_per_reach.png',format='png')

# clears figure
plt.clf()

```

**Reach land cover percent:**

```
# imports modules
import arcpy
# defines parameters
table = r'C:\Users\Schumm\Documents\Belmont
        Lab\GIS_root\banks_land_cover_sp3.shp'
fields = ('reach','LEGEND', 'area_m2')
forested_1_lb = []; cultivated_1_lb = []; low_veg_1_lb = []
forested_2_lb = []; cultivated_2_lb = []; low_veg_2_lb = []
forested_3_lb = []; cultivated_3_lb = []; low_veg_3_lb = []
forested_4_lb = []; cultivated_4_lb = []; low_veg_4_lb = []
forested_5_lb = []; cultivated_5_lb = []; low_veg_5_lb = []
forested_6_lb = []; cultivated_6_lb = []; low_veg_6_lb = []
forested_7_lb = []; cultivated_7_lb = []; low_veg_7_lb = []
forested_8_lb = []; cultivated_8_lb = []; low_veg_8_lb = []
forested_9_lb = []; cultivated_9_lb = []; low_veg_9_lb = []
forested_10_lb = []; cultivated_10_lb = []; low_veg_10_lb = []
forested_1_rb = []; cultivated_1_rb = []; low_veg_1_rb = []
forested_2_rb = []; cultivated_2_rb = []; low_veg_2_rb = []
forested_3_rb = []; cultivated_3_rb = []; low_veg_3_rb = []
forested_4_rb = []; cultivated_4_rb = []; low_veg_4_rb = []
forested_5_rb = []; cultivated_5_rb = []; low_veg_5_rb = []
forested_6_rb = []; cultivated_6_rb = []; low_veg_6_rb = []
forested_7_rb = []; cultivated_7_rb = []; low_veg_7_rb = []
forested_8_rb = []; cultivated_8_rb = []; low_veg_8_rb = []
forested_9_rb = []; cultivated_9_rb = []; low_veg_9_rb = []
```

```

forested_10_rb = []; cultivated_10_rb = []; low_veg_10_rb = []
# calculates the percent of land cover for both sides of each reach from the main stem of
  the Root River
with arcpy.da.SearchCursor(table,fields) as rows:
  for row in rows:
    if row[0] == '1_lb':
      if row[1] == 'Forested':
        forested_1_lb.append(row[2])
      if row[1] == 'Cultivated Land':
        cultivated_1_lb.append(row[2])
      elif row[1] == 'Hay/Pasture/Grassland':
        low_veg_1_lb.append(row[2])
    if row[0] == '2_lb':
      if row[1] == 'Forested':
        forested_2_lb.append(row[2])
      elif row[1] == 'Cultivated Land':
        cultivated_2_lb.append(row[2])
      elif row[1] == 'Hay/Pasture/Grassland':
        low_veg_2_lb.append(row[2])
    if row[0] == '3_lb':
      if row[1] == 'Forested':
        forested_3_lb.append(row[2])
      elif row[1] == 'Cultivated Land':
        cultivated_3_lb.append(row[2])
      elif row[1] == 'Hay/Pasture/Grassland':
        low_veg_3_lb.append(row[2])
    if row[0] == '4_lb':
      if row[1] == 'Forested':
        forested_4_lb.append(row[2])
      elif row[1] == 'Cultivated Land':
        cultivated_4_lb.append(row[2])
      elif row[1] == 'Hay/Pasture/Grassland':
        low_veg_4_lb.append(row[2])
    if row[0] == '5_lb':
      if row[1] == 'Forested':
        forested_5_lb.append(row[2])
      elif row[1] == 'Cultivated Land':
        cultivated_5_lb.append(row[2])
      elif row[1] == 'Hay/Pasture/Grassland':
        low_veg_5_lb.append(row[2])
    if row[0] == '6_lb':
      if row[1] == 'Forested':
        forested_6_lb.append(row[2])
      elif row[1] == 'Cultivated Land':
        cultivated_6_lb.append(row[2])

```

```

elif row[1] == 'Hay/Pasture/Grassland':
    low_veg_6_lb.append(row[2])
if row[0] == '7_lb':
    if row[1] == 'Forested':
        forested_7_lb.append(row[2])
    elif row[1] == 'Cultivated Land':
        cultivated_7_lb.append(row[2])
    elif row[1] == 'Hay/Pasture/Grassland':
        low_veg_7_lb.append(row[2])
if row[0] == '8_lb':
    if row[1] == 'Forested':
        forested_8_lb.append(row[2])
    elif row[1] == 'Cultivated Land':
        cultivated_8_lb.append(row[2])
    elif row[1] == 'Hay/Pasture/Grassland':
        low_veg_8_lb.append(row[2])
if row[0] == '9_lb':
    if row[1] == 'Forested':
        forested_9_lb.append(row[2])
    elif row[1] == 'Cultivated Land':
        cultivated_9_lb.append(row[2])
    elif row[1] == 'Hay/Pasture/Grassland':
        low_veg_9_lb.append(row[2])
if row[0] == '10_lb':
    if row[1] == 'Forested':
        forested_10_lb.append(row[2])
    elif row[1] == 'Cultivated Land':
        cultivated_10_lb.append(row[2])
    elif row[1] == 'Hay/Pasture/Grassland':
        low_veg_10_lb.append(row[2])
if row[0] == '1_rb':
    if row[1] == 'Forested':
        forested_1_rb.append(row[2])
    elif row[1] == 'Cultivated Land':
        cultivated_1_rb.append(row[2])
    elif row[1] == 'Hay/Pasture/Grassland':
        low_veg_1_rb.append(row[2])
if row[0] == '2_rb':
    if row[1] == 'Forested':
        forested_2_rb.append(row[2])
    elif row[1] == 'Cultivated Land':
        cultivated_2_rb.append(row[2])
    elif row[1] == 'Hay/Pasture/Grassland':
        low_veg_2_rb.append(row[2])
if row[0] == '3_rb':

```

```
if row[1] == 'Forested':
    forested_3_rb.append(row[2])
elif row[1] == 'Cultivated Land':
    cultivated_3_rb.append(row[2])
elif row[1] == 'Hay/Pasture/Grassland':
    low_veg_3_rb.append(row[2])
if row[0] == '4_rb':
    if row[1] == 'Forested':
        forested_4_rb.append(row[2])
    elif row[1] == 'Cultivated Land':
        cultivated_4_rb.append(row[2])
    elif row[1] == 'Hay/Pasture/Grassland':
        low_veg_4_rb.append(row[2])
if row[0] == '5_rb':
    if row[1] == 'Forested':
        forested_5_rb.append(row[2])
    elif row[1] == 'Cultivated Land':
        cultivated_5_rb.append(row[2])
    elif row[1] == 'Hay/Pasture/Grassland':
        low_veg_5_rb.append(row[2])
if row[0] == '6_rb':
    if row[1] == 'Forested':
        forested_6_rb.append(row[2])
    elif row[1] == 'Cultivated Land':
        cultivated_6_rb.append(row[2])
    elif row[1] == 'Hay/Pasture/Grassland':
        low_veg_6_rb.append(row[2])
if row[0] == '7_rb':
    if row[1] == 'Forested':
        forested_7_rb.append(row[2])
    elif row[1] == 'Cultivated Land':
        cultivated_7_rb.append(row[2])
    elif row[1] == 'Hay/Pasture/Grassland':
        low_veg_7_rb.append(row[2])
if row[0] == '8_rb':
    if row[1] == 'Forested':
        forested_8_rb.append(row[2])
    elif row[1] == 'Cultivated Land':
        cultivated_8_rb.append(row[2])
    elif row[1] == 'Hay/Pasture/Grassland':
        low_veg_8_rb.append(row[2])
if row[0] == '9_rb':
    if row[1] == 'Forested':
        forested_9_rb.append(row[2])
    elif row[1] == 'Cultivated Land':
```

```

        cultivated_9_rb.append(row[2])
    elif row[1] == 'Hay/Pasture/Grassland':
        low_veg_9_rb.append(row[2])
if row[0] == '10_rb':
    if row[1] == 'Forested':
        forested_10_rb.append(row[2])
    elif row[1] == 'Cultivated Land':
        cultivated_10_rb.append(row[2])
    elif row[1] == 'Hay/Pasture/Grassland':
        low_veg_10_rb.append(row[2])
area_1lb = sum([sum(forested_1_lb),sum(cultivated_1_lb),sum(low_veg_1_lb)])
forested_area_1lb = sum(forested_1_lb)/area_1lb
cultivated_area_1lb = sum(cultivated_1_lb)/area_1lb
low_veg_area_1lb = sum(low_veg_1_lb)/area_1lb
print 'Reach 1 left: forested {0}, cultivated {1}, low vegetation
      {2}'.format(forested_area_1lb,cultivated_area_1lb,low_veg_area_1lb)
area_2lb = sum([sum(forested_2_lb),sum(cultivated_2_lb),sum(low_veg_2_lb)])
forested_area_2lb = sum(forested_2_lb)/area_2lb
cultivated_area_2lb = sum(cultivated_2_lb)/area_2lb
low_veg_area_2lb = sum(low_veg_2_lb)/area_2lb
print 'Reach 2 left: forested {0}, cultivated {1}, low vegetation
      {2}'.format(forested_area_2lb,cultivated_area_2lb,low_veg_area_2lb)
area_3lb = sum([sum(forested_3_lb),sum(cultivated_3_lb),sum(low_veg_3_lb)])
forested_area_3lb = sum(forested_3_lb)/area_3lb
cultivated_area_3lb = sum(cultivated_3_lb)/area_3lb
low_veg_area_3lb = sum(low_veg_3_lb)/area_3lb
print 'Reach 3 left: forested {0}, cultivated {1}, low vegetation
      {2}'.format(forested_area_3lb,cultivated_area_3lb,low_veg_area_3lb)
area_4lb = sum([sum(forested_4_lb),sum(cultivated_4_lb),sum(low_veg_4_lb)])
forested_area_4lb = sum(forested_4_lb)/area_4lb
cultivated_area_4lb = sum(cultivated_4_lb)/area_4lb
low_veg_area_4lb = sum(low_veg_4_lb)/area_4lb
print 'Reach 4 left: forested {0}, cultivated {1}, low vegetation
      {2}'.format(forested_area_4lb,cultivated_area_4lb,low_veg_area_4lb)
area_5lb = sum([sum(forested_5_lb),sum(cultivated_5_lb),sum(low_veg_5_lb)])
forested_area_5lb = sum(forested_5_lb)/area_5lb
cultivated_area_5lb = sum(cultivated_5_lb)/area_5lb
low_veg_area_5lb = sum(low_veg_5_lb)/area_5lb
print 'Reach 5 left: forested {0}, cultivated {1}, low vegetation
      {2}'.format(forested_area_5lb,cultivated_area_5lb,low_veg_area_5lb)
area_6lb = sum([sum(forested_6_lb),sum(cultivated_6_lb),sum(low_veg_6_lb)])
forested_area_6lb = sum(forested_6_lb)/area_6lb
cultivated_area_6lb = sum(cultivated_6_lb)/area_6lb
low_veg_area_6lb = sum(low_veg_6_lb)/area_6lb

```

```

print 'Reach 6 left: forested {0}, cultivated {1}, low vegetation
      {2}'.format(forested_area_6lb,cultivated_area_6lb,low_veg_area_6lb)
area_7lb = sum([sum(forested_7_lb),sum(cultivated_7_lb),sum(low_veg_7_lb)])
forested_area_7lb = sum(forested_7_lb)/area_7lb
cultivated_area_7lb = sum(cultivated_7_lb)/area_7lb
low_veg_area_7lb = sum(low_veg_7_lb)/area_7lb
print 'Reach 7 left: forested {0}, cultivated {1}, low vegetation
      {2}'.format(forested_area_7lb,cultivated_area_7lb,low_veg_area_7lb)
area_8lb = sum([sum(forested_8_lb),sum(cultivated_8_lb),sum(low_veg_8_lb)])
forested_area_8lb = sum(forested_8_lb)/area_8lb
cultivated_area_8lb = sum(cultivated_8_lb)/area_8lb
low_veg_area_8lb = sum(low_veg_8_lb)/area_8lb
print 'Reach 8 left: forested {0}, cultivated {1}, low vegetation
      {2}'.format(forested_area_8lb,cultivated_area_8lb,low_veg_area_8lb)
area_9lb = sum([sum(forested_9_lb),sum(cultivated_9_lb),sum(low_veg_9_lb)])
forested_area_9lb = sum(forested_9_lb)/area_9lb
cultivated_area_9lb = sum(cultivated_9_lb)/area_9lb
low_veg_area_9lb = sum(low_veg_9_lb)/area_9lb
print 'Reach 9 left: forested {0}, cultivated {1}, low vegetation
      {2}'.format(forested_area_9lb,cultivated_area_9lb,low_veg_area_9lb)
area_10lb = sum([sum(forested_10_lb),sum(cultivated_10_lb),sum(low_veg_10_lb)])
forested_area_10lb = sum(forested_10_lb)/area_10lb
cultivated_area_10lb = sum(cultivated_10_lb)/area_10lb
low_veg_area_10lb = sum(low_veg_10_lb)/area_10lb
print 'Reach 10 left: forested {0}, cultivated {1}, low vegetation
      {2}'.format(forested_area_10lb,cultivated_area_10lb,low_veg_area_10lb)
area_1rb = sum([sum(forested_1_rb),sum(cultivated_1_rb),sum(low_veg_1_rb)])
forested_area_1rb = sum(forested_1_rb)/area_1rb
cultivated_area_1rb = sum(cultivated_1_rb)/area_1rb
low_veg_area_1rb = sum(low_veg_1_rb)/area_1rb
print 'Reach 1 right: forested {0}, cultivated {1}, low vegetation
      {2}'.format(forested_area_1rb,cultivated_area_1rb,low_veg_area_1rb)
area_2rb = sum([sum(forested_2_rb),sum(cultivated_2_rb),sum(low_veg_2_rb)])
forested_area_2rb = sum(forested_2_rb)/area_2rb
cultivated_area_2rb = sum(cultivated_2_rb)/area_2rb
low_veg_area_2rb = sum(low_veg_2_rb)/area_2rb
print 'Reach 2 right: forested {0}, cultivated {1}, low vegetation
      {2}'.format(forested_area_2rb,cultivated_area_2rb,low_veg_area_2rb)
area_3rb = sum([sum(forested_3_rb),sum(cultivated_3_rb),sum(low_veg_3_rb)])
forested_area_3rb = sum(forested_3_rb)/area_3rb
cultivated_area_3rb = sum(cultivated_3_rb)/area_3rb
low_veg_area_3rb = sum(low_veg_3_rb)/area_3rb
print 'Reach 3 right: forested {0}, cultivated {1}, low vegetation
      {2}'.format(forested_area_3rb,cultivated_area_3rb,low_veg_area_3rb)
area_4rb = sum([sum(forested_4_rb),sum(cultivated_4_rb),sum(low_veg_4_rb)])

```

```

forested_area_4rb = sum(forested_4_rb)/area_4rb
cultivated_area_4rb = sum(cultivated_4_rb)/area_4rb
low_veg_area_4rb = sum(low_veg_4_rb)/area_4rb
print 'Reach 4 right: forested {0}, cultivated {1}, low vegetation
      {2}'.format(forested_area_4rb,cultivated_area_4rb,low_veg_area_4rb)
area_5rb = sum([sum(forested_5_rb),sum(cultivated_5_rb),sum(low_veg_5_rb)])
forested_area_5rb = sum(forested_5_rb)/area_5rb
cultivated_area_5rb = sum(cultivated_5_rb)/area_5rb
low_veg_area_5rb = sum(low_veg_5_rb)/area_5rb
print 'Reach 5 right: forested {0}, cultivated {1}, low vegetation
      {2}'.format(forested_area_5rb,cultivated_area_5rb,low_veg_area_5rb)
area_6rb = sum([sum(forested_6_rb),sum(cultivated_6_rb),sum(low_veg_6_rb)])
forested_area_6rb = sum(forested_6_rb)/area_6rb
cultivated_area_6rb = sum(cultivated_6_rb)/area_6rb
low_veg_area_6rb = sum(low_veg_6_rb)/area_6rb
print 'Reach 6 right: forested {0}, cultivated {1}, low vegetation
      {2}'.format(forested_area_6rb,cultivated_area_6rb,low_veg_area_6rb)
area_7rb = sum([sum(forested_7_rb),sum(cultivated_7_rb),sum(low_veg_7_rb)])
forested_area_7rb = sum(forested_7_rb)/area_7rb
cultivated_area_7rb = sum(cultivated_7_rb)/area_7rb
low_veg_area_7rb = sum(low_veg_7_rb)/area_7rb
print 'Reach 7 right: forested {0}, cultivated {1}, low vegetation
      {2}'.format(forested_area_7rb,cultivated_area_7rb,low_veg_area_7rb)
area_8rb = sum([sum(forested_8_rb),sum(cultivated_8_rb),sum(low_veg_8_rb)])
forested_area_8rb = sum(forested_8_rb)/area_8rb
cultivated_area_8rb = sum(cultivated_8_rb)/area_8rb
low_veg_area_8rb = sum(low_veg_8_rb)/area_8rb
print 'Reach 8 right: forested {0}, cultivated {1}, low vegetation
      {2}'.format(forested_area_8rb,cultivated_area_8rb,low_veg_area_8rb)
area_9rb = sum([sum(forested_9_rb),sum(cultivated_9_rb),sum(low_veg_9_rb)])
forested_area_9rb = sum(forested_9_rb)/area_9rb
cultivated_area_9rb = sum(cultivated_9_rb)/area_9rb
low_veg_area_9rb = sum(low_veg_9_rb)/area_9rb
print 'Reach 9 right: forested {0}, cultivated {1}, low vegetation
      {2}'.format(forested_area_9rb,cultivated_area_9rb,low_veg_area_9rb)
area_10rb = sum([sum(forested_10_rb),sum(cultivated_10_rb),sum(low_veg_10_rb)])
forested_area_10rb = sum(forested_10_rb)/area_10rb
cultivated_area_10rb = sum(cultivated_10_rb)/area_10rb
low_veg_area_10rb = sum(low_veg_10_rb)/area_10rb
print 'Reach 10 right: forested {0}, cultivated {1}, low vegetation
      {2}'.format(forested_area_10rb,cultivated_area_10rb,low_veg_area_10rb)

```

**Elevation extraction and delta eta script:**

```

# import modules
import arcpy
import numpy as np
import os
import matplotlib.pyplot as plt
# checks spatial analysyst extention if it is available
if arcpy.CheckExtension('Spatial') == 'Available':
    arcpy.CheckOutExtension('Spatial')
else: print 'License is not available'
# define parameters
arcpy.env.overwriteOutput = True
ds = r'C:\Users\Schumm\Documents\Belmont Lab\GIS_root\rr_3m'
fields = ('FID','MEAN', 'STD')
workspace = r'C:\Users\Schumm\Documents\Belmont
           Lab\GIS_root\tributaries\trib_boxes'
arcpy.env.workspace = workspace
tributaries = arcpy.ListWorkspaces()
# calculates zonal statistics as table using raster dataset (ds) and polygon boxes along
reaches in the tributaries of the Root River
# calculates difference in bank elevation (delta eta) between each pair of polygon boxes
(left and right) for tributary in tributaries:
    textfile = workspace + '\\' + 'elevations_' +
os.path.splitext(os.path.basename(tributary))[0] + '.csv'
    # calculates zonal statistics as table
    arcpy.env.workspace = tributary
    for box in arcpy.ListFeatureClasses('*9103*', 'Polygon'):
        table = os.path.splitext(os.path.basename(box))[0] + '_table'
        arcpy.sa.ZonalStatisticsAsTable(box, 'FID', ds, table)
# saves results from zonal statistics to .csv files
with open(textfile, 'ab') as _file_:

    _file_.write('FID{0}', '.format(os.path.splitext(os.path.basename(box))[0][8
:]))
    with arcpy.da.SearchCursor(table, fields) as rows:
        for row in rows:
            _file_.write('{0}', '.format(float(row[0])))
            _file_.write('\n')

    _file_.write('ELEV{0}', '.format(os.path.splitext(os.path.basename(box))[0]
[8:]))
    with arcpy.da.SearchCursor(table, fields) as rows:
        for row in rows:
            _file_.write('{0}', '.format(float(row[1])))
            _file_.write('\n')

```

```

_file_.write('STD{0}',.format(os.path.splitext(os.path.basename(box))[0][
8:]))
with arcpy.da.SearchCursor(table,fields) as rows:
    for row in rows:
        _file_.write('{0}',.format(float(row[2])))
    _file_.write('\n')
# calculates delta eta and delta eta absolute for each .csv file
for box in arcpy.ListFeatureClasses('*9103*', 'Polygon'):
    table_left = os.path.splitext(os.path.basename(box))[0][0:9] +
    'left_merge9103_table'
    with arcpy.da.SearchCursor(table_left,fields) as rows:
        values_left_int = []
        for row in rows:
            values_left_int.append(row[1])
    table_right = os.path.splitext(os.path.basename(box))[0][0:9] +
    'right_merge9103_table'
    with arcpy.da.SearchCursor(table_right,fields) as rows:
        values_right_int = []
        for row in rows:
            values_right_int.append(row[1])
# converts values to numpyarrays so that they can be subtracted
with open(textfile,'ab') as _file2_:
    values_left_int_np = np.array(values_left_int)
    values_right_int_np = np.array(values_right_int)
    # makes sure arrays are the same size, if they are not, the size of the smallest one is
    taken
    if values_left_int_np.size > values_right_int_np.size:
        values_left_int_np.resize(values_right_int_np.shape)
    elif values_right_int_np.size > values_left_int_np.size:
        values_right_int_np.resize(values_left_int_np.shape)
    # subtracts arrays (opposing bank elevations) and appends them to csv file
    delta_eta = values_left_int_np - values_right_int_np
    delta_eta_abs = abs(values_left_int_np - values_right_int_np)
    _file2_.write('DELTA_ETA,')
    for n in delta_eta:
        _file2_.write('{0}',.format(n))
    _file2_.write('\n')
    _file2_.write('DELTA_ETA_ABS,')
    for n in delta_eta_abs:
        _file2_.write('{0}',.format(n))
    _file2_.write('\n')
# creates figure showing left and right bank elevations and delta eta plotted from up to
downstream

```

```

figure = workspace + '\\ + os.path.splitext(os.path.basename(tributary))[0] +
    '_fig'
y1 = values_left_int_np
y2 = values_right_int_np
y3 = delta_eta_abs
_max_ = y1.size*10
x = np.array(range(0,_max_,10))
fig = plt.figure()
axes1 = fig.add_subplot(111)
axes1.plot(x,y1,'0.75',lw=2)
axes1.plot(x,y2,'k')
axes1.set_xlabel('Distance downstream (m)')
axes1.set_ylabel('Bank Elevation (m)')
if np.min(y1) < np.min(y2):
    min_ = np.min(y1)-5
else:
    min_ = np.min(y2)-5
if np.max(y1) > np.max(y2):
    max_ = np.max(y1)+1
else:
    max_ = np.max(y2)+1
axes1.set_ylim(min_,max_)
axes2 = axes1.twinx()
axes2.plot(x,y3,'r', lw=2)
axes2.set_ylabel('Delta Eta (m)').set_color('r')
axes2.set_ylim(0,10)
for tl in axes2.get_yticklabels():
    tl.set_color('r')
axes2.annotate('Upstream', xy=(0,0), xycoords='data',xytext=(-20,-30),
    textcoords='offset points')
axes2.annotate('Downstream', xy=(20000,0), xycoords='data',xytext=(-50,-30),
    textcoords='offset points')
axes2.annotate('Average Delta Eta = {0} m'.format(np.around(np.mean(y3),4)),
    xy=(20000,10), xycoords='data',xytext=(-200,-30), textcoords='offset
    points').set_color('r')
plt.xlim(10000,20000)
plt.savefig(figure)
plt.clf

```

```

# checks the spatial analyst extention license back in
arcpy.CheckInExtension('Spatial')

```